

The development of novel infill materials for composite structural assemblies

Juan Vilches Tapia

A thesis submitted to
Auckland University of Technology
in fulfilment of the requirements for the degree of
Master of Philosophy (MPhil)

2014

Faculty of Design & Creative Technologies

Primary Supervisor: Dr. Thomas Neitzert
Second Supervisor: Dr. Dariusz Alterman

Table of Contents

ATTESTATION OF AUTHORSHIP.....	1
ACKNOWLEDGMENTS	2
ABSTRACT	3
CHAPTER 1	5
1. INTRODUCTION	5
1.1. BACKGROUND	6
1.1.1. Core Materials for Wall Systems	8
1.1.2. Facing Materials.....	11
1.2. THE RESEARCH QUESTION.....	11
1.3. OBJECTIVES OF THE STUDY	12
1.4. OUTLINE OF THE THESIS.....	13
CHAPTER 2	15
2. LITERATURE REVIEW	15
2.1. INTRODUCTION.....	15
2.2. LIGHTWEIGHT CONCRETE.....	15
2.3. FOAM CONCRETE	22
2.4. COMPOSITE STRUCTURAL ASSEMBLIES (CSAs).....	27
2.5. BONDING PHENOMENA.....	29
2.6. SUMMARY	31
CHAPTER 3	33
3. METHODS.....	33
3.1. INTRODUCTION	33
3.2. EXPERIMENTAL INVESTIGATION	34
3.2.1. Foam Concrete Mixture Design	34
3.2.2. Materials and Mixture Composition	36
3.2.3. Preparation of Foam Concrete	38
3.3. TEST METHODS	38
3.3.1. Compressive Strength.....	39
3.3.2. Density.....	39
3.3.3. Fire Resistance of Ultra-lightweight Concrete.....	40
3.3.4. Thermal Conductivity for Ultra-lightweight Concrete	42
3.3.5. Pull-out Experiments	43
3.4. CONCLUSION.....	50
CHAPTER 4	51
4. EXPERIMENTAL RESULTS AND DISCUSSION	51
4.1. INTRODUCTION.....	51
4.2. EXPERIMENTAL INVESTIGATION	51
4.3. FOAM CONCRETE MIXTURE DESIGN.....	52
4.4. TEST RESULTS.....	54
4.4.1. Compressive Strength and Density.....	54

4.4.2.	<i>Fire Resistance of Ultra-lightweight Concrete</i>	56
4.4.3.	<i>Thermal Conductivity of Ultra-lightweight Concrete</i>	61
4.4.4.	<i>Pull-out Experiments</i>	61
4.5.	CONCLUSION	80
CHAPTER 5		82
5. THREE DIMENSIONAL FINITE ELEMENT MODELS TO SIMULATE THE BONDING BEHAVIOR BETWEEN STEEL AND FOAM CONCRETE		82
5.1.	INTRODUCTION	82
5.2.	INPUT PARAMETERS FOR MODELING	83
5.2.1.	<i>Aerated Concrete Properties</i>	83
5.2.2.	<i>Galvanized Steel Properties</i>	86
5.3.	FE MODELLING OF BOND BETWEEN STEEL STRIPS AND FOAM CONCRETE	87
5.4.	EXPERIMENTAL AND MODELING RESULTS	89
5.5.	CONCLUSIONS	97
CHAPTER 6		98
6. CONCLUSIONS AND RECOMMENDATIONS FOR FURTHER STUDIES		98
6.1.	OVERVIEW	98
6.2.	CONCLUSIONS	99
6.3.	RECOMMENDATIONS FOR FURTHER STUDY	102
APPENDIX A. SIKAMENT HE200		105
APPENDIX B. ULTRAFOAM		108
APPENDIX C. QUICK GEL		110
APPENDIX D. LOAD DISPLACEMENT CURVES		111
APPENDIX E. PUBLICATIONS RESULTING FROM THE RESEARCH.		117
7. REFERENCES		118

List of Abbreviations and Symbols

AAC	Autoclaved Aerated Concrete
a/c	ash/cement ratio
A _h	Hole Area
A _s	Surface area of steel strips
ASTM	American Society for Testing and Materials
C	Cement
CA _h	Sum of circumference area of holes
CSAs	Composite Structural Assemblies
E _c	Modulus of Elasticity
EPS	Expanded Polystyrene
FEA	Finite Element Analysis
FEM	Finite Element Model
FC	Foam Concrete
f_c	Compressive strength
FRST	Foundation for Research Science & Technology
FRLWC	Fiber Reinforced Lightweight Concrete
G250	Grade of galvanized steel sheet
HCAR	Hole Circumference Area Ratio
HERA	Heavy Engineering Research Association
k	Ratio of the second stress invariant on the tensile meridian to that on the compressive meridian
LFC	Lightweight Foam Concrete
LWA	Lightweight Aggregate
LWC	Lightweight Concrete
M10	10mm diameter bolts with metric thread
MWEPS	Modified Waste Expanded Polystyrene
OPC	Ordinary Portland Cement
PVC	Polyvinyl Chloride
PS	Polystyrene
PU	Polyurethane
RD _f	relative density of foam
RD _c	relative density of cement
RD _a	relative density of ash
R ²	Correlation Coefficient
S	Hole pattern
s/c	sand/cement ratio
SCLC	Self-compacting Lightweight Concrete
T	Thermocouples
ULWC	Ultra Lightweight Concrete
V _f	volume of foam (l)
W	Water content
w/a	water/ash ratio
w/c	water/cement ratio
w/s	water/sand ratio
x	cement content (kg/m ³)
δ _m	target casting density (kg/m ³)
δ	Concrete density
ε	Eccentricity

σ_{b0}/σ_{c0}	Ratio of initial equi-biaxial compressive strength to uniaxial compressive strength
ΣV_i	Total component volumes

List of Figures

Figure 1-1 Typical composite sandwich panels.....	9
Figure 1-2 CSA sandwich wall panel	9
Figure 2-1 Typical ranges of densities of concretes made with various lightweight aggregates [14].	16
Figure 3-1 The heating unit.....	40
Figure 3-2 Schematic diagram of heating unit.....	41
Figure 3-3 Thermal conductivity equipment (Anacon TCA-8)	43
Figure 3-4 View of the rig for pull-out tests	44
Figure 3-5 Undesirable effects	44
Figure 3-6 Final set-up: Testing mechanism with a freely adjustable ball-joint and a plate with embedded-bolts within foam concrete samples (see also Figure 3.9).....	45
Figure 3-7 Patterns of holes in steel strips	47
Figure 3-8 Casting moulds	48
Figure 3-9 Schematic views of the location of a steel strip in foam concrete specimens between the holding-bolts	48
Figure 3-10 Testing rig with a freely adjustable ball-joint for pull-out tests	49
Figure 4-1 Relationship between air-dry density and compressive strength	55
Figure 4-2 Typical failure modes in compression tests	56
Figure 4-3 Time-temperature curve ULWC 150 (kg/m ³)	57
Figure 4-4 ULWC of 150 (kg/m ³) after test.....	57
Figure 4-5 Time-temperature curve ULWC 200 (kg/m ³)	58
Figure 4-6 ULWC of 200 (kg/m ³) after test.....	58
Figure 4-7 Time-temperature curve ULWC 250 (kg/m ³).....	59
Figure 4-8 ULWC of 250 (kg/m ³) after test.....	59
Figure 4-9 Time-temperature curve ULWC 400 (kg/m ³).....	60

Figure 4-10 Critical line of concrete density	63
Figure 4-11 Pull-out test results	66
Figure 4-12 Relationship between pull-out force and compressive strength....	67
Figure 4-13 Relationship between pull-out force and density	68
Figure 4-14 The effect of sum of area of holes on pull-out force for FC2 concrete	70
Figure 4-15 The effect of sum of area of holes on pull-out force for FC3 concrete.	70
Figure 4-16 The effect of the sum of diameters of holes on pull-out forces for FC2 concrete	73
Figure 4-17 The effect of the sum of diameters of holes on pull-out forces for FC3 concrete	74
Figure 4-18 The effect of sum of circumference areas of holes on pull-out force for FC2 concrete	76
Figure 4-19 The effect of sum of circumference areas of holes on pull-out force for FC3 concrete	77
Figure 4-20 The effect of hole circumference area ratio on pull-out strength for FC2 concrete	79
Figure 4-21 The effect of hole circumference area ratio (HCAR) on pull-out strength for FC3 concrete	79
Figure 5-1 Measured compressive stress-strain curve of foam concrete.....	86
Figure 5-2 Typical finite element model displaying shear stresses	87
Figure 5-3 Typical shear stress distributions for concrete and steel without holes	89
Figure 5-4 Typical bond strength distributions for concrete and steel with 4 holes of 2.83 mm radius.....	90
Figure 5-5 Stress concentration zone in [MPa] for S0 steel strip	91
Figure 5-6 Stress concentration zone in [MPa] for S1-8 steel strip	91
Figure 5-7 Stress concentration zone in [MPa] for S2-8 steel strip	92
Figure 5-8 Stress concentration zone in [MPa] for S4-3 steel strip	92
Figure 5-9 Stress concentration zone in [MPa] for S9-2 steel strip	93

Figure 5-10 Stress concentration zone in [MPa] for S14-3 steel strip	93
Figure 5-11 Load-displacement curves for S0 sample	94
Figure 5-12 Load-displacement curves for S4-3 sample.....	95
Figure 5-13 The effect of hole circumference area ratio (HCAR) on pull-out strength for FE simulation and FC3.	96

List of Tables

Table 2.1 Classification of lightweight concretes [13].....	16
Table 3.1 Chemical composition of mineral admixture.....	37
Table 3.2 Mix proportions.	37
Table 3.3 Pattern of holes in steel strips of 0.75 and 2 mm thickness	49
Table 3.4 Hole area ratios.....	50
Table 4.1 Mixture proportions [kg/m^3]	52
Table 4.2 Target and casting densities	53
Table 4.3 Thermal conductivity results.....	61
Table 4.4 Relationships of hole patterns.....	62
Table 4.5 Pull-out forces	65
Table 4.6 Variations of pull-out forces for different concretes	65
Table 4.7 FC4 pull-out forces and extrapolated pull-out forces.....	68
Table 4.8 Pull-out forces as a function of hole area	69
Table 4.9 Pull-out forces and sum of diameters of holes for FC2 concrete.....	72
Table 4.10 Pull-out forces and sum of diameters of holes for FC3 concrete.....	73
Table 4.11 Pull-out forces and sum of circumference area.....	75
Table 5.1 Input parameters used for concrete damaged plasticity in ABAQUS	85
Table 5.2 Material properties for steel sheets G250	86
Table 5.3 Comparison between FE and experimental results.....	95

Attestation of Authorship

I hereby declare that this submission is my own work and that, to the best of my knowledge and belief, it contains no material previously published or written by another person (except where explicitly defined in the acknowledgements), nor material which to a substantial extent has been submitted for the award of any other degree or diploma of a university or other institution of higher learning.

A handwritten signature in blue ink, appearing to read 'Juan Vilches', with a stylized, cursive script.

Juan Vilches

Acknowledgments

First and above all, I praise God, the almighty for providing me this opportunity and granting me the capability to proceed successfully. This research project would not have been possible without the support of many people. I would like to express my special gratitude and thanks to my supervisor, Prof. Thomas Neitzert who was abundantly helpful and offered invaluable assistance, support, guidance and patience. Thanks to Dr Dariusz Alterman and Dr Maziar Ramezani for their time and guidance on this project. Deepest gratitude are also due to the technicians without whose assistance this study would not have been successful. I also appreciate the financial support of the Chilean government and the Católica del Maule University, during my MPhil study. Thanks to all my colleagues in Chile, especially Dr Juan Figueroa, for providing support and encouragement. I would like to thank Anne Bliss for helping me with English language issues and for spending her valuable time to proofread this document.

I am appreciative of Florian Kern for assisting me and providing advice.

I would like to extend my deepest gratitude to my family: My parents Sara and David Vilches, and all of my brothers and sisters. Thank you for believing in me.

And finally, a person that moved with me and our children to New Zealand, my lovely wife, dear Marcela, without your supports and encouragements, I could not have finished this work. I understand it was difficult for you, therefore, I can just say thanks for everything and God will give you all the best in return.

Abstract

This thesis presents experimental investigations on the development of new/suitable materials for lightweight wall systems. The physical and mechanical characteristics of different mix compositions of foam and ultra-lightweight concrete as well as numerical simulation using finite element analysis in order to describe and predict bonding strength between steel sheets and aerated concrete specimens are presented in the thesis.

A significant achievement of the research was to design a novel set-up of a flexible mechanism to eliminate the influence of undesirable effects of either bending and/or twisting of steel strips during pull-out tests to concentrate on pure uniaxial performance. Furthermore, this thesis provides primary quantitative information about bonding behavior between lightweight concrete and perforated steel strips, and a finite element model (FEM) of the interface behavior of both materials, establishing a basis for future research.

Galvanized plain and perforated steel strips with holes of various numbers and patterns were used in order to verify the effect of the anchorage of concrete embedded into holes. Significant improvements for strips with holes over strips without holes were confirmed through a comparative analysis of pull-out tests.

Diverse components were researched to obtain a lightweight concrete, such as a plasticizer, lightweight aggregates, foaming agents, and mineral admixtures. Three foam concrete (FC) mix compositions were prepared with desired densities of 800, 1000 and 1200 kg/m³, and ultra-lightweight concretes (ULWC) with desired densities of 150, 200, 250 and 400 kg/m³. The compressive

strength obtained for FC varied between 0.91 and 23 N/mm² while for ULWC between 0.07 and 2.1 N/mm².

Differences between target and final densities were found. This may be due to the processing method, i.e. bubbles not able to resist the physical and chemical forces imposed during mixing.

Fire resistance has also been investigated as an important parameter of this ultra-lightweight concrete made with expanded polystyrene (EPS) beads potentially being used as infill material for wall panels. These infill materials should be designed with a density greater than 250 kg/m³, as the insulation failure criterion (160°C) applied during the fire tests indicated sufficient fire resistance compared with less dense lightweight concretes, demonstrating the percentage of cement being a significant parameter for fire resistance properties. In addition, an innovative ultra-lightweight concrete made with EPS beads was developed at 150 kg/m³ density, which can be a filler material for wall systems, if a suitable layer of fire insulation is added to reduce the fire effects.

A very good agreement of cohesive behavior between 3-D FEM modeling and experimental results was obtained with the simulation, i.e. the relationship between displacement and pull-out force in the simulation is similar to that observed in the experimental results of various lightweight concretes and various geometrical configurations of steel strips.

CHAPTER 1

1. Introduction

In the industrialised world, new and modern techniques and materials, such as composites, have become common in today's construction industry. These new materials are lightweight, energy efficient, aesthetically attractive and efficiently handled and erected.

Composite Structural Assemblies (CSAs) are products with performance superior to existing building elements, based on the combinations of materials such as embedded light gauge steel components, settable fillers, and coatings of sheet materials to provide a variety of finishes. The materials are combined or assembled in various ways to provide improved performance in strength and stiffness and associated properties of acoustic filtering, thermal energy conservation, vibration resistance, moisture barriers or absorption, and fire behaviour. The structural strength of these products is determined by the grade and thickness of the steel, the configuration of the internal panel components, and by the features of the infill material.

The current research focuses on novel materials for application in CSAs, and the bonding performance between steel and infill materials. This investigation studied samples of CSAs during and after loading in order to verify the properties and to develop prototypes for later production. The experiments were conducted and the results analysed in order to improve the mechanical properties of CSAs, steel plate design, bonding agents and techniques for assembling various components into usable products. Additionally, designs

were optimized through the selection of various components and additives such as foam products, lightweight aggregates, and plasticiser potentially sourced in the domestic and international market.

1.1. Background

In order to recognize the relevance of this project, it is important to understand the CSA project and its scope. The CSA project relates to the New Zealand government's investment in High Value Manufacturing Processes and the Products and Materials Portfolio for creating advanced composite materials and products, using advanced and newly developed manufacturing technologies. This CSA project was supported by an alliance between the Heavy Engineering Research Association (HERA), industrial companies NZ Steel, Dimond, Grayson Engineering, Winstone Wallboards, and Tandarra Engineering, in conjunction with the University of Auckland and the Auckland University of Technology [1].

In the 2004 Foundation for Research Science & Technology (FRST) funding round, the alliance secured government support for a six year research programme to develop a range of advanced Composite Structural Assembly products. These CSAs were building elements with performance superior to existing building elements, based on the high strength of locally manufactured light gauge steel in combination with other locally produced materials such as wood, concrete, glass-fibre, and gypsum. The novel combination of materials enabled each assembly to achieve performance standards well above those of the individual materials or existing building products [1].

The aspirations of the CSA project were to identify performance requirements for Composite Structural Assemblies, develop manufacturing concepts and processes, evaluate performance, conceptualise designs, outline pathways to market, and to establish a sector group. CSA research was initially focused toward the development of a prefabricated composite wall panel system [2].

In the CSA project, design, advanced Finite Element Modelling and prototype manufacture of a number of wall types were carried out, leading to a wide range of activities that supported the development of new construction components. In the CSA project, these were assembled in various configurations to provide load bearing structures to suit specific needs and purposes as identified by the programme. Advanced FE modelling was conducted for a number of the configurations to predict the structural performance for roof, wall and floor products including the effects of fire. Advanced Finite Element modelling was extended to thermal performance and joint behaviour between the panels. Significant research was done into developing a suitable filler medium and recipes were formulated that gave advantages to the CSA panels [2].

General tests were carried out to determine qualities of various completed structures. Full scale fire testing, press forming, roll forming, spot welding, punching, folding and clinching activities were completed and analysed and recommendations made for manufacturing of the CSA panels. Physical testing included bonding pull out tests, thermal imaging of heat flux transfer through the panel, impact testing, and load deflection tests for walls and floors in order to predict span capabilities in roof and floor panels. Various coatings applicable to steel and to fillers for both exterior and interior CSA panel use were identified, and samples were supplied by a number of different manufacturers [2].

As part of the CSA project, this current research studied the properties of infill materials, the adhesion between aerated concrete and steel, the effects of the steel geometries on bonding behaviour, and developed models to predict the behaviour of bonding between aerated concrete and galvanised steel by finite element analysis.

1.1.1. Core Materials for Wall Systems

A typical sandwich panel (Figure 1-1) is a layered structure that consists of face sheets made of metal or laminated composite and a core that is made of either metallic or low strength compressible honeycomb or foam. Foams are one of the most common forms of core material; they can be developed from a variety of synthetic polymers including polyvinyl chloride (PVC), polystyrene (PS) and polyurethane (PU). Other core materials commonly used for wall systems are honeycomb cores and wood cores. In addition, precast sandwich panels with various surface materials, using lightweight concrete as filler, are being extensively used for partition walls in building construction.

The main challenge of this research was to propose a new core material for wall panels (Figure 1.2), based on foam concrete and lightweight aggregates, to establish the bonding strength, and to develop a numerical simulation to predict the bonding strength between steel and lightweight concrete.

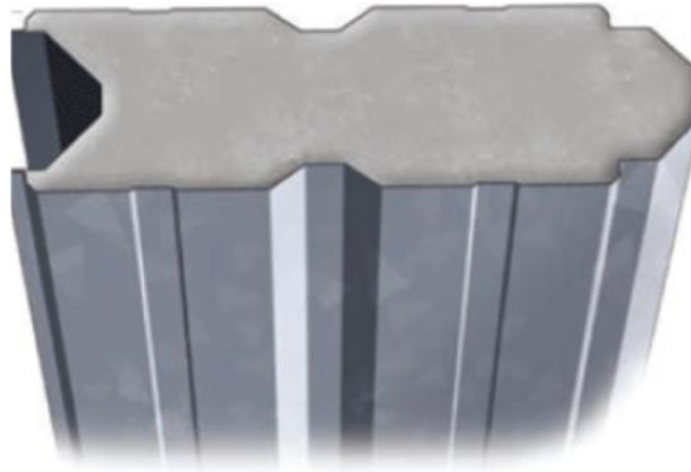


Figure 1-1 Typical composite sandwich panels

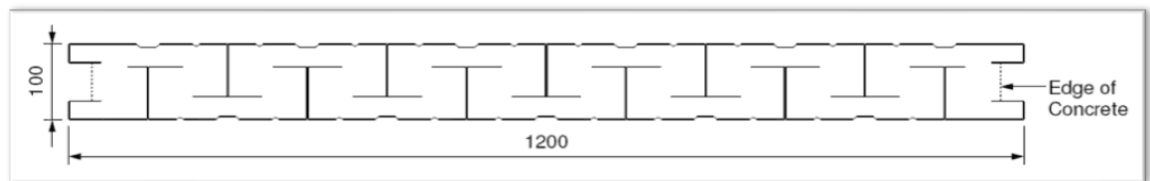


Figure 1-2 CSA sandwich wall panel

1.1.1.1. Lightweight Concrete (LWC)

Lightweight concrete has been used in industrial buildings as precast panels. To achieve adequate features, researchers have used various components and additives within concrete mixtures. Lightweight concrete can be produced by different methods, e.g. by using only fine aggregate and introducing air voids (Foam concrete) into concrete structures with chemical admixtures and mechanical foaming. Cellular concrete is also known as aerated, foam or gas concrete. There are other production methods, but the most popular way to make LWC is to add natural lightweight or artificial aggregates (Lightweight aggregate concrete) [3]. Various components such as steel fibres [3-5]

polypropylene fibres [6], pumice aggregates, silica fume [7] , and fly ash [8], can also be used in LWC.

1.1.1.2. Lightweight Foam Concrete (FC)

A foam concrete composition consists of only a cement matrix (called a paste) or a cement and sand matrix (mortar) with homogeneous voids, which can be created by introducing small air bubbles. Introduction of air voids into concrete is carried out mechanically by foaming agents which are mixed with water [9]. Many factors can affect the production of stable foam concrete, such as the foam preparation system, the foaming agent, the concrete mixture design, and the procedure for mixing foam concrete. Some by-products, such as fly ash have been added to reduce the cost, improve workability of the mix, reduce heat of hydration, and increase the long term strength [10].

The foam can be produced by either a wet or dry foam method. Dry foam is made by forcing the foaming agent solution into a foaming generator, wherein the solution is highly aerated and transformed into firm and stable foam. Dry foam is more stable than wet foam, and the air voids in the concrete have a size smaller than 1 mm in diameter, which makes it easier for blending with the base material for producing a pumpable foam concrete. The foam must be firm and stable so that it resists the pressure of the mortar until the cement takes its initial set and a strong skeleton of concrete is built up around the voids filled with air.

1.1.2. Facing Materials

Although facing materials were not addressed predominantly in this research, a general description is included in this section to enable understanding of the main features of metal face materials commonly used in wall panels.

These metal sheets have variable thickness, but they must be of certain strength in order to fulfil manufacturing and functional requirements, such as roll-forming, bending, coping with local loads and maintaining adequate resistance to corrosion and fire [11]. Panel facings can be made of metal sheets, especially steel (stainless steel, galvanized steel) or aluminium sheeting.

1.2. The Research Question

Composite Structural Assemblies are products based on the high strength of light gauge steel in combination with other materials such as wood, concrete, glass-fibre, gypsum, honeycomb and synthetic polymers (including polyvinyl chloride, polystyrene and polyurethane). Previous studies have established that the rigid faces, which are separated by the lighter core, have usually a high modulus of elasticity. This core must have shear stiffness sufficient to carry the shear force. The core also acts as a highly effective thermal insulation layer [11].

Thus, the current research aims to develop a novel infill material for application in wall systems, based on existing cementitious materials.

Additionally, experimental research has shown the importance of the bonding behaviour of the contact zone between steel and lightweight concrete. The interface between concrete and steel is the principal cause for both the strength and the deterioration or damage of structures, when the composites are under stresses during fabrication, transport, erection and use. Thus, this study investigates the bonding performance and analyzes it through pull-out tests to provide data for the FE Modelling of CSAs. Because the bonding is a general problem for wall panel designs, in particular, and for other uses of concrete that employ a steel to concrete contact zone, this research undertakes an analysis of the influence of various steel strip designs and geometry on bonding behaviour and the influence of the mechanical properties of concrete. With the obtained results, the research enables the development of a numerical simulation based on bonding tests of lightweight and foam concrete.

Experimental investigations of bonding and infill material, analysis of the outcomes, and development of a simulation contribute novel knowledge about building materials. At the same time these investigations provide solutions for composite structural assemblies.

1.3. Objectives of the Study

This research aims:

- To develop novel materials, propose one or more fillers for wall systems, and improve existing design methods for lightweight concrete.

- To establish experimentally the bonding strength and to apply numerical simulation using finite element analysis in order to describe and predict bonding strength between steel strips and foam concrete specimens.

1.4. Outline of the Thesis

The thesis consists of six chapters, namely: introduction, literature review, methodology, test results and discussion, proposed FE model, and, finally, conclusions and recommendations.

Chapter 1: The first chapter describes the background of this investigation, the objectives, and the outline of the work covered in this investigation.

Chapter 2: This chapter provides an overview of previous research related to infill materials for Composite Structural Assemblies and bonding phenomena. This chapter reviews three bodies of literature pertaining to this study. First, it discusses several studies of lightweight concrete. Following that, a conceptual framework, with literature that particularly focuses on the components of the wall panel, is described in order to give a general overview of these wall systems. Finally, the literature discussing of bonding phenomena is explored to provide understanding of the key elements of this problem.

Chapter 3: This chapter includes the appropriate methodology for investigating lightweight concrete and bonding to develop novel infill materials.

Chapter 4: This chapter contains an experimental study for improvement of the mechanical properties of new concrete materials in conjunction with steel. Experiments are carried out to optimize the experimental design, develop

experimental models, compare the properties with original materials and investigate the influence of various components. The bonding performance analysed through pull-out tests provides the main data for the FE analysis of CSAs. The analysis of the influence of various steel strips with and without holes is studied to understand bonding behaviour of the concrete and steel. A numerical simulation, based on bonding tests of lightweight and foam concrete, was developed in Chapter 5 in order to predict the performance of the bond between steel and lightweight concrete. The pull-out test results and discussions are also presented in this chapter.

Chapter 5: This chapter contains the numerical modeling to predict the performance of the bond between steel and lightweight concrete. It focuses on the development of a finite element model that simulates the bonding behaviour between steel plates and lightweight concrete. The numerical model is validated against the experimental results available in the current study. The model is used to predict the effect of geometry of steel strips that have a significant influence on the bonding behaviour either for testing or industrial purposes.

Chapter 6: This final chapter presents conclusions reached upon completion of the study. The chapter also presents several recommendations for future investigation with regards to concrete aggregates, wall panels, pull-out tests, and for utilizing these materials in future construction.

CHAPTER 2

2. Literature Review

2.1. Introduction

This chapter provides an overview of previous research related to infill materials for Composite Structural Assemblies (CSAs) and to the bonding phenomena associated with them. This chapter reviews the literature in order to provide a conceptual framework that includes the theoretical foundation of the structural behavior of CSAs and the previous research, which must be taken into account when analyzing novel infill materials for wall or floor panels.

This chapter reviews three bodies of literature pertaining to this study. First, several studies of lightweight concrete are reviewed. After that, a conceptual framework, which particularly focuses on the components of wall panels, is described in order to give a general view of these wall systems. Finally, bonding phenomena are also explored to provide an understanding of the key elements of the bonding problem. These three issues, lightweight concrete, components, and bonding phenomena, serve as the framework for developing novel materials and, in a later chapter, to propose one filler for wall systems.

2.2. Lightweight Concrete

The majority of studies about lightweight concrete have analyzed, by means of experimental tests, the behaviour of lightweight concrete made from diverse components.

Lightweight concrete can be classified into three groups based on their use and physical properties: for structural use, for both structural/insulating purpose, and for insulating. Structural lightweight concrete normally contains lightweight aggregates, such as shales, clays, slates, expanded slag, expanded fly ash, and natural porous volcanic stones [12]. Structural/insulating dual purpose concrete may incorporate air contents and structural lightweight aggregates, or they may be produced with both structural and insulating lightweight aggregates. Lightweight insulating concretes are very light, but not appropriate for structural use, as reported by Holm and Ries [12]. Other authors [2, 3] classify lightweight concretes based on their properties, as shown in Table 2.1 [13], and a full spectrum of densities of lightweight concretes is available in Figure 2-1 [14].

Table 2.1 Classification of lightweight concretes [13].

Property	Structural	Structural/insulating	Insulating
Compressive strength [MPa]	>15.0	>3.5	>0.5
Coefficient of thermal conductivity [W/mK]	-	<0.75	<0.30
Approximate density range [kg/m ³]	1600-2000	<1600	<<1450

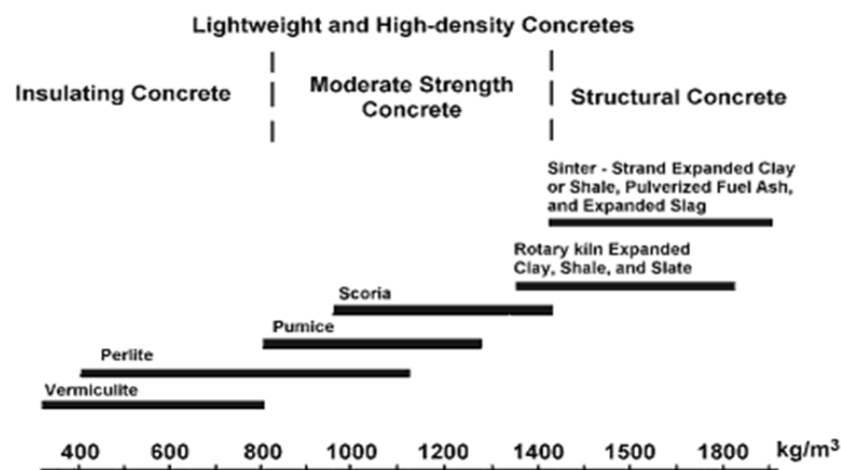


Figure 2-1 Typical ranges of densities of concretes made with various lightweight aggregates [14].

Several investigations in the past aimed to understand the behaviour of lightweight concrete (LWC). These studies have considered various components, namely pumice aggregates [15, 16], scoria [17, 18], silt [19], expanded polystyrene spheres (EPS) [20], silica fume [21], fly ash [8, 22], steel fibers [3-5], polypropylene fibers PVA (polyvinyl alcohol) fibers [23], and zeolite [24] to achieve adequate features in the concrete mixtures. Some of these research results follow below.

Yasar et al. [15] developed a structural lightweight concrete made with basaltic pumice as aggregate and fly ash as mineral admixtures. They obtained a lightweight concrete with 1850 kg/m^3 dry unit weight, and 25 MPa cylinder compressive strength, containing 20% of fly ash as a replacement of the cement by weight basis. It was found that the use of fly ash seems to be necessary for the production of cheaper and environment-friendly structural lightweight concrete.

Gündüz [16] studied the use of pumice lightweight aggregate to produce non-structural lightweight concrete. This research showed that lightweight concrete can be produced by using fine, medium and coarse pumice aggregate mixes. The dry unit weights obtained was between 988 and 1272 kg/m^3 . It was found that some properties (water absorption, drying shrinkage and thermal conductivity) decreased in value with a higher range of different pumice aggregate/cement ratios.

Khandaker and Hossain [17] developed a structural lightweight concrete using scoria as aggregate. All scoria concretes used scoria aggregate replacement within the range of 50% and 100% of coarse aggregate by volume. The strength

developed was over 15 MPa and air dry density between 1850 and 2150 kg/m³. They propose that scoria concrete can be used in building construction as an energy saver because of its good heat-insulating characteristics.

Kılıç et al. [18] studied a structural lightweight high strength concrete made with basaltic-pumice (scoria) as lightweight aggregate. The control lightweight concrete mixture was modified in three different ways by replacing 20% of the cement with fly ash, by replacing 10% of the cement with silica fume, and finally a ternary lightweight concrete mixture was also prepared by replacing 20% of cement with fly ash and 10% of cement with silica fume. Air dry unit weights were between 1800 and 1860 kg/m³. Test results showed that the use of mineral additives (fly ash, silica fume, natural pozzolan, metakaolin and calcined clay) seems to be necessary to produce structural lightweight high strength concrete. They also recommended a mixture composition with cement, fly ash and silica due to its satisfactory strength and environmental friendliness.

Wang and Tsai [19] studied physical and mechanical properties of lightweight aggregate concrete made from dredged silt. In this study, the concrete was filled using 60% of lightweight aggregate and fly ash to replace 15% of sand as well as slag to replace 5% of cement. Unit weights of the concrete samples were between 1637 to 2007 kg/m³. The hardened properties, such as the compressive strength, ultrasonic pulse velocity and thermal conductivity were found to decrease with increasing water/binder ratio but rise when the density of aggregate is increased. It was found that dredged silt can help to improve durability of lightweight aggregate concrete.

Le Roy et al. [20] developed lightweight concrete (LWC) made from expanded polystyrene spheres (EPS) as lightweight aggregates. The concrete was prepared with water, superplasticizer, silica fume, sand and cement as components. Unit weights of the concrete samples were between 600 and 1400 kg/m³. Proper precautions were taken to inhibit the material's hydrophobia and to reduce the electrostatic effects of EPS spheres. The experimental results show that the compressive strength of the concrete is increased by reducing the EPS sphere size. They proposed the inclusion of new components to prepare other cement-based materials, such as hollow glass microspheres, which would probably increase the strength of the concrete.

Chen and Liu [21] investigated the effects of mineral admixtures including fly ash, blast furnace slag and silica fume on workable high strength lightweight concrete. The results showed that both blast furnace slag and silica fume can improve the concrete strength; however, it reduces the workability of the concrete. According to the results of the study, fly ash improves the workability of the mixture, but affects negatively the homogeneity of the mixture.

Bekir and Canbaz [8] analysed the effect of different fibers on the mechanical properties of concrete containing fly ash. They found that addition of fly ash to the mixture may improve the workability and strength losses caused by fibers.

Jones and McCarthy [22] investigated the use of unprocessed low-lime fly ash in foam concrete, as a replacement for sand. Densities of the foam concrete were between 1000 to 1400 kg/m³, while cube strengths were from 1 to 10 N/mm². The research results showed that this type of fly ash can significantly improve rheology and compressive strength development, and provide

immunity to sulfate attack. It was also found that there was a need to increase considerably the amount of foam required to achieve the target density, due to the high carbon content of this fly ash.

Akin et al. [3] studied the effect of steel fibers on the mechanical properties of pumice aggregate concrete. Different pumice ratios (25%, 50%, 75%, and 100%) and steel fiber ratios (0.5%, 1.0%, and 1.5%) by volume were used in the mixtures instead of natural aggregate. Lightweight concrete with unit weights ranging between 1450 to 2140 kg/m³ were tested. The test results showed that increasing pumice aggregate ratios decrease the density and mechanical properties of the concretes, whilst the increase of steel fiber ratios in the mixtures enhance unit weight, compressive strength, splitting-tensile strength and flexural strength of concretes up to 8.5%, 21.1%, 61.2% and 120.2% respectively. In contrast, modulus of elasticity and deformation capability was decreased with an increase of pumice aggregate and steel fiber ratios in the mixture.

The optimization of fibre size, fibre content, and fly ash content in hybrid polypropylene-steel fibre concrete with low fibre content based on general mechanical properties of the concrete was investigated by Qian and Stroeven [4]. The research results show that fly ash content can uniformly disperse fibres. Compressive strength was significantly influenced by adding small fibre types, but the splitting tensile strength was only slightly affected. While a large fibre type gave rise to opposite mechanical effects.

The effect of steel fibres on strength and ductility of normal and lightweight high strength concrete was investigated by Balendran et al. [5], by adding steel fibres

to lightweight aggregate concrete and limestone aggregate concrete. The density of the concrete mixes varied between 2015 and 2470 kg/m³ and the fibre content was 1% by volume. The experimental results showed that compressive strength was slightly affected by a low content of fibre, while splitting tensile strength, flexural strength and toughness improved substantially after tests.

A study was undertaken by Arisoy and Wu [23] focusing on mix design of PVA (polyvinyl alcohol) fiber reinforced lightweight concrete (FRLWC). They developed this lightweight concrete obtaining high flexural strength, high flexural ductility, and excellent toughness. The densities of the lightweight concrete varied between 800 to 1600 kg/m³.

Natural zeolite as an aggregate and bubble-generating agent in autoclaved aerated concrete (AAC) production was studied by Karakurt et al [24]. The usage of natural zeolite has beneficial effects on the physical and mechanical properties of AAC. The test results demonstrated that the optimum replacement amount was 50% for samples with a compressive strength, unit weight and thermal conductivity of AAC as 3.25 MPa, 553 kg/m³ and 0.1913 W/mK respectively. It was found that calcined zeolite acts as both an aggregate and a bubble-generating agent.

Although numerous investigations have been made of LWC, to date, there are only a few studies available about ultra-lightweight concrete. The current research is focused on insulating concretes, as they have sufficient strength for the intended application, low densities and better thermal insulation.

2.3. Foam Concrete

Foam concrete can be defined as either a cement paste or mortar that contains stable air or gas cells uniformly distributed in the matrix by suitable foaming agents. This aerated concrete possesses excellent thermal insulation properties, high flowability, low density and controlled low strength. However, some uncertainty factors have also been identified for preparing a stable concrete mix, namely the foam preparation system, the kind of foaming agent, and foam concrete mix preparation, as reported by Ramamurthy et al. [10], and Kearsley and Mostert [25] in their study about concrete mixture design.

Narayanan and Ramamurthy [26] classified the investigations of the properties of aerated concrete in terms of physical, chemical, mechanical and functional performance characteristics (i.e. thermal insulation, moisture transport, durability, fire resistance and acoustic insulation). They found that the properties of aerated concrete are influenced by the density, which is to be specified along with the moisture content.

Kunhanandan and Ramamurthy [9] evaluated the relationships between pore structure parameters and foam concrete properties. They found that volume, size and spacing of air voids influence strength and density of the aerated concrete. In addition, Kearsley and Wainwright [27] investigated the effect on the porosity and permeability of foam concrete by replacing volumes of cement with fly ash. They found that porosity depended on the dry density of the concrete, and permeability increased with increasing porosity and ash content [27]. Thus, this current research project seeks to verify properties of samples and investigates the influence of various components on low density concretes.

There is no standard method for designing an aerated concrete mix, and most of the methods proposed [25, 28-31] can determine batch quantities only if the mix proportions are known. For instance, ASTM C 796-97 provides an equation to determine the dry density of foam concrete which is written in terms of weight of cement and volume of batch. Otherwise, Kearsley and Mostert [25] proposed two equations to determine target casting density and volume of foam concrete, which are based on foam volume and cement content. The current research deals with the mix proportion design of aerated concrete to verify these equations and to minimize undesirable factors during the mixing process.

The foam can be produced by either a wet or dry foam system, as reported by Ramamurthy et al. [10]. Wet foam is produced by spraying a solution of a foaming agent over a fine mesh. Stable dry foam is made by forcing the foaming agent solution into a foam generator, where the solution is highly aerated and transformed into a firm and stable foam. This stable foam must resist the pressure of the cement based slurry until the concrete structure is set and strong enough to maintain the overall structure [10]. Otherwise, it may negatively influence the physical (drying shrinkage, density, porosity and air void system, as well as sorption) and mechanical (compressive and tensile strength, and modulus of elasticity) target properties of the foam concrete. As a result, the density, strength or other properties of the concrete might be significantly different from the desired properties, and adversely affected by these factors.

Kunhanandan and Ramamurthy [32] studied the influence of filler type and fineness of sand on the properties of foam concrete made by using pre-foam foam. They found that the consistency of the mixture for achieving pre-foam

foam concrete of a designed density depends on the filler type. In addition, the flowability of foam concrete was influenced by the foam volume [32]. Thus, the production of a stable foam concrete mix depends on many factors, such as kind of foaming agent, adequate mixing process, uniform air-voids distribution, material selection, mixture design strategies, and the production technique of foam concrete, as reported by Ramamurthy et al. [10]. The current research project evaluates chemical products that can produce firm and stable foam.

An important property of foam concrete is its density, which can be measured by the moisture condition of the material. This moisture condition includes as-cast density (wet density or plastic concrete density), air-dry density (at a stated age and curing condition), and oven-dry density, as reported by Fouad [33]. Ramamurthy et al. [10] stated that compressive strength decreases exponentially with a reduction in density of aerated concrete. Kearsley proposed a mix composition of foam concrete with a high fly ash content [25], which considered a methodology of foam concrete design to achieve an adequate compressive strength and density.

However, many factors can influence the strength of cellular concrete. Ramamurthy [10] stated, "*there is a need to investigate compatibility between foaming agent and chemical admixtures, use of lightweight coarse aggregate and reinforcement including fibres, for enhancing the potential of foam concrete as a structural material*". Although numerous investigations have been undertaken about lightweight aggregate concrete [5, 7, 34-36] and foam concrete [9, 10, 37], quantitative information on ultra-lightweight concrete [38] is extremely sparse. Some of these studies are summarized below.

Wu et al. [34] studied experimentally the mix proportion design and workability of self-compacting lightweight concrete (SCLC). They used expanded shale as lightweight aggregate. The compressive strength and density was 42.6 MPa and 1879 kg/m³ for SCLC1, while for SCLC2 it was 50.1 MPa and 1920 kg/m³. The results show that the two SCLC had good workability and can be used for the design of practical concrete structures.

The contribution of hybrid fibers to properties (workability, mechanical and shrinkage) of high-strength lightweight concrete was investigated by Chen and Liu [7]. The density of this LWC was 1830 kg/m³. It was found that the sedimentation of aggregates is reduced during mixing and the uniformity of the mix is improved by adding fiber to the lightweight concrete mixture; in contrast, the slump value is reduced. In addition, adding hybrid fibers to the mix improved the mechanical properties and reduced the brittleness of lightweight concrete and restrained the long-term shrinkage.

Kayali et al. [35] investigated the effect of polypropylene and steel fibers on high strength lightweight aggregate concrete. The fine aggregate (sand) was partially replaced by fly ash in the lightweight concrete. The density of this lightweight aggregate concrete varied between 1860 to 1940 kg/m³. Polypropylene fiber addition increased the indirect tensile strength and the modulus of rupture in comparison with sintered fly ash. Steel fibers also increased significantly the indirect tensile strength and the modulus of rupture. However, steel fiber additions decreased the modulus of elasticity.

Kan and Demirboğa [36] developed a novel material for semi-structural lightweight concrete production, by using recycled waste expanded polystyrene

foam (EPS). Modified waste expanded polystyrene (MWEPS) aggregates were obtained by keeping waste EPS foams in a hot air oven at 130 °C for 15 min. Natural aggregate was replaced by MWEPS aggregate at the levels of 0%, 25%, 50%, 75%, and 100% by volume. Lightweight concrete densities obtained were about 900 to 1700 kg/m³. The compressive strengths of MWEPS concrete varied from 12.58 MPa to 23.34 MPa respectively. The current research seeks to develop lighter lightweight concrete, based on these previous investigations.

Othuma [37] studied the thermal properties of lightweight foam concrete (LFC) at high temperatures and its application to composite walling systems. Mechanical properties of unstressed LFC were obtained from compression and bending tests at elevated temperatures for LFC densities of 650 and 1000 kg/m³. A composite wall panel was tested, which consisted of two outer skins of steel sheeting (0.4mm and 0.8mm thickness) with LFC core material. The results indicate that the proposed panel system, using 100mm LFC core and 0.4mm steel sheeting, has appropriate load carrying capacity to be used in residential construction for up to four floors.

Laukaitis et al. [38] investigated the effect of recycled polystyrene waste as well as blown polystyrene granules on cement composite properties. The density of this foam composite was 150–170 kg/m³, the thermal conductivity coefficient 0.06–0.064 W/mK, and the compressive strength 0.25–0.28 N/mm². The size and shape of granules used have a significant effect on bonding between foam cement concrete and polystyrene granules. Strength and thermal conductivity of the composite depend on its density and the type of granules used.

The majority of the previous researches obtained lightweight concrete densities between 600 to 1900 kg/m³. The lightest LWC (150 kg/m³) was developed by Laukaitis et al. [38], by using recycled polystyrene waste and blown polystyrene granules. They analysed strength and thermal properties as well as interactions between three different kinds of polystyrene granules with a composite matrix. EPS granules are a combustible material at higher temperature, and its use in LWC can increase the fire risk. However, the fire performance of EPS products was not quantified in this study. Therefore, fire resistant properties as an important parameter of lightweight concrete will be analysed in the current research.

There have been few studies concerning ultra-lightweight concrete as infill material for composite panels. Hence, the current research attempts to discover the properties and abilities of foam concrete and ultra-lightweight concrete as infill materials for wall systems. This study analyzes the properties of lightweight foam concrete in terms of physical (density), mechanical (compressive strength) and functional characteristics (thermal conductivity and fire resistance) by means of experimental investigation. The investigation studied and designed mixture compositions to create a novel infill material for wall panels.

2.4. Composite Structural Assemblies (CSAs)

Modern sandwich panels consist of two strong facings separated by and bonded rigidly to the centre core of lighter and weaker material. The sandwich elements combine the positive properties of facings, which carry both a tensile

and a compressive load, while the core separates the face skins and carries the shear loads [11].

The use of sandwich panels in the construction of building structures offers many advantages, as it leads to structures that are lightweight, cost effective and durable. These products are very popular because they are easy to install and have good thermal and acoustic properties [39]. A combination of different facing and infill materials can be used to build sandwich panels, such as steel or aluminium sheet and rigid foams, cork, balsa wood, rubber, solid plastic material, honeycombs of metal, and metal [40, 41]. Facing materials must resist local loads and have adequate resistance to corrosion and fire.

In spite of the advantage of plastic foam materials being lightweight, they can be severely degraded under the thermal conditions caused by fire due to high flammability and poor fire resistance of the polymer foam core [11, 42, 43]. Laminated glass fibre reinforced panels were submitted to severe fire conditions to investigate the thermal response for these panels by furnace fire testing and thermal modeling, as reported by Dodds et al. [44]. In their investigation they used an insulation failure criterion for the furnace fire tests, which is utilised in the current research as well. Thus it is important to consider composite panel fillers that can act as an effective thermal insulation layer and provide an additional barrier for fire effects; this filler must be bonded with the faces of the panel.

The current research has focused on finding an insulating concrete which can be used as a potential infill material for composite systems, by verifying its

properties, and assessing the influence of its components on low density concretes.

2.5. Bonding Phenomena

The bond between concrete and steel elements is one of the most important properties contributing to the successful functioning of a composite panel [45]. The main contribution to bond strength comes from the chemical adhesion, and the friction resistance occurring between the steel facing and concrete as a result of the surface effects. Composite structures made of various materials [46], e.g. sandwich panels, can fail in several ways depending on material properties of components, design methods and loading cases, but most important is the co-operation of all elements. The lack of compatibility between elements leads to bond failure, sliding of reinforcement bars and/or steel strips, local deformations, and finally cracking. Destructive measurements of the shear strength through pull-out [47] and push-in tests are commonly used methods to assess the quality of a connection between steel elements and fillers, e.g. concrete or polyurethane foams. The bond behaviour can be characterized by the mode of failure, bond strength, and bond–slip relationships [48], as reported by Tang et al. Thus, experiments, which can support the understanding of the fundamental failure phenomena between components of composites, are essential for establishing bonding strength behaviour.

There are several ways to increase bonding strength between elements of composite panels, such as applying adhesives [49, 50] or welding small elements/spots or even bars to a surface, but they are usually not cost-effective

and sometimes not applicable to many situations. They require extremely large amounts of elements, which have to be folded, punched and/or combined in order to increase bonding strength [46]. There are a few studies of structural bond properties between lightweight concrete and steel bars through pull-out test, e.g. [51]. This study analysed the use of solid waste oil palm shells as coarse aggregates for the production of structural lightweight concrete, and conducted pullout test on both plain and deformed steel bars. It was found that the experimental bond strength of this lightweight concrete behaves similar to other structural lightweight aggregate concretes.

Most of the previous investigations about bonding behavior focused mainly on experimental and theoretical studies of shear stress between reinforcing bars and concrete specimens [47, 52-58], plastic bars and concrete samples [59], but not directly on steel strips, which are applicable to this project.

In addition, Pokharel and Mahendran [40], Khalfallah and Ouchenane [60] , and Schilde and Seim [50] have conducted Finite Element Analysis (FEA) of reinforced concrete structures or sandwich panels. The common object of these studies has been to produce a reliable analysis that takes into account the effective bond behaviour between reinforcing bars or steel sheets and concrete specimens.

Other authors [61] developed a new methodology to build 3D non-linear Finite Element Models (FEM) to simulate the longitudinal slip mechanics of composite slabs in pull-out tests. These previous studies of pull-out tests may be useful for proposing a procedure to assess the bonding behavior and develop a FE model for the current research.

In spite of numerous investigations that have been made of pull-out experiments, quantitative information about bonding behavior between lightweight concrete and steel strips, and FE modeling between steel and concrete materials is practically non-existent. Thus, further investigations of these materials and their bonding are necessary in order to obtain a comprehensive understanding that would provide the necessary data in order to develop a numerical simulation for bonding strength between lightweight concrete and steel strips.

2.6. Summary

This literature review reports about experimental studies of lightweight concrete, and especially structural lightweight concrete, which were carried out using lightweight aggregates or foam agents in the concrete mixtures. The influence of diverse components, such as steel fibers, polypropylene fibers, pumice aggregates, silica fume, fly ash, polypropylene, and other materials on compressive, splitting, tensile, bending and bonding strength has been studied, inconclusively in some areas, as explained in this chapter. Additionally, the lightweight concrete properties themselves depend on many factors, such as mixture proportions, age, curing method, moisture content, the physical and chemical characteristics of component materials, method of mixture and distribution of fibers.

The current research seeks to investigate insulating concrete as a potential infill material for wall systems, to examine properties of samples, and to investigate the influence of various components on low density concretes. In addition, this

study aims to verify equations in order to design the mix proportion of aerated concrete and minimize the effect of undesirable factors during the mixing process. This investigation also evaluates chemical products that may produce firm and stable foam, and analyses properties of lightweight foam concrete in terms of physical, mechanical and functional characteristics through experimental investigations. Finally the research studies bonding behavior between aerated concrete and steel strips in order to obtain a comprehensive understanding that would provide data to develop a numerical simulation for bonding strength between both materials.

The search of the literature reveals that very little quantitative information about bonding behavior between lightweight concrete and steel strips is available, and FE modeling between both materials is practically non-existent. Thus, the current study proposes to supply such information by developing eventually one infill material for wall panels and determining the adhesion properties. This study also takes a novel approach to discovering quantitative results by studying pull-out strength of various lightweight insulating concrete mixes and various geometrical configurations of steel strips suitable for wall panels.

CHAPTER 3

3. Methods

3.1. Introduction

The main research goals of this project are to develop novel materials, i.e. one or more fillers for wall systems, improve existing design methods for lightweight concrete, and attempt to describe bonding processes between steel and concrete specimens experimentally and by applying FE methods.

Different formulae of fillers have been investigated to obtain the required lightweight concrete mechanical properties, using diverse components, such as plasticizer, lightweight aggregates, foaming agents, and mineral admixtures.

Analyses of the results for improvement of the mechanical properties of new materials have been undertaken. Experiments were carried out to optimize the experimental design, develop experimental models, verify properties of samples and investigate the influence of various components.

In addition, a numerical simulation was conducted in order to predict the adhesion between steel and lightweight concrete based on bonding trials.

Finally, the results of investigations of the bonding behaviour between lightweight concrete and steel strips enable a better understanding of the use of lightweight concrete in wall panels.

This chapter describes the various methodologies and pieces of equipment used throughout the research project.

3.2. Experimental Investigation

The most appropriate methodology for investigating lightweight concrete and bonding is experimental research with the aim to develop a model of bonding behaviour between concrete and steel commonly used in wall panels. Thus, the research should examine the properties of infill materials, the effects of steel strip geometries on the adhesion of steel and lightweight concrete, and predict the behaviour of bonding between aerated concrete and galvanised steel by FE methods.

Air voids are introduced into the concrete structure through mechanical means either by mixing a foaming agent with the water and aerating to form foam before the liquid is added to the mix, or by mixing foaming agent directly with the matrix [9]. The foam concrete composition consists as only a cement matrix (named paste) or a cement and sand matrix (mortar) with homogeneous voids, which can be created by introducing small bubbles.

3.2.1. Foam Concrete Mixture Design

This study considers a methodology of lightweight concrete design (as explained below) to achieve adequate compressive strength and density for infill materials for wall panels. Foam concrete mixtures were prepared at 800, 1000, and 1200 kg/m³ density, by using stable foam concrete compositions, which were designed based on Kearsley's and Mostert's investigations [25]. Properties of this foam concrete were analysed for the two following qualities: density and compressive strength, based on the standard testing methods for physical and mechanical properties.

In addition, four separate mixtures of ultra-lightweight concrete were prepared at 400, 250, 200 and 150 kg/m³ density, by using Expanded Polystyrene beads (EPS) and foam concrete. Four properties of this ultra-lightweight concrete were analysed, such as density (physical property), compressive strength (mechanical property), fire resistance and thermal conductivity (functional characteristics). To obtain these densities, the quantity of EPS beads was varied in the EPS concrete mixes to reduce the concrete density of a lightweight concrete from initially 700 kg/m³ to the required target densities.

Experiments showed that by using a theoretical design method (Kearsley's and Mostert's investigations [25], it is possible to predict the compressive strength and density for lightweight concrete mixtures, as shown in equations 3.1 and 3.2.

$$\delta m = x + x(w/c) + x(a/c) + x(s/c) + x(a/c)(w/a) + x(s/c)(w/s) + RD_f V_f \quad (3.1)$$

$$1000 = x/(RD_c) + x(a/c)/RD_a + x(s/c)/RD_s + x(a/c)(w/a) + x(s/c)(w/s) + V_f \quad (3.2)$$

Where:

δm	–	target casting density (kg/m ³)
x	–	cement content (kg/m ³)
w/c	–	water/cement ratio
a/c	–	ash/cement ratio
s/c	–	sand/cement ratio
w/a	–	water/ash ratio
w/s	–	water/sand ratio
V_f	–	volume of foam (l)
RD_f	–	relative density of foam
RD_c	–	relative density of cement
RD_a	–	relative density of ash

RD_s – relative density of sand

After an initial analysis, it was possible to simplify and suggest two new equations, 3.3 and 3.4, which give the similar results as Kearsley's and Mostert's equations [25]. Generally, the sum of the material weights per m^3 should be equal to the required density, as shown in equation 3.3, and the volume of foam can be obtained from equation 3.4.

$$\text{Density} = C+W+LWA+V_f \cdot RD \cdot 1000 \quad (3.3)$$

$$V_f = (1 - \Sigma V_i) \cdot 1000 \quad (3.4)$$

Where:

- C – cement content, kg/m^3
- W – water content, kg/m^3
- LWA – lightweight aggregate content, kg/m^3
- ΣV_i – total component volumes, m^3

3.2.2. Materials and Mixture Composition

Ordinary Portland Cement (OPC) was used for all the ultra-lightweight and foam concrete mixtures. The chemical composition of the cement and fly ash (FA), which were obtained from the Golden Bay Cement company [62], are given in Table 3.1. The lightweight aggregate for ultra-lightweight concrete used in this study consisted of EPS beads of 1 mm diameter. A superplasticizer Sikament HE200 (Appendix A) was used only for ultra-lightweight concrete of a density lower than 250 kg/m^3 , at 5 ml of plasticizer per kg of cement. The

superplasticizer was used to improve the workability of the ultra-lightweight concrete (ULWC).

Table 3.1 Chemical composition of mineral admixture

Composition [%]	OPC	FA
Silicon dioxide (SiO_2)	22.8	40.1
Aluminum oxide (Al_2O_3)	4.2	20.4
Iron oxide (Fe_2O_3)	2.3	10.1
Calcium oxide (CaO)	64.8	19
Magnesium oxide (MgO)	1.0	3.4
Sodium oxide (Na_2O)	0.19	2.1
Potassium oxide (K_2O)	0.49	0.5
Sulfur trioxide (SO_3)	0.42	0.8
Titanium dioxide (TiO_2)	-	1.5

Foam concrete (FC) mixtures were prepared with densities of 800, 1000, and 1200 kg/m^3 , and ultra-lightweight concretes (ULWC) were prepared with densities of 400, 250, 200, and 150 kg/m^3 , by using stable foam concrete compositions, which were designed based on equations 3.3 and 3.4. The mix proportions for foam concrete are shown in Table 3.2.

Table 3.2 Mix proportions.

No	Target Density [kg/m^3]	Cement [kg/m^3]	Ash [kg/m^3]	Water [l]	Foam, [kg/m^3]	EPS [kg/m^3]	Superplasticizers [ml/m^3]
FC1	800	382.92	191.46	191.46	33.67		
FC2	1000	485.95	242.98	242.98	32.76		
FC3 and FC4	1200	589.00	294.50	294.50	21.56		
ULWC1	400	248.50		124.25	20.11	7.28	
ULWC2	250	151.49		75.75	12.24	10.93	757.45
ULWC3	200	118.83		59.41	9.62	12.14	594.15
ULWC4	150	86.43		43.22	6.98	13.36	432.16

3.2.3. Preparation of Foam Concrete

The foam concrete was obtained by mixing cement, water, and foam in a mortar mixer. The foam was prepared with a foam generator at a density of 56 kg/m^3 . The Portland Cement and water were mixed for 5 minutes. Finally, the foam was added to the mortar, followed by an additional 2 minutes of mixing.

To prepare the foam, Ultrafoam (Appendix B) was used as the foaming agent and Quick Gel as the viscosifier (Appendix C). These were mixed with water in the foam generator, until the foam bubble size was uniform and stable (usually 2 minutes). Then, the foam was added to the cement matrix while under stir, with continual mixing for 1 to 2 minutes. When the mix of foam and the cement matrix was uniform, the prepared foam concrete was poured into the test mold with slight vibrations to fill up the mold completely.

Under standard conditions, specimens were demoulded after 24 hours and then moist cured in a standard curing room for a further 28 days, in order to test the samples with a standard testing machine.

3.3. Test Methods

The main standard test methods for ultra-lightweight concrete and foam concrete are described in this chapter, such as the evaluation of density (physical properties), compressive strength (mechanical properties), and bonding behaviour between lightweight concrete and steel. Functional characteristics for ultra-lightweight concrete were investigated, such as fire resistance and thermal conductivity.

3.3.1. Compressive Strength

Before mixing, stable foam concrete compositions were designed based on equations 3.3 and 3.4. Standard cylinders of 100 mm diameter and 200 mm height were used for the compressive strength tests, which were carried out in a testing machine of 100 kN capacity at a loading displacement rate of 0.1 mm/s. The reported compressive strength results are the mean values of three tests.

Three cylinders were tested for compressive strength after 28 days according to ASTM C39 Standard Test Method for Compressive Strength of Cylindrical Concrete Specimens [63]. All specimens were cured in a fog room for 28 days. At the end of this curing period destructive tests were applied to all of the concrete specimens to determine the mechanical properties of lightweight concrete. The outcomes of these experiments were analysed by comparing target density (1200, 1000, 800, 400, 250, 200 and 150 kg/m³) with real density of the tests, to reach the optimum mechanical properties of the targeted materials. These results are discussed in Chapter 4.

3.3.2. Density

Fouad [64] classified foam concrete density depending on the moisture condition of the material. These densities are: wet density or plastic concrete density, air-dry density (at a stated age and curing conditions), and the oven-dry density.

Wet density is required for casting control purposes. Usually, the air-dry density of cellular concrete can be close to 80 kg/m³ less than its wet density, as

reported by Fouad. Thus, after mixing was completed, the wet density of the foam concrete was checked to assure that it was close to the required air-dry density (1200, 1000, 800, 400, 250, 200, and 150 kg/m³).

The air-dry density of the foam concrete was obtained by dividing the weight of the cylinder by its volume. The weight of the cylinders was measured by using a digital balance scale, while the dimension of the cylinders was measured with a caliper. For this research, in total, 39 samples of ultra-lightweight concrete and 15 samples of foam concrete were tested.

3.3.3. Fire Resistance of Ultra-lightweight Concrete

Ultra-lightweight concrete samples were prepared at densities of 400, 250, 200, and 150 kg/m³. After 7 days, a small scale sandwich panel with a square footprint of 100 mm² was placed on top of a heating unit, as shown in Figure 3-1 and Figure 3-2.



Figure 3-1 The heating unit

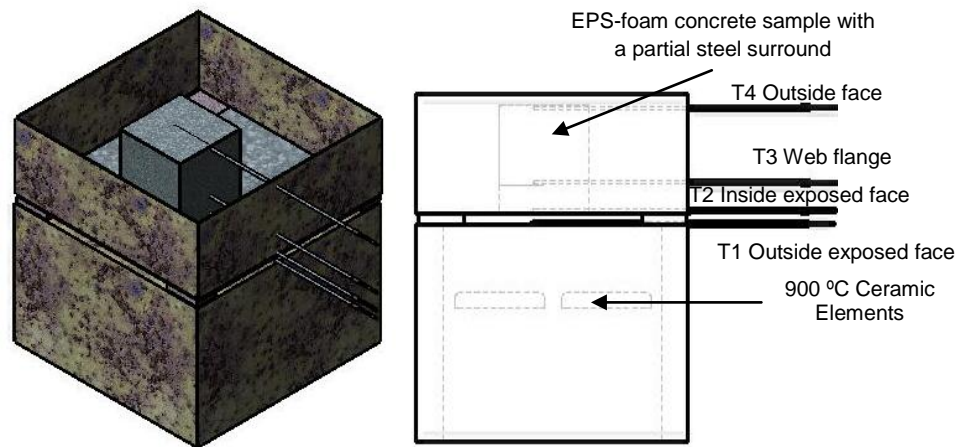


Figure 3-2 Schematic diagram of heating unit

The EPS-foam concrete sample was perforated to insert four thermocouple scions into the sample. A square galvanized steel sheet (305 mm² and 0.55 mm thick) was placed on top of the heating unit. This steel sheet represents the opposite side of the sandwich panel. An EPS-foam concrete sample was placed on the square galvanized steel sheet. A thin steel mold was placed on the square galvanized steel sheet and separated from this device with four pieces of heat resistant fibers. The thermocouples were inserted into the center of the foam concrete sample in a vertical line (Figure 3-1 and Figure 3-2), and the steel mold was filled with insulating fibers around the foam concrete block. Thermocouples were connected to a four thermocouple datalogger outside the heating unit.

The heating unit was turned on and the ceramic elements were set to reach the maximum temperature of 900 °C. An insulation failure criterion was applied to the fire tests [44]. The small scale sandwich panels were considered to have failed when the cold face temperature had reached 160 °C, which occurred when thermocouple T4 reached the threshold value of 160°C. Every 5 seconds

the temperature was recorded with a thermometer. The temperature of thermocouples T1, T2, and T3 were simultaneously recorded. Thus, a chart (time versus temperature profiles) was created to collect experimental data in order to analyse the results.

3.3.4. Thermal Conductivity for Ultra-lightweight Concrete

Foam concrete has excellent thermal insulating properties derived from its microcellular structure. A thermal conductivity range of 0.06–0.16 W/mK can be obtained for foam concretes of 200–650 kg/m³ densities [65]. Thermal conductivity coefficients k can reach 0.06–0.064 W/mK for lighter concretes of 150–170 kg/m³ with cement composites and EPS granules as components [38].

Three conductivity samples of a size of 200x200x40 mm were prepared with ultra-lightweight concrete of 500 and 150 kg/m³ densities. A thermal conductivity analyzer (Anacon TCA-8) was used for thermal conductivity factor measurements of the insulation samples, as shown in Figure 3-3. The measurements were made with a sample contacting a 10cm diameter hot and cold plate, maintained at 37 °C and 10 °C respectively. The Anacon TCA-8 thermal conductivity analyzer maintains a fixed temperature difference across a sample by controlled hot and cold plate temperatures. A heat-flow transducer produces a signal proportional to the heat passing through the sample. The TCA-8 automatically measures the thickness of the sample and combines the reading with the heat-flow measurement to yield a direct digital readout of thermal conductivity.



Figure 3-3 Thermal conductivity equipment (Anacon TCA-8)

The tests were run and thermal conductivity values were determined during the period when the thermal conductivity values were stable. During the test, the thermal conductivity obviously changed until it achieved a consistent value.

3.3.5. Pull-out Experiments

The pull-out test method was used to evaluate the shear bonding strength between steel and lightweight aerated concrete. The initial pull-out test method included a lightweight aerated concrete cube (100x100x100 mm) with galvanized steel sheet (200 x 50 mm) embedded 100 mm into the middle of the concrete cube. The concrete sample was held with steel plates at the top of the sample. The pulling force was applied directly on the free area of the steel sheet. The pull-out forces were maintained centric to the strips to avoid any eccentricity through loading. The initial test method and sample is illustrated in Figure 3.4 and Figure 3-5.

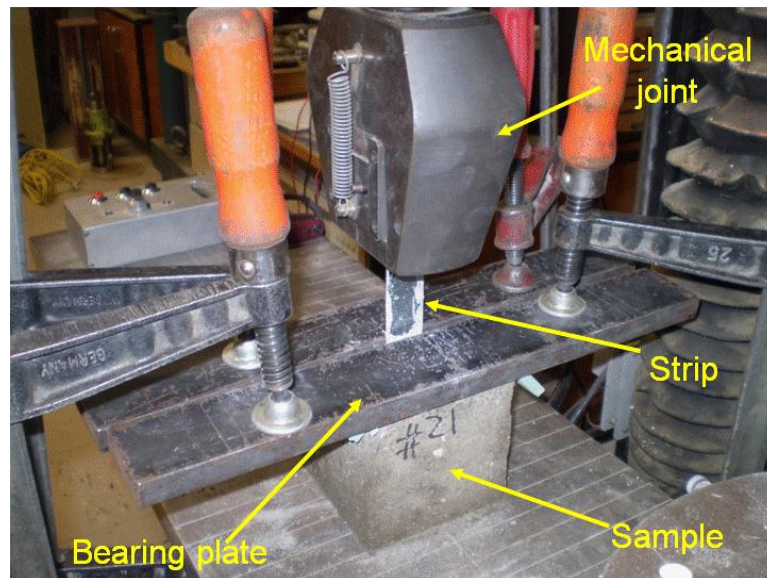


Figure 3-4 View of the rig for pull-out tests

The usual experimental set-ups for reinforcing rods are not adequate for testing steel strips due to eccentricity of loads that cause a bending of strips, and due to clamping forces from experimental accessories [66].

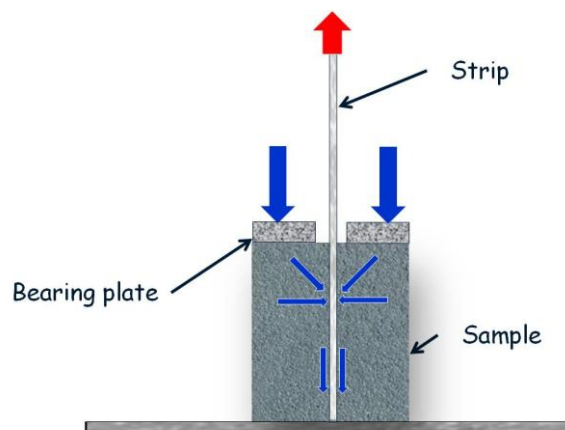


Figure 3-5 Undesirable effects

Thus, effort was undertaken to design a testing mechanism that would eliminate the influence of undesirable effects (Figure 3.5) of either bending and/or twisting

the steel strips during pull-out tests, and to concentrate on pure uniaxial tests, as illustrated in Figure 3.6. A flexible mechanism eliminated these effects.



Figure 3-6 Final set-up: Testing mechanism with a freely adjustable ball-joint and a plate with embedded-bolts within foam concrete samples (see also Figure 3.9)

Pull-out tests were carried out with the aim of predicting the bonding strength between lightweight concrete and steel strips. The influence of steel strip geometries was checked as well. The steel strips were cut by using a laser cutting machine. The steel geometries are shown in Figure 3.7.

Finally numerical modeling was done based on the experimental bonding results between aerated concrete and galvanised steel using Finite Element Analysis (FEA) to predict the behaviour of bonding between both materials. Abaqus was used as a commercial finite element software package. Finally, a comparison between experimental load-displacement and finite element simulations was completed.

150 aerated concrete specimens were prepared and tested with these testing procedures, which provided data for this study.

Three standard foam concrete cylinders of 100 mm diameter were prepared for each of the pull-out experiments, to determine the compressive strength and density of the foam concrete and to verify the strength properties as desired in the mix design. Thus, four different mix compositions of aerated concrete were prepared at 1200, 1000, and 800 kg/m³ density of foam concrete and 200 kg/m³ of ultra-lightweight concrete. All of them used steel strips of 0.75 mm thickness. In addition, the mix composition of foam concrete prepared at 1200 kg/m³ density included steel strips of 0.75 and 2 mm thickness.

150 pull-out tests (5 mix compositions, 10 hole pattern, each set repeated 3 times) studying the effect of various parameters such as steel strip geometries, which included thickness, number and diameter of holes, size-dependence, as well as the position of holes, plus a variety of set-ups were run at AUT University. This testing provided significant information for this research [49, 66], such as knowledge about mixing concrete procedures, achieving experimental bonding results, and finally obtaining a numerical model for the bonding between foam concrete and steel plates with and without holes.

The major purpose of the pull-out test experiments was to find relationships between 10 hole patterns (Figure 3-7) in the steel strips and mechanical properties of aerated concrete in order to evaluate the pull-out force. Enhancing the bonding between steel elements and fillers for sandwich panels was realized through 10 patterns of holes in steel strips, as shown in Figure 3.7.

Three specimens for each single set of strips were prepared and tested to determine the shearing strength and bonding behaviour during pull-out tests.

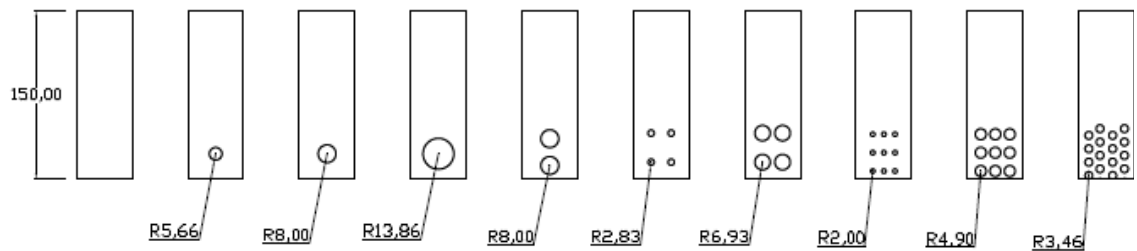


Figure 3-7 Patterns of holes in steel strips

This investigation hypothesised that the shearing strength of the foam concrete, which filled the holes of strips, is higher than the sole bonding strength of a contact layer of steel strips without holes. The pull-out tests were performed for the aerated concrete specimens with the dimension of 150x100x100 mm for steel strips of 50 mm in width. Plates were put in a casting mould (Figure 3.8) and the whole set-up was easily assembled and disassembled. Steel strips were placed in the middle of specimens and embedded 50 mm into the aerated concrete among the holding bolts (Figure 3.8). Galvanized steel strips (Bluescope NZ Steel product G250) of 0.75 mm in thickness with various diameters, numbers and distribution of holes were also tested, as shown in Figure 3-7.



Figure 3-8 Casting moulds

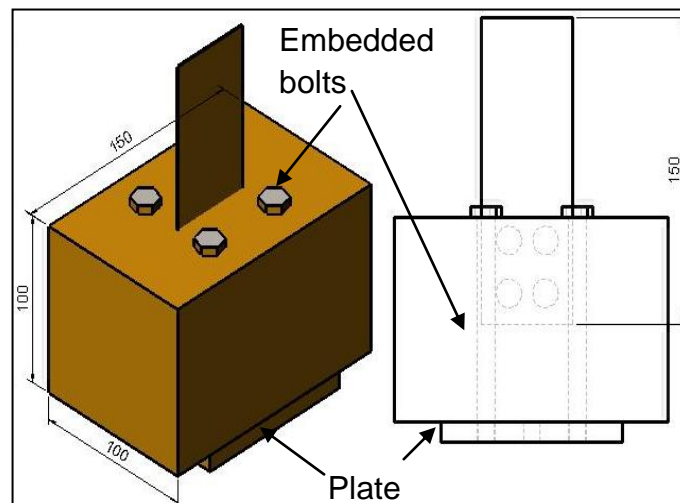


Figure 3-9 Schematic views of the location of a steel strip in foam concrete specimens between the holding-bolts

The pull-out tests were carried out using a universal testing machine equipped with a testing rig with a freely adjustable ball-joint for pull-out tests (Figures 3.6 and Figure 3.10). Four M10 bolts were embedded through cubic foam concrete samples and fixed to a plate at the bottom of the foam concrete cube, to hold the sample in place. The adjustable ball-joint for pull-out tests assures the pull-

out forces are centric to the strips during loading. The load was applied to the metal strip through a mechanical joint (Figure 3.6), and evenly increased while controlling the displacement at a rate of 0.05 mm/s.

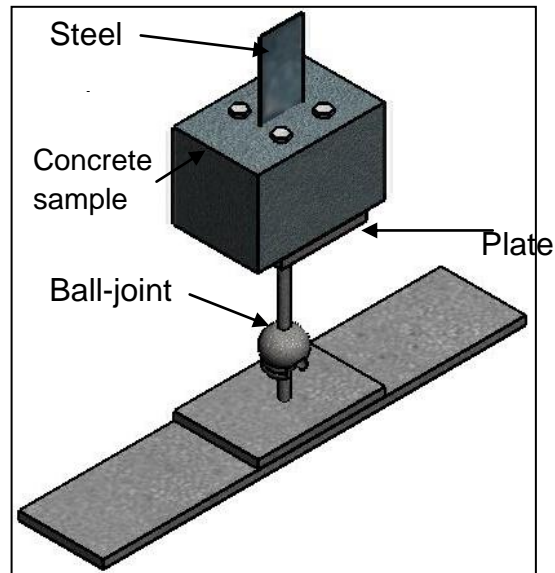


Figure 3-10 Testing rig with a freely adjustable ball-joint for pull-out tests

Both the load applied and the displacement of a steel strip were measured and recorded on a computer until a strip was extracted from a cubic sample, which made it possible to evaluate the force needed to pull-out a strip from the concrete. Thus, a load-deformation curve was obtained from each experiment. The combinations of hole patterns and concrete densities, the thickness of plates, and the diameter of the holes in the tested steel strips with various concretes are presented in Table 3.3 and Table 3.4. The choice of hole diameters to achieve the same total hole area with different configurations, or the increased hole area by 2, 4, 5.2, 6, and 6.8 times, are presented in Table 3.4.

Table 3.3 Pattern of holes in steel strips of 0.75 and 2 mm thickness

Concrete density [kg/m ³]	Number of holes	Radius [mm]
FC1200, FC1000, FC800 and ULWC200	0	0
	1	5.66
	1	8
	1	13.86
	2	8
	4	2.83
	4	6.93
	9	2
	9	4.9
	14	3.46

Table 3.4 Hole area ratios

Number of holes	Radius [mm]	Hole diameter ratios
1	5.66	Reference
4	2.83	1
9	2	1.1
1	8	2
2	8	4
14	3.46	5.2
9	4.9	6.8
1	13.86	6
4	6.93	6

3.4. Conclusion

This chapter has presented an appropriate methodology for investigating lightweight concrete and bonding to develop novel infill materials. The current research optimizes existing design methods for lightweight concrete, examines physical and mechanical properties of lightweight concrete, and will propose one filler for wall systems. Furthermore, this chapter presents a variety of steel strips with holes that may provide stronger bonding than flat steel without holes.

Chapter 4

4. Experimental Results and Discussion

4.1. Introduction

This chapter discusses the results of the experimental protocols as described in the previous chapter.

The results presented in this chapter demonstrate mechanical (compressive strength), physical (density), and functional characteristics (thermal conductivity and fire resistance) for different mix compositions of lightweight foam concrete, as well as bonding behaviour between foam concrete, ULWC and steel strips. The main results of this section were published in [66].

4.2. Experimental investigation

Seven target densities in total of 1200, 1000 and 800 kg/m³ were proposed for foam concretes, and 400, 250, 200 and 150 kg/m³ for ultra-lightweight concretes (ULWC) respectively. Both target densities and real densities were compared after testing to verify the effectiveness of the equations used in the mixture design.

The experiments were conducted, and the test results obtained from these experiments are discussed below.

4.3. Foam Concrete Mixture Design

A procedure for designing the mix composition of foam concrete was proposed by Kearsley and Mostert in 2005 [25], as described in Chapter 3.

Prior to casting the concrete samples, the densities of the mix compositions were obtained by using equations 3.3 and 3.4 explained in Chapter 3. Thus, three foam concrete (FC) mix compositions were prepared with target densities of 800, 1000 and 1200 kg/m³, and ultra-lightweight concretes (ULWC) were prepared with target densities of 150, 200, 250 and 400 kg/m³, by using stable foam concrete compositions. The mix proportions for foam concrete are shown in Table 4.1.

Table 4.1 Mixture proportions [kg/m³]

Concrete	Target Density	Cement	Ash	Water	Foam	EPS	Superplasticizers [ml/m ³]
FC1	800	382.92	191.46	191.46	33.67		
FC2	1000	485.95	242.98	242.98	32.76		
FC3 and FC4	1200	589.00	294.50	294.50	21.56		
ULWC1	400	248.50		124.25	20.11	7.28	
ULWC2	250	151.49		75.75	12.24	10.93	757.45
ULWC3	200	118.83		59.41	9.62	12.14	594.15
ULWC4	150	86.43		43.22	6.98	13.36	432.16

The mixes were prepared with the ratios as indicated in Table 4.1, and the differences between the target densities and casting densities are compared in Table 4.2.

Table 4.2 Target and casting densities

Concrete	Target Density [kg/m ³]	Casting Density [kg/m ³]	Density differences [%]
FC1	800	885.39	10.67%
FC2	1000	1049.81	4.98%
FC3	1200	1260.47	5.04%
FC4	1200	1585.53	32.13%
ULWC1	400	430.90	7.73%
ULWC2	250	237.74	4.90%
ULWC3	200	231.63	15.65%
ULWC4	150	132.55	11.63%

All casting densities on average of foam concrete (FC1 to FC3) were within 7% of the targets, while for ULWC the casting densities on average were close to 10% of the targets, as shown in Table 4.2, with the exception of the ULWC3. The casting density of the FC4 concrete mixture was 32% greater than the target. This may be due to bubbles not able to resist the physical and chemical forces imposed during mixing. In spite of the proportions in the mixture were not modified for FC4 concrete, an intense mixing more likely destroyed some bubbles of the foam, increasing the density of the foam concrete.

The excessive difference between target and casting density of the foam concrete (FC4) confirms that important precautions must be taken when preparing foam concrete, namely the foam preparation system, the kind of foaming agent, foam concrete mix preparation, the percentage of additives, and the duration of the mixing.

4.4. Test Results

Four series of foam concrete (FC1, FC2, FC3 and FC4) and four series of ultra-lightweight concrete (ULWC1, ULWC2, ULWC3 and ULWC4) were prepared, as shown in Table 4.1. Fly ash was used as replacement for cement in the FC, at a level of 50% by weight. EPS beads of different percentages by weight were added to the FC to create ULWC. The mix designs of these concretes are shown in Table 4.1. Cylindrical specimens were produced for each series of concrete.

4.4.1. Compressive Strength and Density

Foam concrete strength is normally measured by using the ASTM C39 standard. When a compressive load is applied, micro-cracks propagate and cause brittle collapse of the foam concrete sample [67].

ULWCs were prepared based on stable foam concrete of 700 kg/m^3 density. The concrete mix compositions were designed containing a percentage of EPS-beads to reduce the density to the lowest possible value, as described in Table 4.1.

The compressive strength of foam concrete is influenced by the density of the concrete, cement content, water/cement ratio, foam type and curing method.

The relationship between air-dry density and compressive strength is shown in Figure 4.1.

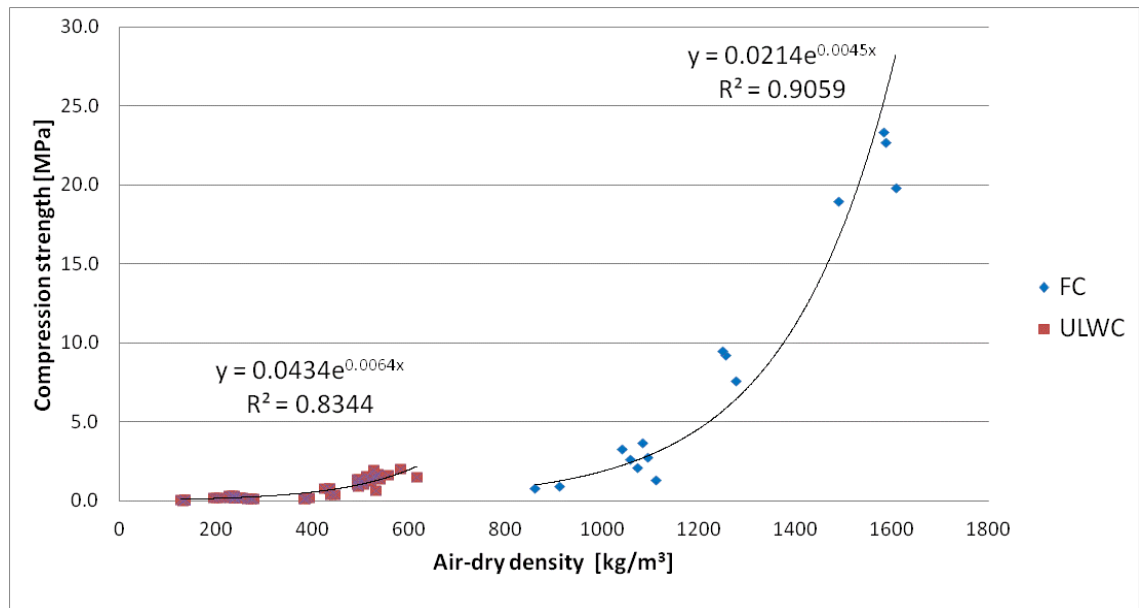


Figure 4-1 Relationship between air-dry density and compressive strength

As shown in Figure 4.1, the compressive strength versus density was plotted for various mix compositions of foam concrete and ULWC. The compressive strength decreases exponentially with the reduction in density of the lightweight aerated concrete.

Figure 4.2. shows the usual failure modes of the foamed concrete after a compression test. It is observed that cracks occur on the top part of the cylindrical sample. A collapse extends through the whole length of the cylinder, as the load is continuously increased.

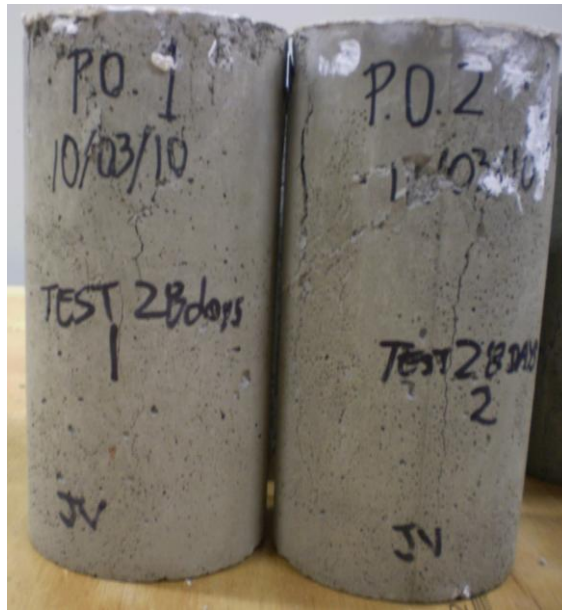


Figure 4-2 Typical failure modes in compression tests

4.4.2. Fire Resistance of Ultra-lightweight Concrete

Aerated concrete is incombustible and has excellent fire resistance properties as compared to normal weight concrete. Fire resistance tests on different densities of foam concrete indicated that the fire endurance is enhanced by increasing the density, as reported by Ramamurthy et al. [10].

The fire test results are shown in Figure 4.3 to Figure 4.9.

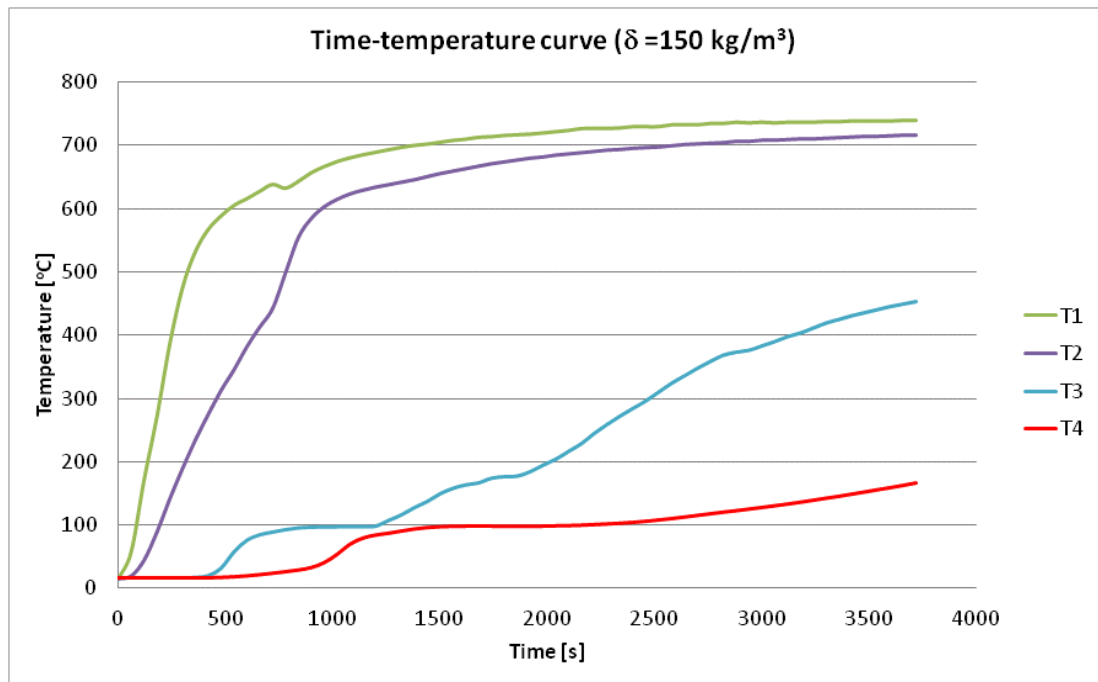


Figure 4-3 Time-temperature curve ULWC 150 (kg/m^3)



Figure 4-4 ULWC of 150 (kg/m^3) after test

The insulation failure criterion value of $>160 \text{ }^\circ\text{C}$ was reached after 60 minutes for the ULWC sample of 150 kg/m^3 . The ULWC had completely disintegrated, as shown in Figure 4.4. After 17 minutes, a small amount of smoke was

observed. This became abundant after 36 minutes, and then began to diminish 20 minutes later. This is because EPS beads are burned progressively.

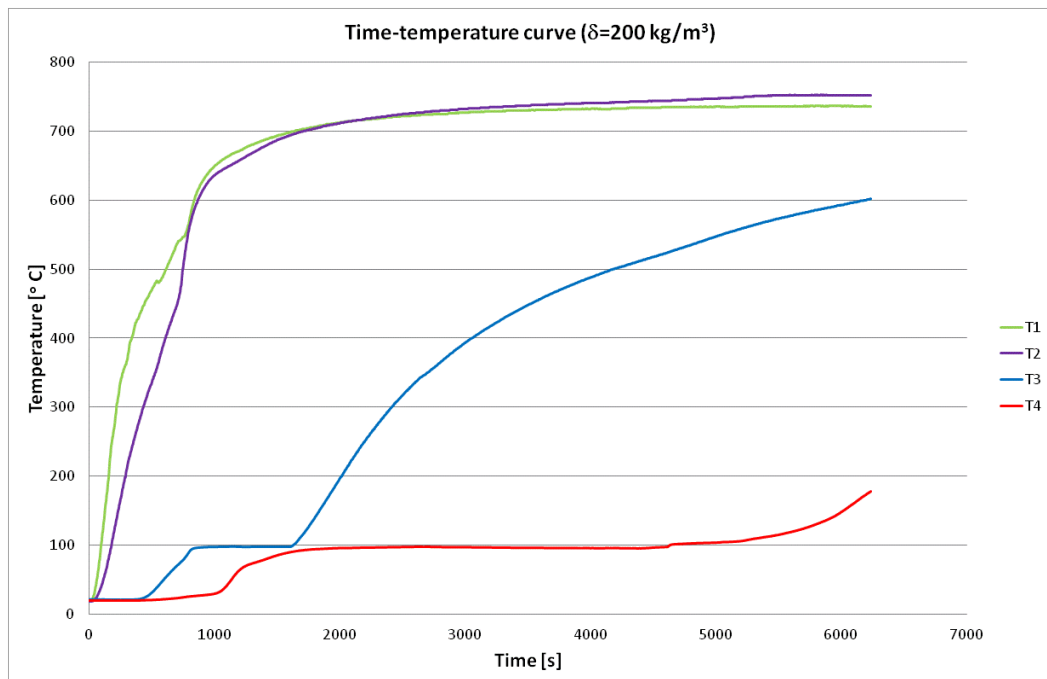


Figure 4-5 Time-temperature curve ULWC 200 (kg/m^3)

It was observed that the threshold value of $> 160^\circ\text{C}$ was reached after 1h 41m for the ULWC sample of 200 kg/m^3 density (Figure 4.5). The ULWC-200 sample had almost disintegrated and provided no strength to touching anymore. This sample is shown in Figure 4.6.



Figure 4-6 ULWC of 200 (kg/m^3) after test

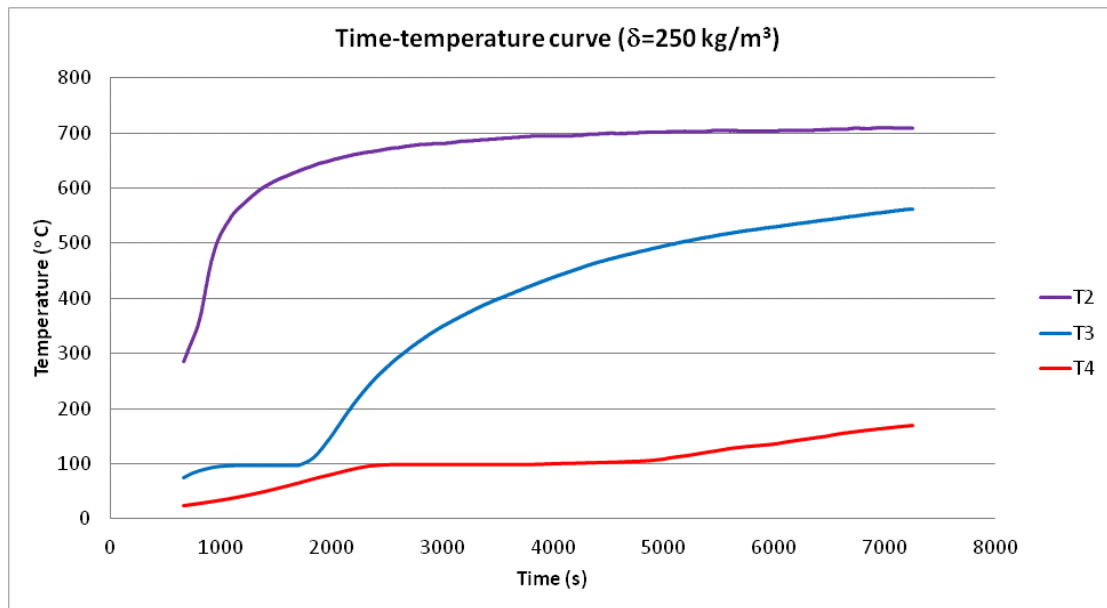


Figure 4-7 Time-temperature curve ULWC 250 (kg/m³)

The insulation threshold value of > 160 °C was reached after 1h 56m for the ULWC sample of 250 kg/m³ density (Figure 4.7). The ULWC sample had partially disintegrated, as shown in Figure 4.8. After 1 h 55m a small amount of smoke was produced. The thermocouple T1 was not detected by the equipment.



Figure 4-8 ULWC of 250 (kg/m³) after test

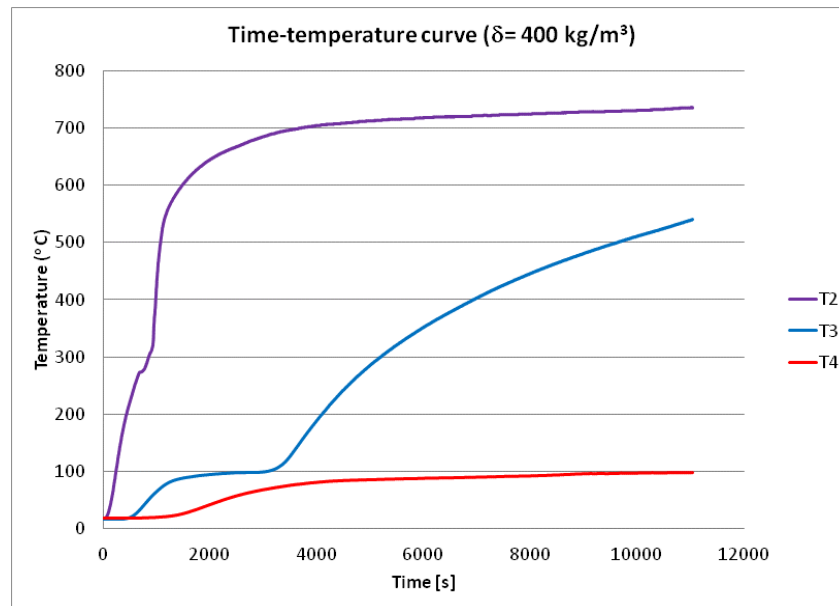


Figure 4-9 Time-temperature curve ULWC 400 (kg/m³)

It was necessary to stop the test after 3 hours because the heating elements were running at maximum power and continuing for more than 3 hours can damage them. The insulation threshold value $> 160\text{ }^{\circ}\text{C}$ was not reached after 3 hours for the ULWC sample of 400 kg/m^3 density (Figure 4.9). Data for the thermocouple T1 was not recorded by the equipment.

The results from this investigation indicate that the percentage of cement is a significant parameter for fire resistance properties. For the small scale sandwich panels from 150 kg/m^3 to 400 kg/m^3 the fire resistance improved from failure at 60 minutes with 150 kg/m^3 to no failure after 3 hours with 400 kg/m^3 . This means that the fire resistance of samples with a density of 400 kg/m^3 was more than 3 times higher than the samples of 150 kg/m^3 . In addition, the fire resistance was 68% and 93% higher for samples with 200 kg/m^3 and 250 kg/m^3 density respectively, when comparing with samples of 150 kg/m^3 density.

4.4.3. Thermal Conductivity of Ultra-lightweight Concrete

Two conductivity samples of 200x200x40 mm were prepared with ultra-lightweight concrete of 150 kg/m³ density. One of the two samples of ULWC of 150 kg/m³ was prepared with a thin layer of plaster on the contact surface. The experiment was designed to determine the thermal conductivity of ULWC.

The thermal conductivity results are shown in Table 4.3.

Table 4.3 Thermal conductivity results

Concrete	Thermal Conductivity [W/m.K]	Density [kg/m ³]
ULWC-150-Plaster	0.0724	150
ULWC-150	0.0848	150

Further experiments with different densities of the concretes should be made to analyse the thermal conductivity coefficient.

4.4.4. Pull-out Experiments

The pull-out experiment results between steel strips and lightweight concrete are presented and discussed here. The influence of the geometry of holes of steel strips embedded into concrete was studied by carrying out tests of steel strips with holes and without holes, in order to separate the contribution of the frictional bond component from the strength derived from the material in the holes.

The main purpose of the pull-out experiments was to find relationships between 10-hole patterns and mechanical properties of aerated concrete in order to evaluate and predict the bonding between steel and lightweight concrete through a numerical simulation.

The aerated concrete strength was studied in order to determine the influence of the concrete on the bonding strength between the concrete and the steel strips.

Ten different hole patterns were prepared including different numbers of holes (0, 1, 2, 4, 9 and 14), radius, and distribution (Table 4.4). In codifying the hole pattern produced, steel plates were denominated as S0, S1-6, S4-3, S9-2, S1-8, S2-8, S14-3, S1-14, S4-7 and S9-5, for each number and approximate radius of holes. Three specimens for each single set (three identical samples) of strip design were prepared and tested to determine the bonding strength during pull-out tests.

The reference hole area was 100.6 mm^2 with a 11.32 mm diameter. The reference area was increased 2, 4, 5, 6, and 6.75 times, in order to verify the effect of the anchorage of the concrete embedded into holes in various designs.

Table 4.4 Relationships of hole patterns

Hole pattern	Number of holes [--]	Radius of holes [mm]	Ah [mm ²]	Ah/As [--]	Increment in area of holes [--]
S0	0	0	0	0	-
S1-6	1	5.66	100.6	0.042	Reference
S4-3	4	2.83	100.6	0.042	1.00
S9-2	9	2	113.1	0.047	1.12
S1-8	1	8	201.1	0.087	2.00
S2-8	2	8	402.1	0.192	4.00
S14-3	14	3.46	526.5	0.267	5.23
S1-14	1	13.86	603.5	0.318	6.00
S4-7	4	6.93	603.5	0.318	6.00
S9-5	9	4.9	678.9	0.373	6.75

Note: Ah/As – hole surface area over strip surface area, As – surface area of strip after the holes are put in.

The effect of several factors on pull-out forces are analysed below, namely density and strength of the concrete, sum of hole area, thickness of steel plate, sum of diameter of holes and sum of circumference of hole area. Therefore, the pull-out results were displayed differently as a function of these factors to analyse the relationship.

4.4.4.1. The Effect of Strength and Density of Concrete

Lightweight foam concretes with a wide range of concrete densities (885, 1049 and 1260 kg/m³) were studied for density effects on pull-out forces, which had the same steel plate thickness (0.75 mm). Samples S9-5 with holes and S0 without holes were selected for the analysis.

The scatter plot of the pull-out force vs. air dry density is shown in Figure 4.10.

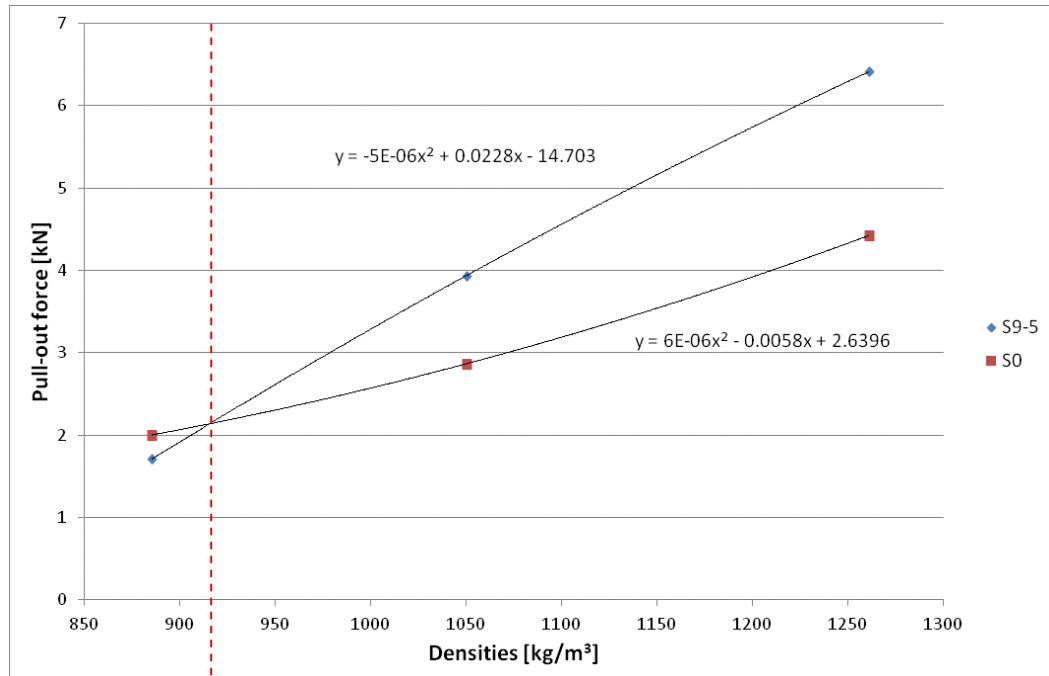


Figure 4-10 Critical line of concrete density

The dashed vertical line in Figure 4.10 indicates the critical concrete density for tested steel strips where holes begin to become beneficial on the right hand side of the line and where they are reducing the pull-out forces on the left hand side.

The analysis of the test results leads to the conclusion that pull-out strength is increased with the increase of foam concrete densities. It may be concluded that holes cut into the steel strips can be used to improve the pull-out forces for concrete with higher densities than 915 kg/m^3 for the materials and geometries involved. However a negative effect on pull-out forces was found for lighter concretes. The main reason for this is that the area of chemical adhesion was reduced due to holes cut into the steel strips, and the mechanical interlock introduced by the concrete inside the holes was not enough to compensate for the loss of adhesion in weaker concretes. Thus, holes cut into steel strips are recommended beyond a certain threshold value for greater densities of concrete, as highlighted by the critical line.

This study discusses variations that occur in the pull-out force for the four different foam concretes by comparing their strengths. 150 pull-out samples were prepared including different number of holes, diameters, distribution of holes in the steel strips, and 0.75 mm thicknesses of the steel plates. The concrete samples were codified as FC1, FC2 and FC3 respectively. The foam concrete strength was measured by using ASTM standard C39. Results from the test show that foam concrete reached compressive strengths of 0.91, 2.97 and 8.8 MPa respectively.

The pull-out results as averages for each single set were analysed and the outcomes are shown in Table 4.5, Table 4.6 and Figure 4.11.

Table 4.5 Pull-out forces

Pull-out force [kN]			
Hole pattern	FC1	FC2	FC3
S1-6	2.0765	3.2408	5.0355
S4-3	1.7928	3.0302	4.9541
S9-2	1.6144	3.3141	5.3549
S1-8	1.7238	2.8707	5.1523
S2-8	1.1924	3.0036	5.4635
S14-3	1.3658	3.4998	6.1834
S1-14	1.3587	2.9085	4.9742
S4-7	1.3282	3.8173	5.7837
S9-5	1.7078	3.9330	6.4073

Table 4.6 Variations of pull-out forces for different concretes

Increased Pull-out force		
Hole pattern	FC2 vs FC1 [Δ %]	FC3 vs FC2 [Δ %]
S0	43.15	52.94
S1-6	56.07	55.38
S4-3	69.02	63.49
S9-2	105.28	61.58
S1-8	66.53	79.48
S2-8	151.89	81.90
S14-3	156.25	76.68
S1-14	114.06	71.03
S4-7	187.41	51.51
S9-5	130.29	62.91

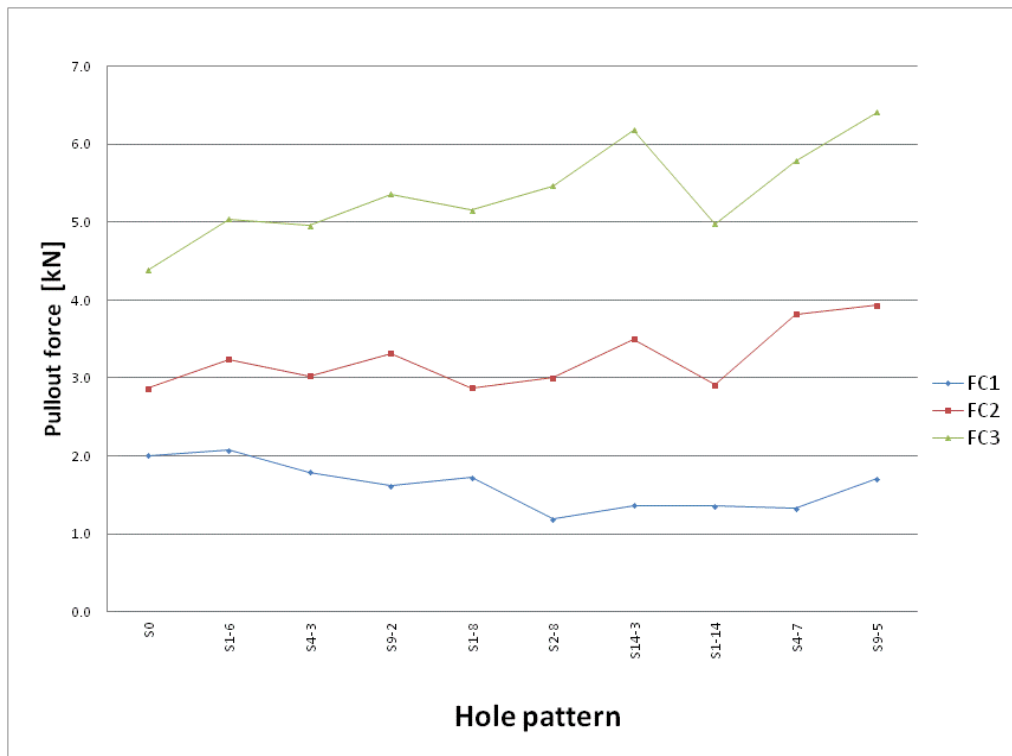


Figure 4-11 Pull-out test results

The results showed that the pull-out forces for FC3 samples were 1.5 to 1.8 times higher than the samples of FC2 (Table 4.6) , thus providing more strength, while the pull-out forces for FC2 samples were increased between 1.4 and 2.9 times higher than for the samples of FC1 (Table 4.6).

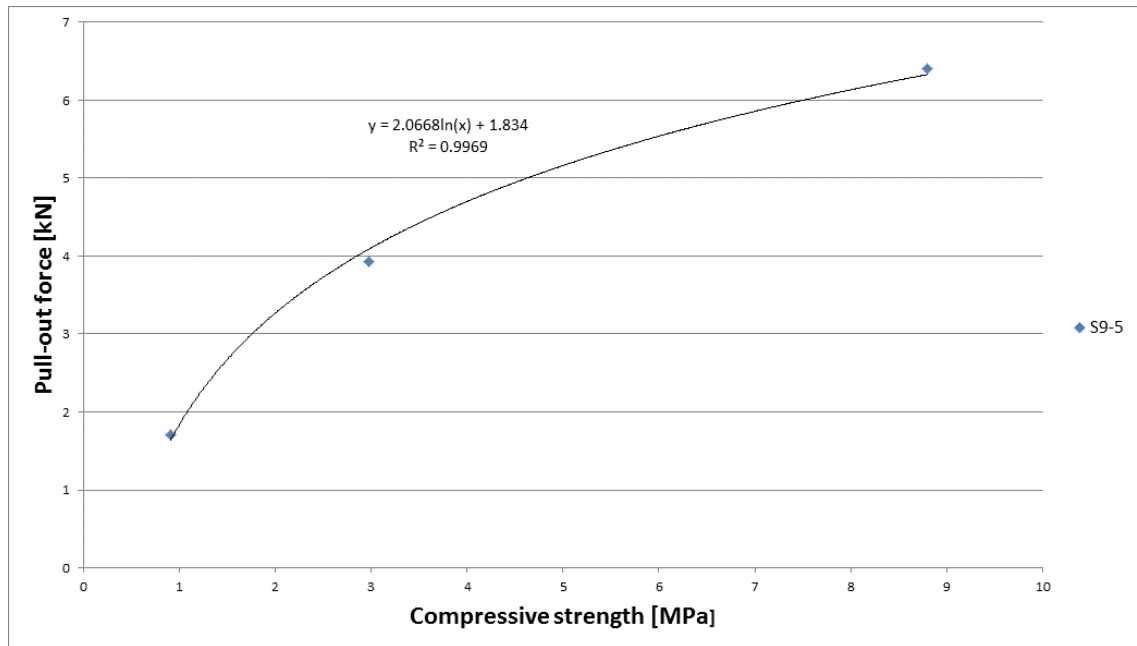


Figure 4-12 Relationship between pull-out force and compressive strength

These results show that pull-out forces are increased with increasing concrete strength, as expected, and the effect was quantified. The increase in pull-out force with increasing concrete strength is leveling off for the investigated samples, as shown in Figure 4.12. Sample S9-5 was selected for the analysis due to this specimen obtained the maximum pull-out force.

4.4.4.2. The Effect of the Thickness of Steel Strips

In an attempt to assess the effect of the thickness of the steel strips on bonding behavior, 3 times 10 pull-out samples with 2 mm thick steel and the same patterns of holes were tested with foam concrete (FC4) of 1585 kg/m³ density. The pull-out results for FC4 and the 2 mm thick strips were compared indirectly with FC3 samples, as FC3 used steel strips of 0.75 mm thickness and foam concrete with 1260 kg/m³ density. Three different densities (885, 1049 and 1260 kg/m³) were used in the experiments, as shown in Table 4.7.

Table 4.7 FC4 pull-out forces and extrapolated pull-out forces

Hole Pattern	Pull-out force [kN]			
	FC1 (0.75 mm)	FC2 (0.75 mm)	FC3 (0.75 mm)	FC4 (2mm thickness)
S1-6	2.0765	3.2408	5.0355	8.6105
S4-3	1.7928	3.0302	4.9541	8.5640
S9-2	1.6144	3.3141	5.3549	8.7067
S1-8	1.7238	2.8707	5.1523	8.5041
S2-8	1.1924	3.0036	5.4635	8.6038
S14-3	1.3658	3.4998	6.1834	9.2782
S1-14	1.3587	2.9085	4.9742	8.5423
S4-7	1.3282	3.8173	5.7837	8.2684
S9-5	1.7078	3.9330	6.4073	9.7403

Two samples were selected (S9-2 and S9-5) to demonstrate the increased pull-out strength by sheet thickness, as shown in Figure 4.13. All data are included in Table 4.7.

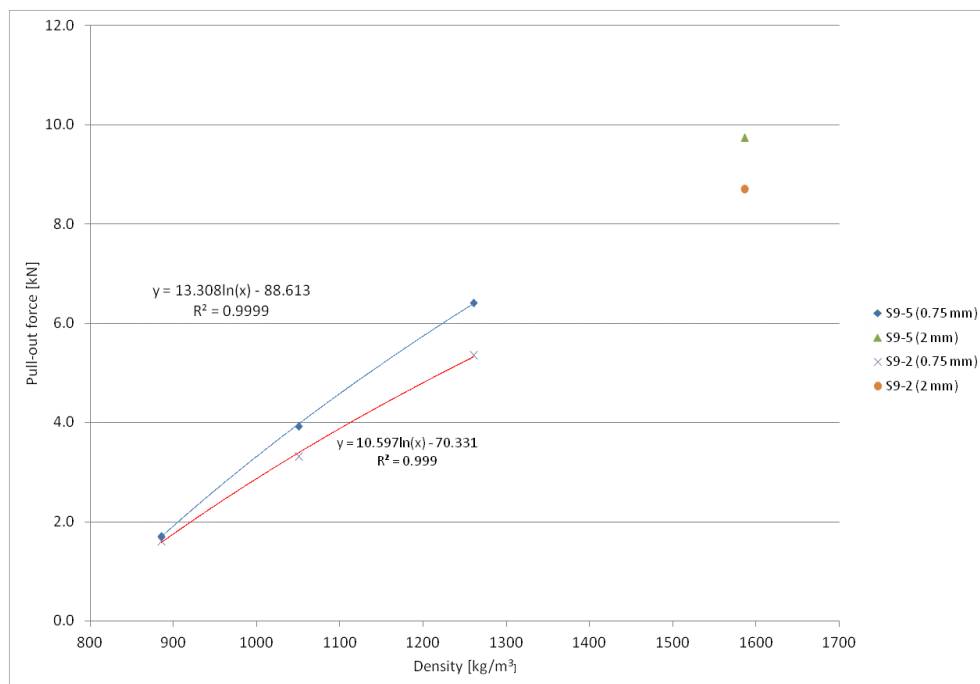


Figure 4-13 Relationship between pull-out force and density

It may be observed that the pull-out force made with 2 mm thickness were higher than that of specimens made with 0.75 mm thickness (Table 4.7 and Figure 4.13). Further experiment should be considered to compare pull-out forces with 0.75 mm and 2 mm thickness for the same concrete.

4.4.4.3. The Effect of Hole Area

In this study, pull-out experiments were conducted to investigate the effect of the hole area on pull-out forces between aerated concrete and embedded steel strips. The pull-out forces were graphed to analyse how strength increases with hole area, for FC2 and FC3 concretes, as presented in Table 4.8, Figure 4.14 and Figure 4.15. FC1 concrete was discarded because of the low strength of the material, which affected negatively the pull-out forces, as explained earlier.

Table 4.8 Pull-out forces as a function of hole area

Hole pattern	Ah [mm ²]	Pull-out force [kN]	
		FC2	FC3
S0	0	2.8643	4.3806
S1-6	100.6	3.2408	5.0355
S4-3	100.6	3.0302	4.9541
S9-2	113.1	3.3141	5.3549
S1-8	201.1	2.8707	5.1523
S2-8	402.1	3.0036	5.4635
S14-3	526.5	3.4998	6.1834
S1-14	603.5	2.9085	4.9742
S4-7	603.5	3.8173	5.7837
S9-5	678.9	3.9330	6.4073

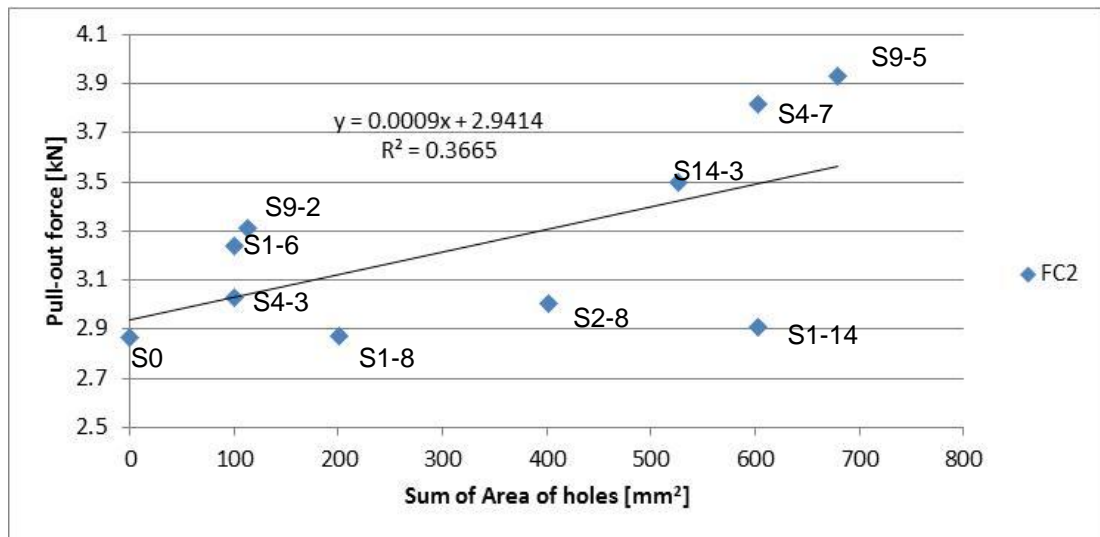


Figure 4-14 The effect of sum of area of holes on pull-out force for FC2 concrete

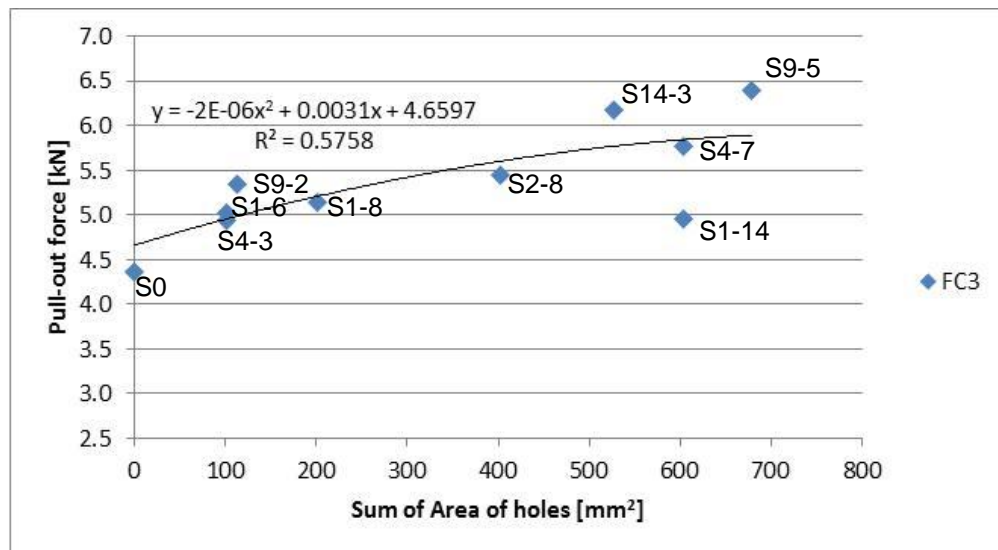


Figure 4-15 The effect of sum of area of holes on pull-out force for FC3 concrete.

The whole pull-out results for the 10 series of samples are graphed in Figure 4.14 and Figure 4.15.

A linear trend line was selected to analyse the pull-out results for FC2 concrete, due to any polynomial trend line not matching the underlying science of the

relationship. The correlation coefficients ($R^2 = 0.3665$ and 0.5758) show a weak relationship of data for FC2 and FC3 samples respectively.

In general terms the pull-out forces increase when the area of holes also increase, with the exception of the sample S1-14. The experiments had been designed, that for two total hole areas, 100 mm^2 and 600 mm^2 , a number of hole configurations existed. Samples S1-6, S4-3 and S9-2 have a common total hole area of 100 mm^2 and samples S1-14 and S4-7 have a common hole area of 600 mm^2 . It can be seen from Figures 4.14 and 4.15 that samples with multiple holes show a higher pull-out force, than samples with only one hole for the same total hole area.

Figures 4.14 and 4.15 also show, that samples with many holes are usually located over the trend line. In contrast, samples with one or two holes (S1-8, S2-8 and S1-14) fall underneath the trend line. As a design rule it can be concluded that steel strips with similar dimension as the ones tested, it is advantageous to rather manufacture a number holes for a given total hole area, than to combine a given total hole area in only one or two holes. This trend might be opposite to the manufacturing costs, but the bonding strength between steel and concrete within the assembled product is improved.

Nevertheless from the correlation coefficients of the curve fittings it can be concluded that the sum of area of holes is not a very exact parameter to describe the relationship between hole geometries of steel strips embedded in concrete and pull-out forces.

Therefore, an effort to find different relationships, i.e. between sum of diameter and sum of circumference of holes, which might improve correlation coefficients, are presented below.

4.4.4.4. Effect of the Sum of Diameters of Holes

The pull-out results were displayed in a different way as a function of the hole diameter. The pull-out forces and sum of diameter of holes for FC2 and FC3 concrete mixtures are shown in Table 4.9, Table 4.10, Figure 4.16 and Figure 4.17.

Table 4.9 Pull-out forces and sum of diameters of holes for FC2 concrete

Hole pattern	Number of holes [--]	Sum of Diameters [mm]	Pull-out force FC2 [kN]
S0	0	0.00	2.8643
S1-6	1	11.32	3.2408
S1-8	1	16.00	2.8707
S4-3	4	22.64	3.0302
S1-14	1	27.72	2.9085
S2-8	2	32.00	3.0036
S9-2	9	36.00	3.3141
S4-7	4	55.44	3.8173
S9-5	9	88.20	3.9330
S14-3	14	96.88	3.4998

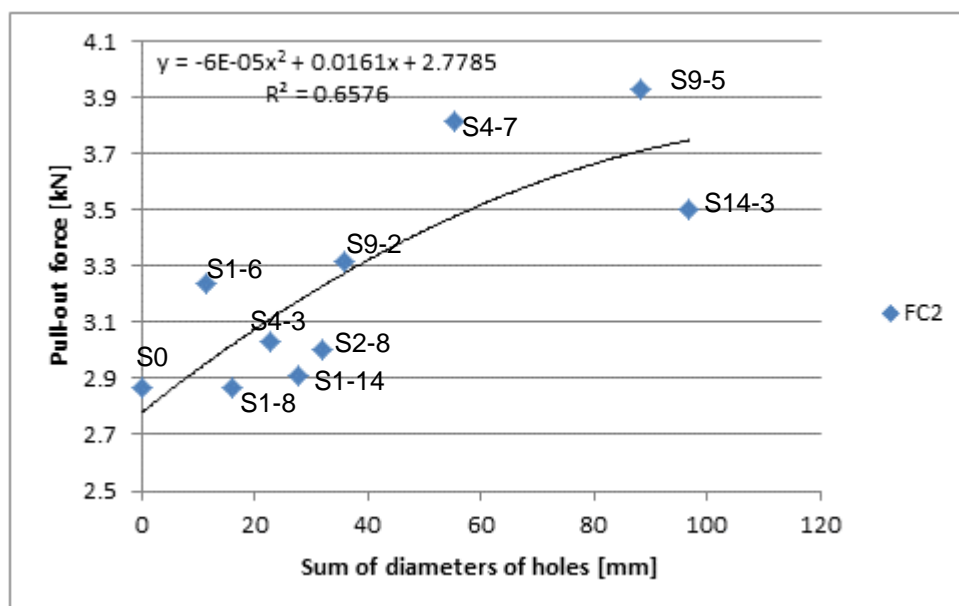


Figure 4-16 The effect of the sum of diameters of holes on pull-out forces for FC2 concrete

Table 4.10 Pull-out forces and sum of diameters of holes for FC3 concrete

Hole pattern	Number of holes [--]	Sum of diameters [mm]	Pull-out force FC3 [kN]
S0	0	0.00	4.3806
S1-6	1	11.32	5.0355
S1-8	1	16.00	5.1523
S4-3	4	22.64	4.9541
S1-14	1	27.72	4.9742
S2-8	2	32.00	5.4635
S9-2	9	36.00	5.3549
S4-7	4	55.44	5.7837
S9-5	9	88.20	6.4073
S14-3	14	96.88	6.1834

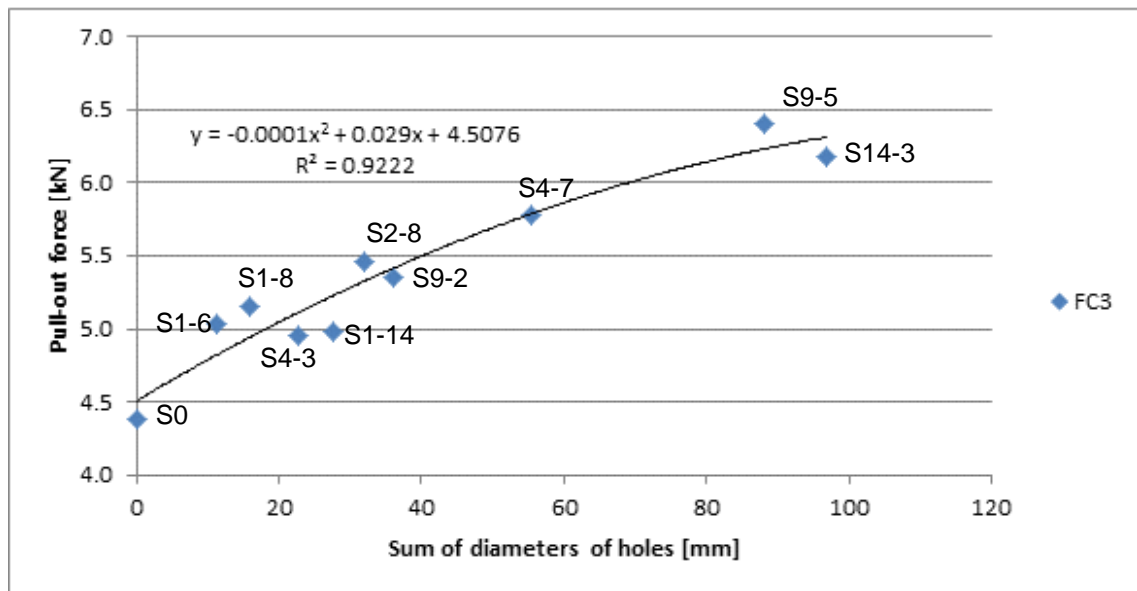


Figure 4-17 The effect of the sum of diameters of holes on pull-out forces for FC3 concrete

There is a stronger correlation between pull-out force and sum of diameters of holes ($R^2 = 0.9222$) for FC3 samples. Regarding FC2, Figure 4.16 shows an acceptable correlation coefficient ($R^2 = 0.6576$). From the available experimental data, it is clear that pull-out forces increase when the sum of diameters also increases. For the selected range of samples certain saturation seems to occur in the sense that pull-out forces do not increase by the same amount for a larger sum of diameter of holes than for smaller sums.

It was also found that there is a better correlation between the pull-out force and the sum of diameters of holes rather than area of holes.

4.4.4.5. Effect of the Sum of Circumference Areas of Holes

A further attempt of finding appropriate parameters, which could describe relations between the contact strip area and the geometrical parameters of

holes, was undertaken. Previous results on bonding energy as a potential parameter were reported by Alterman et al. [46].

The relationship between the sum of hole circumference areas and pull-out forces was analysed to describe the relationship between strip geometry and pull-out forces better.

The strips with the greatest circumference areas of all holes occurred to have higher pull-out forces, which is presented in Table 4.11 and Figure 4.18 to Figure 4.19.

Table 4.11 Pull-out forces and sum of circumference area

Hole pattern	Number of holes [--]	Radius of holes [mm]	Ah [mm ²]	CA _h [mm ²]	As [mm ²]	HCAR [--]	Pull-out force [kN]		
							FC1	FC2	FC3
S0	0	0	0	0	5000	0	2.0009	2.8643	4.3806
S1-6	1	5.66	100.6	1.334	4798.7	0.000278	2.0765	3.2408	5.0355
S4-3	4	2.83	100.6	2.667	4798.7	0.000556	1.7928	3.0302	4.9541
S9-2	9	2	113.1	4.241	4773.8	0.000888	1.6144	3.3141	5.3549
S1-8	1	8	201.1	1.885	4597.9	0.000410	1.7238	2.8707	5.1523
S2-8	2	8	402.1	3.770	4195.8	0.000899	1.1924	3.0036	5.4635
S14-3	14	3.46	526.5	11.413	3946.9	0.002892	1.3658	3.4998	6.1834
S1-14	1	13.86	603.5	3.266	3793.0	0.000861	1.3587	2.9085	4.9742
S4-7	4	6.93	603.5	6.531	3793.0	0.001722	1.3282	3.8173	5.7837
S9-5	9	4.9	678.9	10.391	3642.3	0.002853	1.7078	3.9330	6.4073

Hole circumference area ratio (HCAR) is obtained by dividing the sum of circumference area of holes by surface area of steel strips after the holes are cut, as follows:

$$\text{HCAR} = \text{CA}_h / (\text{As})$$

where: CA_h – sum of circumference areas of holes

As – surface area of strip after the holes are cut

Ah – hole area

In this section, the relationship between circumference area of holes (CA_h) and pull-out forces is analysed. Figure 4.18 and Figure 4.19 show the overall scatter-plot for average pull-out forces vs. CA_h based on experimental results.

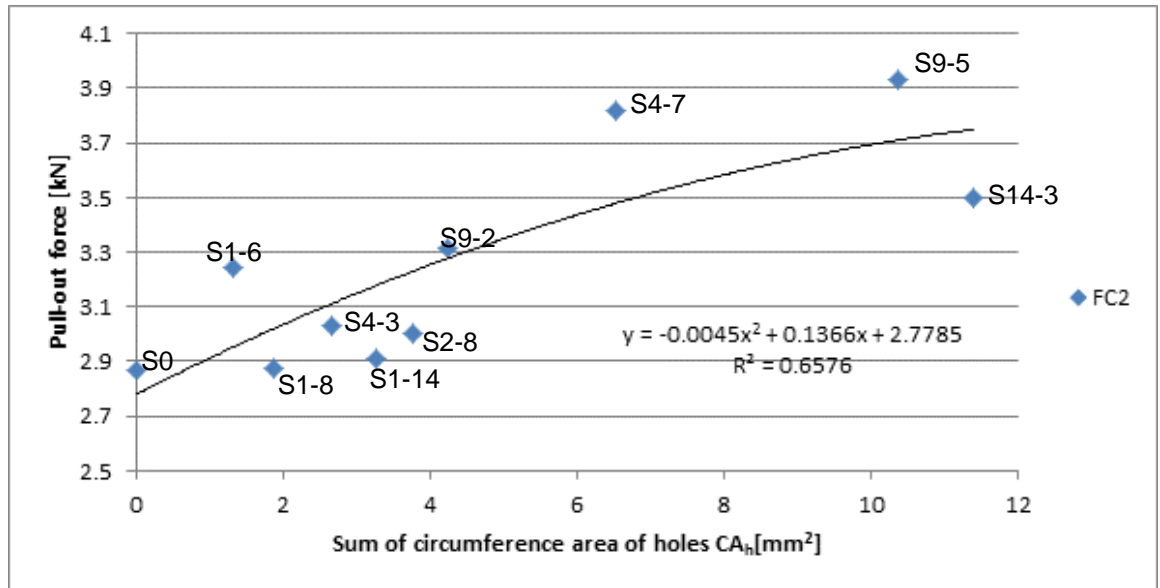


Figure 4-18 The effect of sum of circumference areas of holes on pull-out force for FC2 concrete

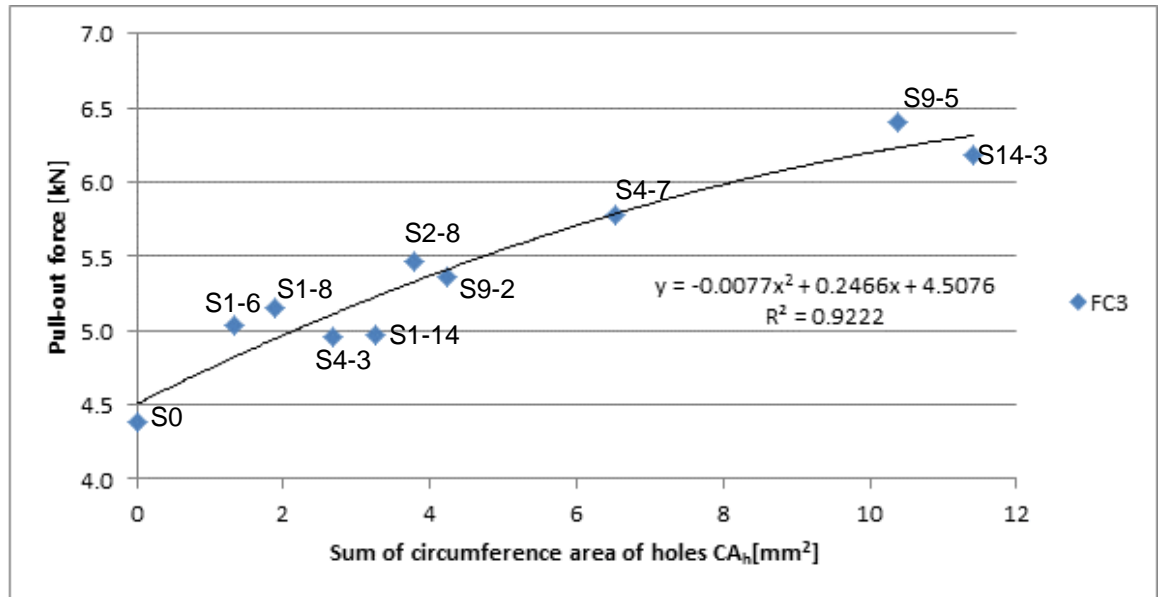


Figure 4-19 The effect of sum of circumference areas of holes on pull-out force for FC3 concrete

From the figures it can be seen that for an identical strip thickness obviously the same correlation coefficient between pull-out force and CA_h ($R^2 = 0.6576$ and 0.9222) exists like previously when plotting over the sum of diameters of holes. This occurs because CA_h is a linear function of the diameters of holes. But an additional factor is now considered as a part of the CA_h calculations, which is the thickness of holes. Therefore CA_h is more appropriate for pull-out analysis when dealing with different thicknesses of steel plates than just the diameter of the holes.

It can also be found again that pull-out forces plotted over CA_h values are showing a diminishing return for higher CA_h values.

Overall, geometrical parameters affecting pull-out forces analysed in this chapter were sum of area of holes (A_h), sum of diameter of holes, and sum of circumference area of holes (CA_h). The results indicated that the sum of

diameter of holes and sum of circumference area of holes give stronger correlations with pull-out forces, while weaker correlations exist between the pull-out forces and the sum of area of holes. The parameter CA_h provides not only a better correlation of data but also includes the thickness of steel strips, as an additional parameter.

4.4.4.6. Effect of Hole Circumference Area Ratio on Pull-out Strength

A comparative approach to analyse bonding behavior between foam concrete and steel strips is developed in this section. This approach is based on a dimensionless parameter HCAR being related to pull-out strength to come up with a comparative analysis.

The pull-out strength is calculated by dividing the maximum pull-out force by surface area of the steel strip after holes are cut.

Figure 4.20 and Figure 4.21 show a graphical representation of the data.

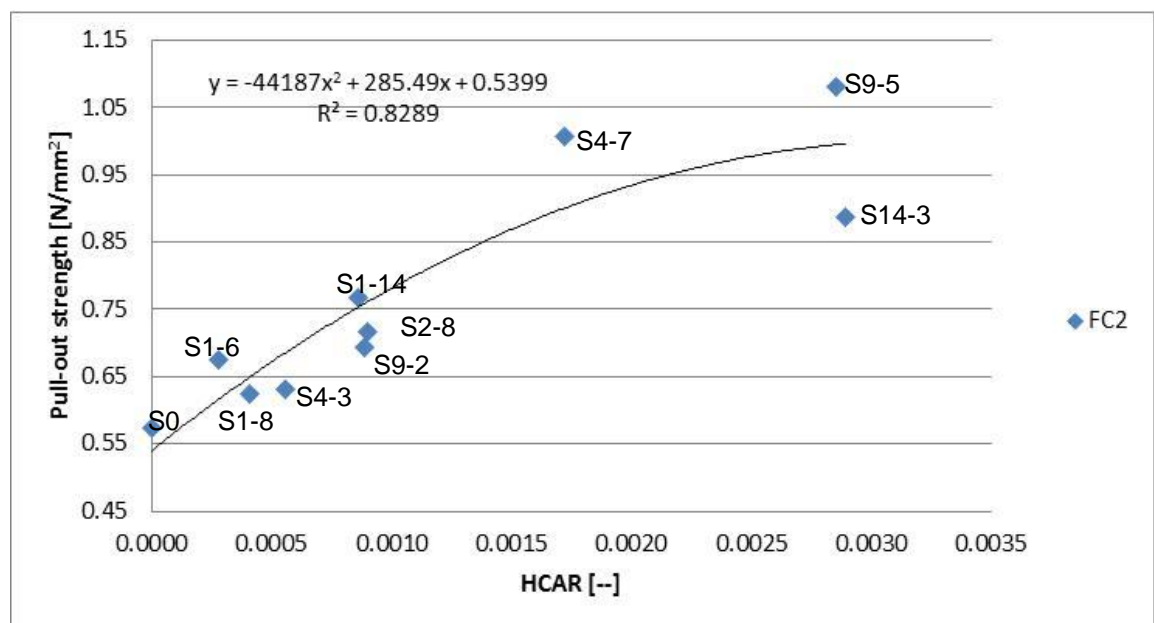


Figure 4-20 The effect of hole circumference area ratio on pull-out strength for FC2 concrete

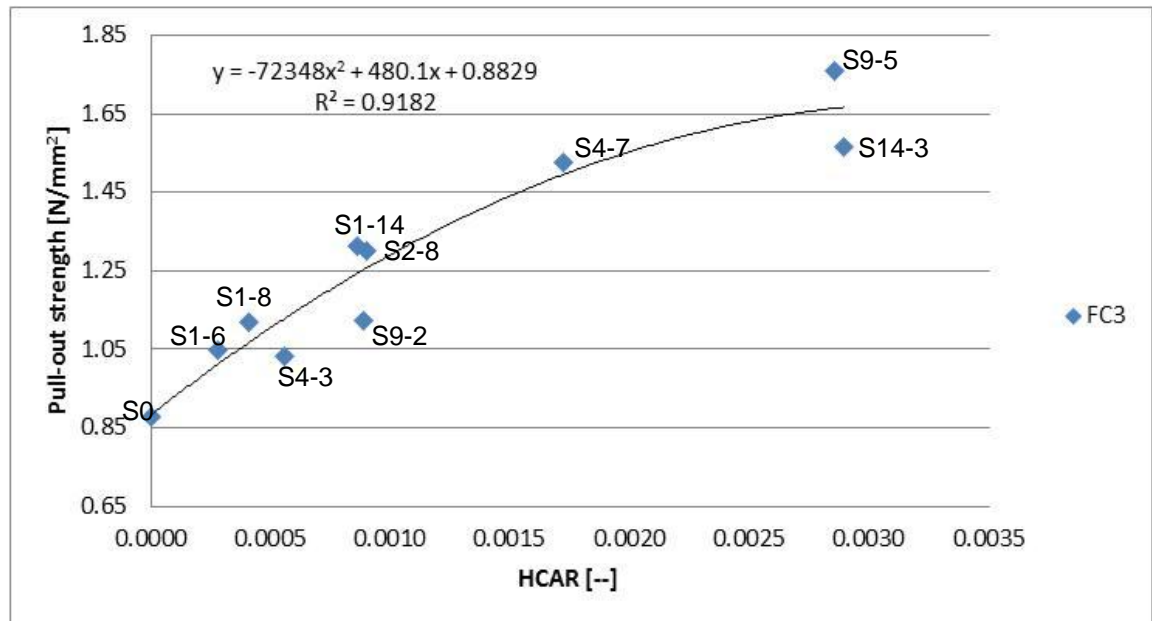


Figure 4-21 The effect of hole circumference area ratio (HCAR) on pull-out strength for FC3 concrete

The correlation coefficient ($R^2 = 0.9182$) reveals strong and positive correlation of data for FC3 samples, while the correlation coefficient ($R^2 = 0.8289$) for FC2 samples shows a still appropriate correlation of data.

Wall panels can be found in different widths, but the most common wall dimensions are between 100 to 150 mm wide. Thus, the embedded depth of the steel plates is between 50 to 100mm respectively. The steel plates used in this study were 50mm wide, which act as the embedded depth of steel sheet into the infill material of the current CSA panel. Figures 4.20 and Figure 4.21 are providing data of pull-out strength for steel plates with similar widths as the investigated ones, since the dimensionless parameter HCAR is being used for the x-axes.

4.5. Conclusion

This chapter has presented the experimental results regarding mechanical properties of foam concrete. Additionally, this chapter has demonstrated the physical and functional characteristics of different mix compositions of ultra-lightweight concrete, as well as the bonding behaviour between foam concrete and steel strips.

Precautions must be taken when preparing foam concrete to prevent differences between casting densities of lightweight foam concrete and target densities. When mixing variables such as the foam preparation system, the kind of foaming agent, foam concrete mix preparation, the percentage of additives, and the duration of the mixing process affect the cast densities.

The results from this investigation indicate that ultra-lightweight concrete based on EPS beads is an excellent potential infill material for wall panels. It is recommended that these infill materials should be designed with a density greater than 250 kg/m^3 , as the insulation failure criterion (160°C) applied during the fire tests indicated sufficient fire resistance compared with less dense lightweight concretes. An innovative ultra-lightweight concrete was also developed at 150 kg/m^3 density. Foam concrete and EPS beads were mixed to reduce the density of the concrete to the lowest possible value. This novel ultra-lightweight concrete could be also a potential filler material for wall systems, if some precautions are taken to reduce the fire risk. Further experiments can be undertaken to mitigate the fire risk, for instance, adding a suitable layer of fire insulation.

The comparative analysis of pull-out tests confirmed significant improvements for strips with holes over the pull-out forces of strips without holes. Sum of diameter of holes and/or sum of circumference area of holes (CA_h) were found to give better correlation with pull-out forces than just the total hole area. This study established that holes cut into steel strips are recommended only for concrete densities greater than 915 kg/m^3 , as a negative effect on pull-out forces was observed for lower concrete densities, because the loss of surface adhesion area of the strip is not compensated for by the shear strength of the concrete in the holes. In addition, it was found that contrasting pull-out strength with hole circumference area ratio (HCAR) provides the strongest correlation of data and is the best alternative for the analysis for different widths and thicknesses of steel plates.

A numerical simulation is developed in Chapter 5 in order to theoretically confirm the pull-out test results.

CHAPTER 5

5. Three Dimensional Finite Element Models to Simulate the Bonding Behavior Between Steel and Foam Concrete

5.1. Introduction

This chapter describes the development of three dimensional (3D) finite element models to simulate the bonding behavior between steel and foam concrete, based on pull-out experiments. The complex bonding phenomena were explored experimentally to provide a better understanding of the key elements of failure in the behavior of steel–concrete bonding. The Finite Element Method (FEM) has been established as the most suitable tool for studying the bonding behavior between steel and concrete, which can cause structural problems of these composites. A large number of numerical models have been related to bonding behavior between reinforcing bars and concrete specimens [47, 53-58], and between plastic bars and concrete samples [59]. However, there are very few investigations reported in the literature that develop a simulation of steel strips and foam concretes. Furthermore, no studies concerning FE modeling of bonding strength between perforated steel strips and aerated concrete were found. Thus, the need for analysis of the bonding behavior between foam concrete and perforated steel plates is imperative for a better understanding of the bonding phenomena, through a modeling of the adhesion within these composite materials.

In the present research the pull-out results collected from the experiments provided the main input data values for the simulation of bonding between steel

strips with holes and foam concrete. The input for FEM were compression tests of the FC3 concrete samples and tensile tests of the steel strips.

FE modeling, using the commercial finite-element software package, ABAQUS, were carried out to verify the pullout force produced for the mechanical interlock between steel plates and aerated concretes, under different experimental conditions. This three-dimensional finite element analysis was conducted to obtain the response of the pull-out force with steel plates in terms of applied load-deflection in the foam concrete samples. Thirty pull-out samples were selected for the analysis in the present study. S0 is the control sample of steel plates without holes, while the other twentyseven samples were performed with one, two, four, nine and fourteen holes in the steel strips. Validation of the current finite element model was carried out by comparing the results from the ABAQUS finite element analysis with those obtained from experimental results.

5.2. Input Parameters for Modeling

Experimental results were used to provide input parameters, namely the uniaxial compression stress-strain curve of the FC3 concrete sample and steel properties defined from tensile test results.

5.2.1. Aerated Concrete Properties

Mechanical properties are important parameters in finite element analysis. They are characterized by elastic modulus, stress-strain relationship, Poisson's ratio and concrete damage plasticity parameters. Experimental results from the FC3

concrete mixture, being the most reliable ones, were selected to provide the main input parameters for the finite element model.

The modulus of elasticity of foam concrete is a function of its density and compressive strength [10, 68]. The compressive strength and density obtained from the experiments were 8.8 MPa and 1260 kg/m³ for this aerated concrete, which may be used in masonry units, as classified by Suryani and Mohamad [69]. In this study, the modulus of elasticity of foam concrete was determined in accordance with BS 1881-121 [68] using the following equation:

$$E_c = 0.0017 \cdot \delta^2 \cdot f_c^{0.33} \quad (5.1)$$

Where

δ – LWC density [kg/m³]

f_c – Compressive strength [MPa]

Thus, the elastic modulus of this aerated concrete is 5535 MPa. The estimated Poisson's ratio commonly used for this kind of modeling is 0.2 [49].

This section describes the selected concrete damage plasticity model provided in ABAQUS for the analysis of concrete and other quasi-brittle materials. Concepts of isotropic damaged elasticity in combination with isotropic tensile and compressive plasticity were used to represent the inelastic behavior of concrete. The concrete damaged plasticity model in ABAQUS is based on the assumption of scalar (isotropic) damage and is designed for applications in which the concrete is subjected to arbitrary loading conditions, including cyclic loading. The model takes into consideration the degradation of the elastic stiffness induced by plastic straining both in tension and compression. It also

accounts for stiffness of recovery effects under cyclic loading, as described in ABAQUS documentation [70]. Table 5.1 shows the model's parameters characterizing its performance under compound stress. The parameters in Table 5.1 are used for all FE-models.

Two parameters are required to define the yield function; the first parameter is the ratio of initial equi-biaxial compressive strength to uniaxial compressive strength σ_{b0}/σ_{c0} , which describes the behavior of concrete under biaxial stress. The default values used were 0.667, as described by Behfarnia and Sayah [71].

The amount of plastic volumetric strain developed during plastic shearing is assumed constant during plastic yielding and is controlled by the dilation angle. A typical dilation angle of 38° was assumed for the analysis, while the default flow potential eccentricity value in ABAQUS is $\varepsilon = 0.1$, as described by Behfarnia and Sayah [71].

The viscosity parameter is used for the visco-plastic regularization of the concrete constitutive equations. The default value in ABAQUS is 0.0, which means that a rate-independent analysis is carried out [70].

Table 5.1 Input parameters used for concrete damaged plasticity in ABAQUS

Parameter	Value
Dilation angle	38°
Eccentricity	0.1
σ_{b0}/σ_{c0}	1.16
k	0.667
Viscosity parameter	0.0

The uniaxial compression stress-strain curve was defined using the experimental values, as shown in Figure 5.1.

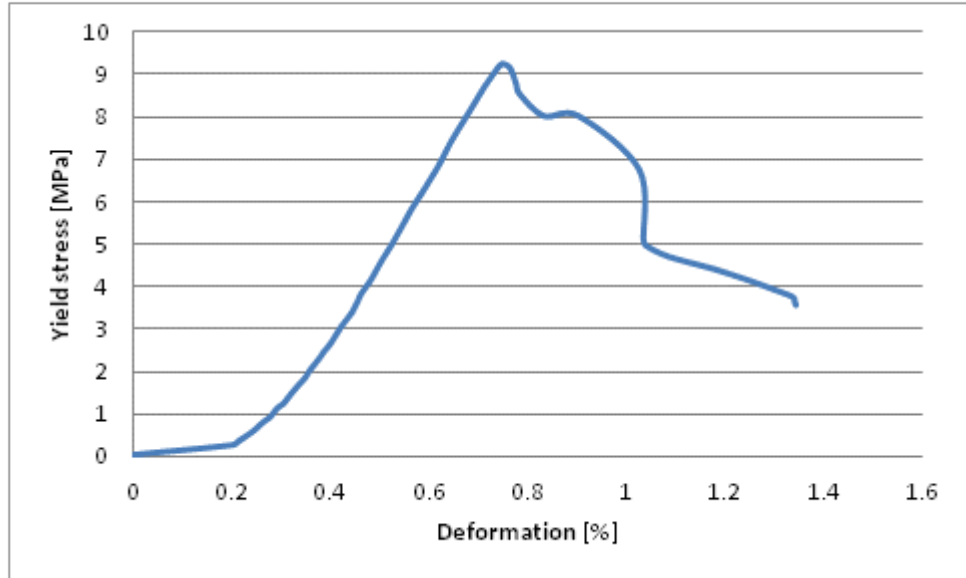


Figure 5-1 Measured compressive stress-strain curve of foam concrete

5.2.2. Galvanized Steel Properties

A galvanized steel sheet 0.75 mm thick and of grade G250 was used in this study. Appropriate mechanical properties for G250 0.75 mm thick were obtained from tensile tests. The experiments were performed in the AUT laboratory. An elastic modulus of 200GPa and a Poisson's ratio of 0.3 were used for the modeling. The plastic flow curve was generated from experimental data, as shown in Table 5.2.

Table 5.2 Material properties for steel sheets G250

Yield stress [MPa]	Plastic strain [--]
306	0
325	0.02
330	0.05
335	0.075
344	0.1
350	0.15
353	0.2
355	0.25
357	0.3

5.3. FE Modelling of Bond Between Steel Strips and Foam Concrete

The material properties that have been used for the validation model were those obtained from the FC3 concrete mixture during the experimental investigation and the galvanized steel sheet G250 grade as described above.

A typical 3D finite element model for simulating the bond-slip behaviour between foam concrete and steel strips of the pull-out test are shown in Figure 5.2, as an example. Only a quarter of the model needed to be simulated because of its symmetry. The 3D finite element model for concrete blocks and steel plates were of sizes 100x50x50mm and 150x25x0.375mm, respectively. The steel plates were placed in the middle of the concrete blocks, and embedded 50mm deep. The virtual models include the effect of bond behavior by simulating the contact between steel and concrete.

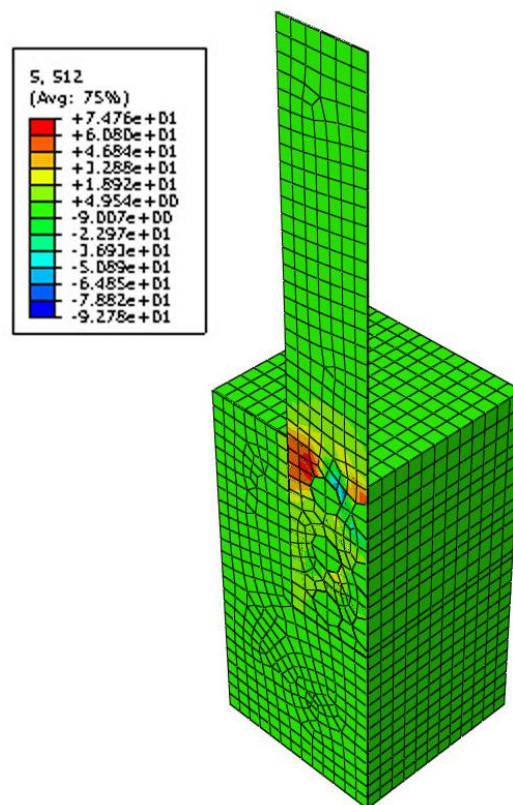


Figure 5-2 Typical finite element model displaying shear stresses

A static solution procedure was used for the computation of the system response to develop this model, where a general-static analysis step was created and the Nlgeom button was turned on for large displacement analysis in the ABAQUS model.

The ABAQUS user's manual specifies cohesive behavior as a part of the surface interaction properties that are assigned to a contact pair. Cohesive behavior can be assigned to contact pairs using surface-to surface formulation, with the exception of finite sliding. It is often desirable in debonding applications for the cohesive surfaces to begin the analysis just touching each other. A cohesive behavior with eligible slave nodes with “only slave nodes initially in contact” was used as well as a traction separation method with the “default contact enforcement method” [70].

Regarding interaction properties, “surface-to-surface” contact interaction was selected for cohesive behavior, which describes contact between two deformable surfaces or between a deformable surface and a rigid surface. “Node to surface” was selected for the discretization method. The contact conditions were established such that each “slave” node on one side of a contact interface effectively interacts with a point of projection on the “master” surface on the opposite side of the contact interface [70].

The mesh for the samples was created using standard linear solid elements C3D8R (8-node linear brick, reduced integration, hourglass control). These three-dimensional continuum elements allow stress and displacement analysis. Hex-dominated element shape and sweep technique were used for more accuracy of the simulated model [70].

5.4. Experimental and Modeling Results

The developed model is verified through comparison with experimental data. The typical bond strength distributions in the different zones at the interface are shown in Figure 5.3 and Figure 5.4.

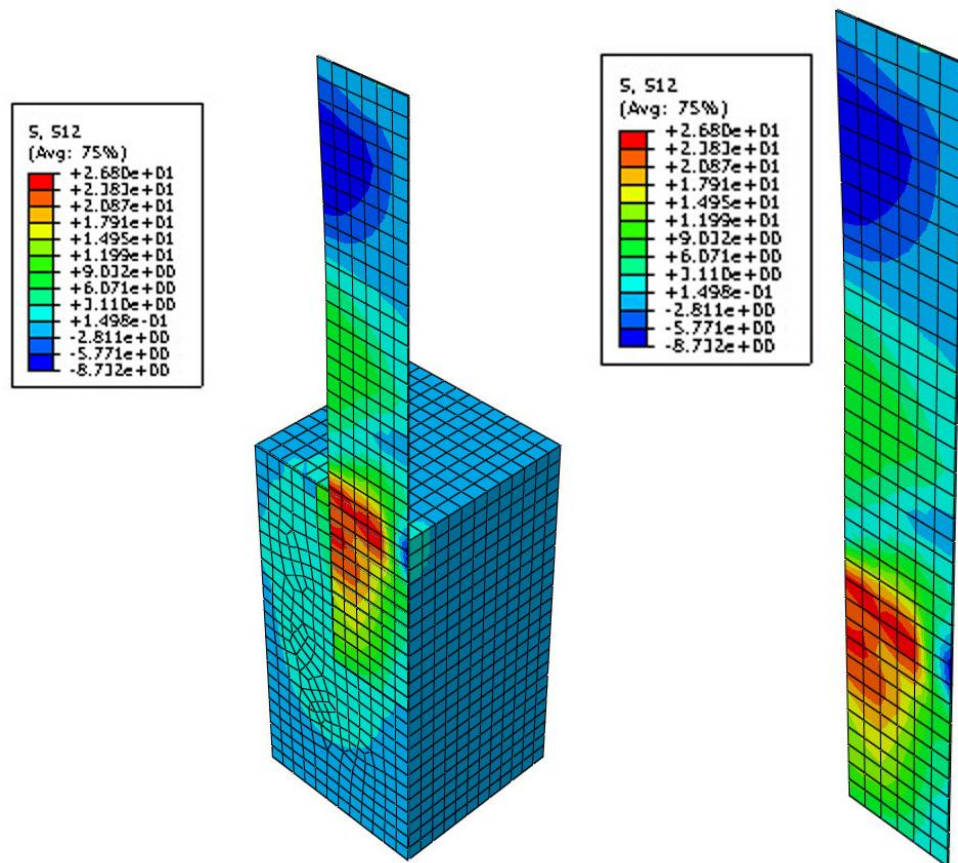


Figure 5-3 Typical shear stress distributions for concrete and steel without holes

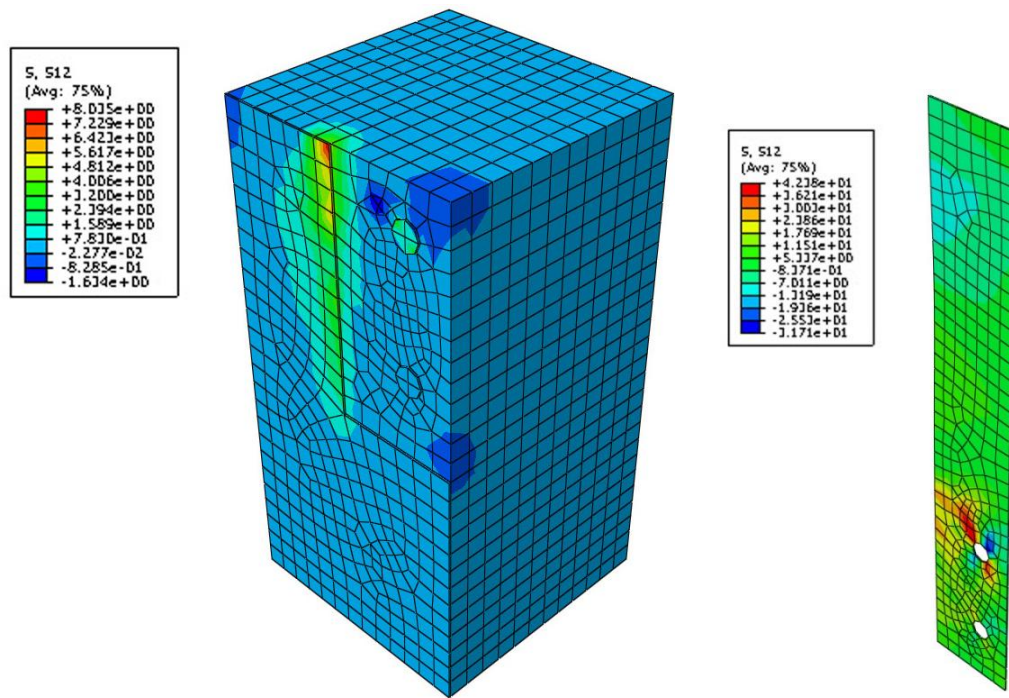


Figure 5-4 Typical bond strength distributions for concrete and steel with 4 holes of 2.83 mm radius

The analysis of the shear stress values obtained from ABAQUS modeling revealed that maximum stress concentrations were located at the top of the concrete block for all finite element models, as shown in Figure 5.5 to Figure 5.10. It confirms the failure initiation at this zone.

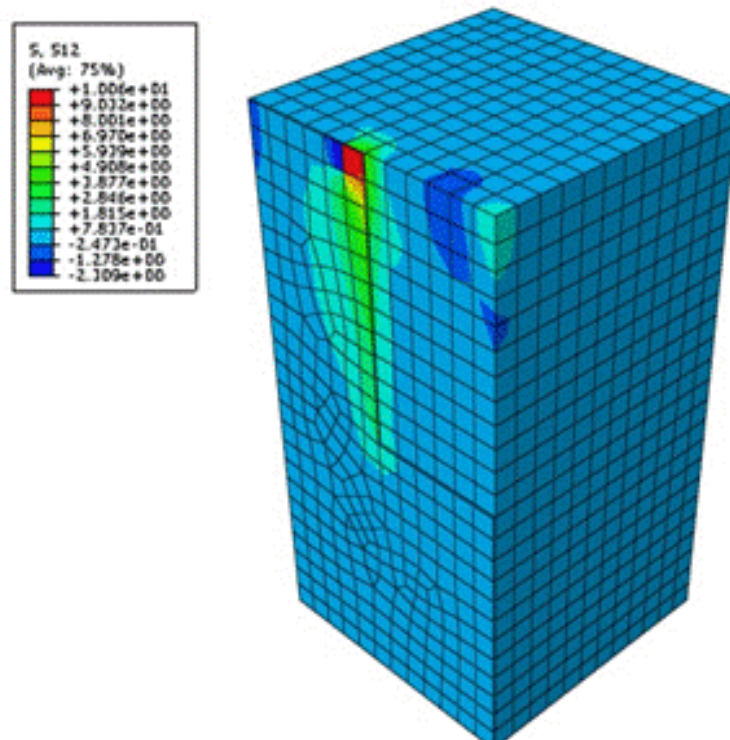


Figure 5-5 Stress concentration zone in [MPa] for S0 steel strip

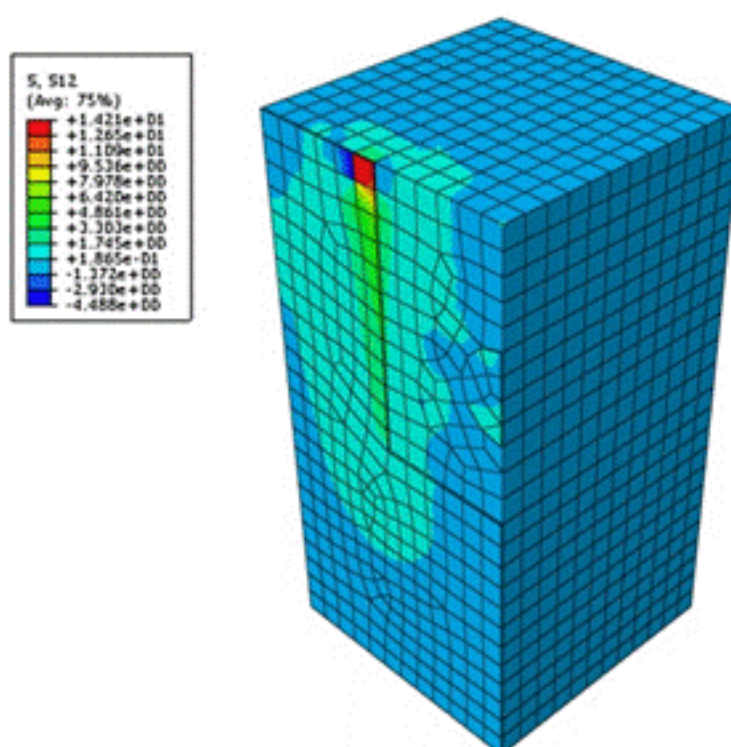


Figure 5-6 Stress concentration zone in [MPa] for S1-8 steel strip

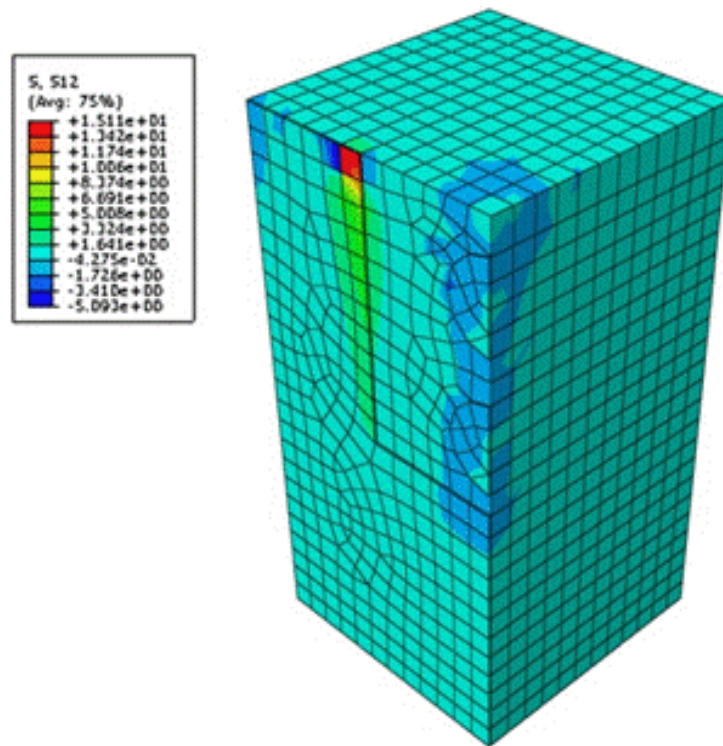


Figure 5-7 Stress concentration zone in [MPa] for S2-8 steel strip

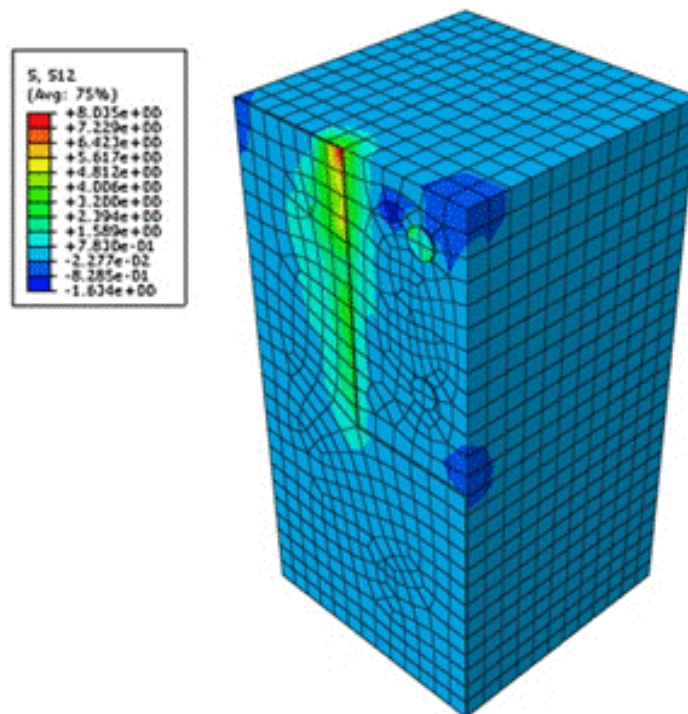


Figure 5-8 Stress concentration zone in [MPa] for S4-3 steel strip

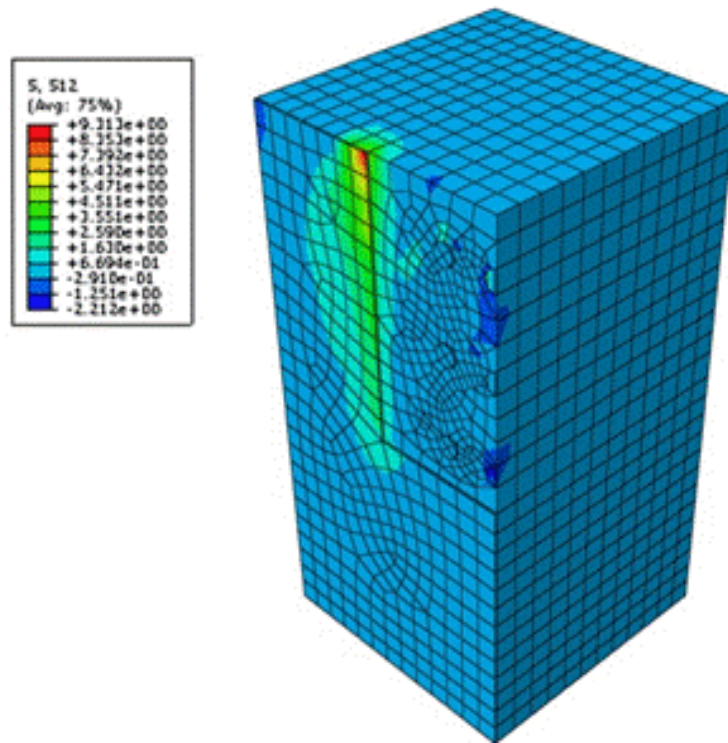


Figure 5-9 Stress concentration zone in [MPa] for S9-2 steel strip

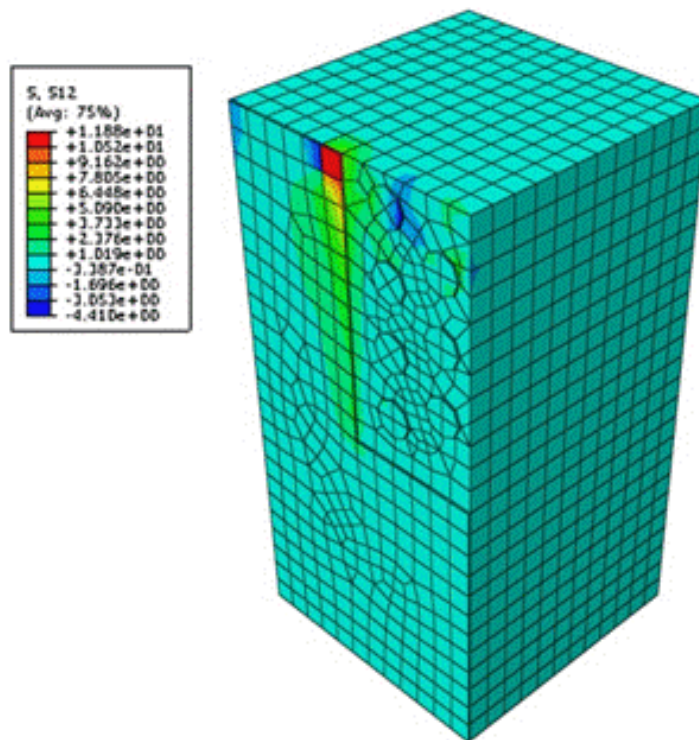


Figure 5-10 Stress concentration zone in [MPa] for S14-3 steel strip

For evaluation purposes three experimental curves were obtained from the pull-out tests. The simulation results obtained from the Abaqus modeling averages

the experimental data. Figure 5.11 and Figure 5.12 present the relationship between displacement and load for only two of the ten patterns (S0 and S4-3). Detailed load-displacement curves for the ten hole patterns are included in Appendix D. The relationship between displacement and pull-out force in the simulation is again similar to that observed in the experimental model.

The contour plots are generated automatically in ABAQUS and the colors depend on the level of stress in the concrete block. The difference in the level of stresses in the concrete block due to differences in the hole patterns can be seen.

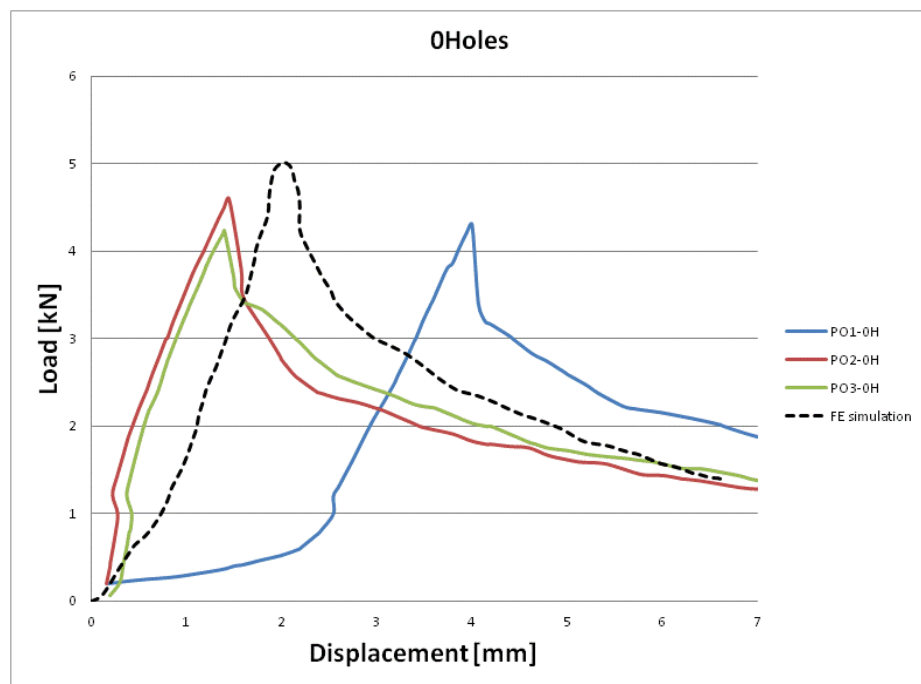


Figure 5-11 Load-displacement curves for S0 sample

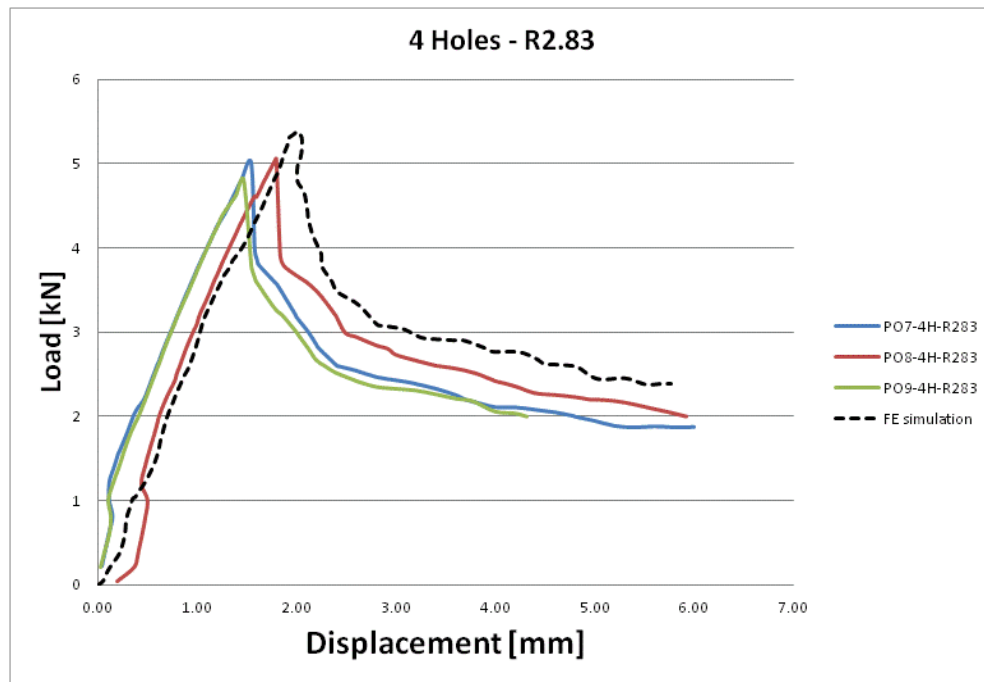


Figure 5-12 Load-displacement curves for S4-3 sample

A comparison of data collected from pull-out experiments and FE simulations are provided in Table 5.3.

Table 5.3 Comparison between FE and experimental results

	Experimental results		FE simulation results		FE-Experimental results differences	
Hole pattern	Max load [kN]	Displacement [mm]	Max load [kN]	Displacement [mm]	Δ load [%]	Δ displacement [%]
S0	4.3806	2.2882	5.0030	2.0510	14.21%	-10.37%
S1-6	5.0355	1.6870	5.3416	2.2897	6.08%	35.73%
S1-8	5.1523	2.0273	5.5950	2.7931	8.59%	37.78%
S1-14	4.9742	2.0394	5.2701	1.5866	5.95%	-22.20%
S2-8	5.4635	2.3613	5.8370	2.3153	6.84%	-1.95%
S4-3	4.9541	1.6057	5.3738	2.0145	8.47%	25.46%
S4-7	5.7837	2.5365	6.2553	2.6206	8.15%	3.31%
S9-2	5.3549	2.1467	6.1664	2.5351	15.16%	18.09%
S9-5	6.1532	3.1377	6.8025	2.6376	10.55%	-15.94%
S14-3	6.3898	2.6388	7.6226	2.9100	19.29%	10.28%

The difference in force between FE simulations and experimental results is less than 10% for six of the ten hole patterns. This may be attributed to variations in

the pull-out test experiments and the FEM only being an approximation of reality.

Finally, pull-out strength was plotted over HCAR in order to compare FE simulation with experimental results. Similar distributions of data were obtained with the model and also a better correlation coefficient ($R^2=0.9753$) than from the experiments, as shown in Figure 5.8. This points towards variations in the experimental data, which can be overcome by increasing the sample size further.

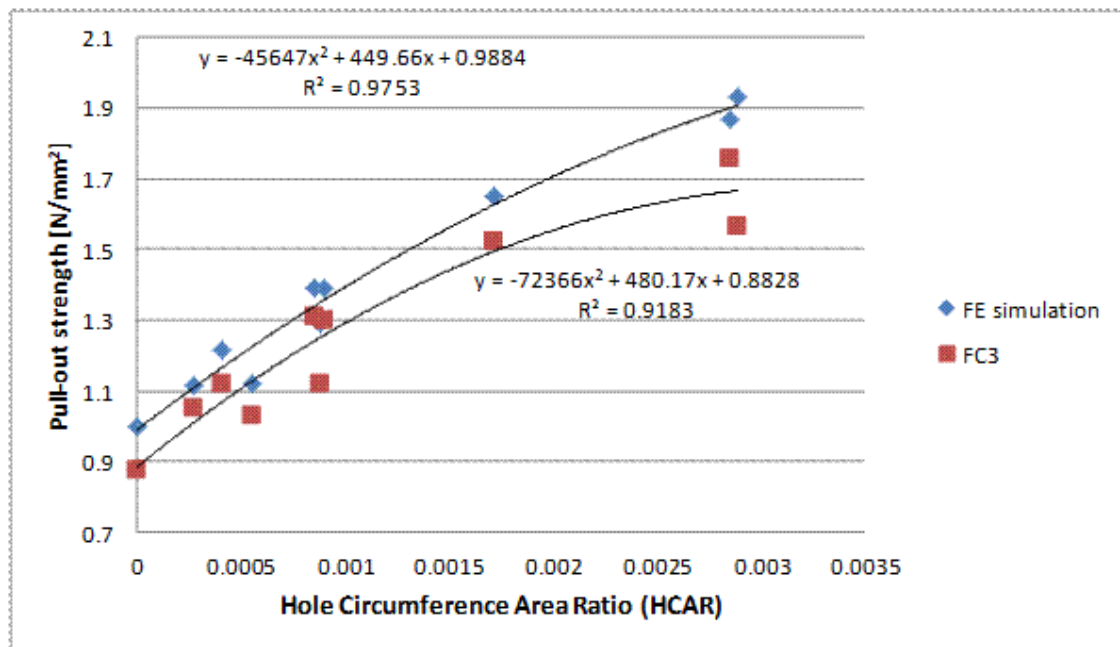


Figure 5-13 The effect of hole circumference area ratio (HCAR) on pull-out strength for FE simulation and FC3.

The concrete mixture gained pull-out strength by increasing the hole circumference area ratio, which indicates that more concrete contained in a larger circumference and diameter holes results in greater pull-out strength.

The FE results were always higher than the experimental results in terms of maximum pull-out force. The difference between the experiments and FE

simulations is generally due to the material model and the friction model implemented to the FE simulation. In general, all FE simulations show the same trend and predict slightly higher max pull-out force in all cases. This shows the consistency of the FE simulations and together with the fact that the errors are relatively in the same range, ensures that the FE model works properly. The reason that the FE model predicts higher pull-out force could be due to the values of the coefficient of friction and/or material data used in simulations. In general, for the same coefficient of friction and cohesive model, the same trend for all hole patterns was obtained. The main results of evaluation of the pull-out strength of galvanised steel strips in a cement-based material were published in [72].

5.5. Conclusions

This study demonstrates the use of a finite element model to simulate the bonding behavior between aerated concrete and perforated steel plates. The results clearly show that there is a good agreement of cohesive behavior between modeling and experimental results. Therefore, this model and its parameters may help to develop a predictable pull-out force with different geometries of steel plates in future design solutions.

CHAPTER 6

6. Conclusions and Recommendations for Further Studies

6.1. Overview

This study focuses on the development of novel infill materials for applications in Composite Structural Assemblies and investigates the bonding performance between steel and infill materials.

This project involves the experimental determination of mechanical properties of foam concrete. Additionally, this study presents the physical and functional characteristics of different mix compositions of ultra-lightweight concrete, as well as the bonding behaviour between foam concrete and steel strips.

Galvanized steel strips were used plain and perforated with holes of various numbers and patterns in order to verify the effect of the anchorage of concrete embedded into holes. Diverse components were researched to obtain a required lightweight concrete, such as a plasticizer, lightweight aggregates, foaming agents, and mineral admixtures. Three foam concrete (FC) mix compositions were prepared with desired densities of 800, 1000 and 1200 kg/m³, and ultra-lightweight concretes (ULWC) were prepared with desired densities of 150, 200, 250 and 400 kg/m³. The compressive strength obtained for FC were between 0.91 and 23 N/mm² while for ULWC were between 0.07 and 2.1 N/mm².

6.2. Conclusions

Based on the analysis of all test results generated in this research, the following conclusions are drawn:

1. Infill Materials

The developed different mix compositions of lightweight concrete were analysed regarding mechanical properties (compressive strength), physical (density) and functional characteristics (fire resistance), as well as the adhesion between foam concrete and steel strips. The investigation confirms that the compressive strength decreases exponentially with the reduction in density of lightweight aerated concrete. The mechanical and functional properties of this foam concrete are influenced not only as far as the density of the concrete is concerned, but also by the cement content, water/cement ratio, foam type and curing method.

All casting densities of foam concrete were on average within 7% of the targets, while for ULWC the casting densities on average were close to 10% of the targets. This may be due to bubbles not able to resist the physical and chemical forces imposed during mixing. Thus, it would be recommendable to take extra precautions during mixing, as intense mixing more likely destroys some bubbles of the foam, increasing the density of the foam concrete.

Fire resistance is also an important parameter to understand as this ultra-lightweight concrete made with EPS beads might be used as infill material for wall panels. These infill materials should be designed with a density greater than 250 kg/m^3 , as the insulation failure criterion (160°C) applied during the fire

tests indicated sufficient fire resistance compared with less dense lightweight concretes, being the percentage of cement a significant parameter for fire resistance properties. In addition, an innovative ultra-lightweight concrete made with EPS beads was developed at 150 kg/m^3 density, which could be a potential filler material for wall systems, if a suitable layer of fire insulation is added to reduce the fire risk.

2. Experimental Bonding Tests

Most of the previous investigations of bonding behavior focused mainly on experimental and theoretical studies of shear stress between reinforcing bars and concrete specimens, plastic bars and concrete samples but not directly on steel walls and steel strips for that matter. This study takes a novel approach to discovering quantitative results by studying pull-out strength of various lightweight insulating concrete mixes and various geometrical patterns of steel strips.

Significant improvements for strips with holes over the pull-out forces of strips without holes were confirmed through a comparative analysis of pull-out tests.

A negative effect on pull-out forces was observed for lower concrete densities than 915 kg/m^3 , caused by the loss of surface adhesion area of the strip, which is not compensated by the shear strength of the concrete in the holes.

The hole circumference area ratio (HCAR) is the best parameter for the analysis for different widths and thicknesses of steel plates, as it has stronger and positive correlation of data than sum of area of holes or sum of diameter of holes. The largest increase in pull-out strength of 46% was found for samples

with 9 holes of 5 mm radius (S9-5) in comparison with steel strips without holes. In addition, HCAR considers not only different hole patterns but also different widths and thicknesses of steel strips.

A larger hole circumference area ratio increases the pull-out strength, which means that more concrete contained in a larger circumference results in greater pull-out strength.

3. Theoretical Bonding Model

The search of the literature reveals that very little quantitative information about bonding behavior between lightweight concrete and steel strips is available, and theoretical modeling of the bond between both materials is practically non-existent. This study develops a Finite Element Model (FEM) for pull-out strength simulation based on the experimental results of various lightweight concretes and various geometrical configurations of the steel strips.

A very good agreement of cohesive behavior between 3-D modeling and experimental results was obtained with the simulation, i.e. the relationship between displacement and pull-out force in the simulation is similar to that observed in the experimental results.

The difference on average between FE simulations with the chosen parameters and experimental results is less than 10% for six of the ten hole patterns. This difference may be attributed to variations in the pull-out test experiments, which were based on three repetitions per data point.

6.3. Recommendations for Further Study

The presented research in this thesis can be developed further and the following recommendations may help to proceed the study.

1. Infill Materials

There have been few studies concerning ultra-lightweight concrete as infill material for composite panels. The current research has focused on finding an insulating concrete which can be used as a potential infill material for composite systems, by verifying its properties, and assessing the influence of its components on low density concretes.

Ultrafoam was used as the foaming agent and Quick Gel as the viscosifier to produce firm and stable foam. These components were mixed with water in a foam generator, until the foam bubble size was uniform and stable. However, appropriate precautions (the foam preparation system, the kind of foaming agent, foam concrete mix preparation, the exact percentage of additives, and the duration of the mixing process) must be taken when preparing foam concrete to prevent differences between casting densities and target densities.

The majority of the previous researches obtained lightweight concrete densities between 600 to 1900 kg/m³. The lightest LWC was developed by Laukaitis et al. However, the fire performance of products containing EPS was not quantified by them. Therefore, the current research focused on insulating concretes, as they have sufficient strength for the intended application, low densities and better thermal insulation.

This study considered a primary approach about functional characteristics in small scale experiments of wall panels. Therefore there are other variables to be considered in future research, for instance determination of the effect on fire performance of full-scale sandwich panels, investigation of the contribution of the developed infill materials in full-scale sandwich panels on fire resistance under monotonic loading, and analysis of the bonding behaviour between the infill materials and steel sheet in full-scale sandwich panels under monotonic loading. Further experiments on full-scale sandwich panels can be undertaken to mitigate the fire risk further by adding a suitable layer of fire insulation.

2. Pull-out Experiments

Results of this investigation show that holes in steel strips should be applied for concrete densities greater than 915 kg/m^3 , as a negative effect on pull-out forces was found for lighter concretes.

This is the first study of holes in strips, and there are more factors to be investigated in future research. Therefore, future studies could consider new specimens with additional geometrical configurations of steel strips to understand the effect of these parameters on pull-out strength of aerated concrete, for example, rather than round holes, use triangular holes or square holes, or holes cut at angles rather than straight through the steel. Additional studies should be undertaken to analyse the effect of interlocking between a steel plate and aerated concrete elements through embossments on the profiled steel sheets, which bear the horizontal shear force.

Future research should be undertaken to analyse microcracks in the foam concrete during pull-out tests through a non-destructive procedure and by

microscopy to understand its behaviour under loading and to improve this composite.

Additional studies should also be undertaken to analyse the effect of bolts in pull-out tests, as well as a FE simulation could be developed to assist the understanding of the roll of bolts in the concrete.

3. Theoretical Modeling

The current research marks an important first step in developing a program on quantitative information about bonding behavior between lightweight concrete and perforated steel strips, and FE modeling of the bond between both materials. Additional modeling of full-scale sandwich panels can be undertaken to analyse the bonding behaviour between foam concrete and steel strips by using the parameters established in this study and this could further verify the findings.

Appendix A. Sikament HE200

The appendix contains the specifications of superplasticizer Sikament HE200 used to prepare the foam concrete.

Construction

Product Data Sheet
Edition 1,2005
Identification no. CA-4
Version no.1

Sikament®-HE 200

Concrete Admixture for High Early Strength Concrete


Product Description	Sikament®-HE 200 is a superplasticizer and accelerator for concrete and mortar. It promotes high early strengths in concrete without negatively influencing the final strengths. Suitable for use in tropical and hot climatic conditions.
Uses	Sikament®-HE 200 is being used in ready-mix-plants and pre-cast yards, where high early strengths after 8 - 24 hrs are required. The use of Sikament®-HE 200 facilitates early trowelling and smoothing of the concrete surface at low temperatures without loss of cohesion. Therefore, the product is highly suitable for the production of slabs and soffit systems especially in winter when concrete is not vacuumed. Sikament®-HE 200 does not contain chlorides and may be used without any restrictions for reinforced concrete and pre-stressed concrete. However, it should not be used together with expansive and shrinkage compensating admixtures.
Advantages	Sikament®-HE 200 causes a much better cement dispersion, resulting in a concrete of plastic consistency without loss of cohesion. Depending on the dosage of Sikament®-HE 200, the w/c ratio may be reduced by more than 10 %, at the same time producing an increase of high early strengths of more than 50% in comparison with a normal Sikament enhanced concrete. Should even higher early strengths be required, Sika Rapid-1 may be added to the concrete.
Test Standards	Sikament®-HE 200 complies with ASTM C-494 Type C & F and EN 934-2:2001 depending upon dosage and mix.

Product Data

Type	Organic polymer and blends
Form	Brown Liquid
Packaging	200 lt. drums and 1000 lt. flow bins Bulk supply in tanker trucks is possible on demand
Storage Condition	Store in a dry area between 5°C and 35°C. Protect from direct sunlight
Shelf life	12 months minimum from production date if stored properly in original unopened packaging

Technical Data

Density	Approximately 1.20 kg/lit
----------------	---------------------------



Sikament®-HE 200 1/2

pH value	Approximately 8.5
Chloride content	Nil (EN 934-2)
Application Details	
Dosage	1.2 - 3.0 % by weight of cement for high early strengths, plastic concrete. It is advisable to carry out trial mixes to establish the correct dosage.
Dispensing	Sikament®-HE 200 is added to the gauging water or is poured into the concrete mixer simultaneously with the gauging water. It may also be added into the transit mixer at the place of discharge. In this case after its addition a mixing time of at least one minute per m³ concrete must be observed. Prior to its discharge, the concrete must be checked visually for uniform consistency.
Concrete Placing	With the use of Sikament®-HE 200, concrete of high quality is produced. The standard rules of good concreting practice (production as well as placing) must also be observed with Sikament®-HE 200 concrete.
Compatibility	Sikament®-HE 200 can be combined with Sika Rapid-1, Sika Fume, SikaPump, Sika-Aer and Plastiment admixtures. Pre-trials are recommended for combinations with this product. Do not combine Sikament®-HE 200 with expansive admixtures, such as Intraplast EP, Intracrete EH etc. It is also compatible with sulfate resistant cement.
Curing	Fresh concrete must be cured properly, especially at high temperatures in order to prevent plastic and drying shrinkage. Use Sika Antisol products as a curing agent or apply wet hessian.
Cleaning	Clean all equipment and tools with water immediately after use.
Remarks	When accidental overdosing occurs, the set retarding effect increases. During this period the concrete must be kept moist in order to prevent premature drying out.
Notes	All technical data stated in this Product Data Sheet are based on laboratory tests. Actual measured data may vary due to circumstances beyond our control.
Safety	For information and advice on the safe handling, storage and disposal of chemical products, users should refer to the most recent Material Safety Data Sheet containing physical, ecological, toxicological and other safety-related data.



Sika Gulf B.S.C (c)
 Bldg. 825, Road 115, Siba Area 601
 P.O. Box 15776
 Adiya, Kingdom of Bahrain
 Tel: +973 17732 180
 Fax: +973 17732 476
 E-mail: sika.gulf@bh.sika.com
 Web: <http://www.sika.com/bh>



Sikament®-HE 200 2/2

Legal Notes

The information, and, in particular, the recommendations relating to the application and end-use of Sika products, are given in good faith based on Sika's current knowledge and experience of the products when properly stored, handled and applied under normal conditions in accordance with Sika's recommendations. In practice, the differences in materials, substrates and actual site conditions are such that no warranty in respect of merchantability or of fitness for a particular purpose, nor any liability arising out of any legal relationship whatsoever, can be inferred either from this information, or from any written recommendations, or from any other advice offered. The user of the product must test the product's suitability for the intended application and purpose. Sika reserves the right to change the properties of its products. The proprietary rights of third parties must be observed. All orders are accepted subject to our current terms of sale and delivery. Users should always refer to the most recent issue of the local Product Data Sheet for the product concerned, copies of which will be supplied on request.



Sika Gulf B.S.C (c)
Bldg. 925, Road 115, Site Area 001
P.O. Box 15776
Adiyah, Kingdom of Bahrain
TEL: +973 17736 100
Fax: +973 17732 470
E-mail: sika.gulf@bh.sika.com
Web: <http://www.sika.com.bh>



Appendix B. Ultrafoam

The appendix contains the specifications of ultrafoam used to prepare the foam for this research.



ULTRA-FOAM®

High Performance Foaming Agent

Description	ULTRA-FOAM, is a biodegradable mixture of anionic surfactants and foaming agents. ULTRA-FOAM can be added to fresh, hard, or high salinity water for airfoam, airgel-foam, or mist drilling applications.	
Applications/Functions	<ul style="list-style-type: none">• Enhance the rate of cuttings removal• Increase the ability of lifting large volumes of water• Improve hole-cleaning capability of the airstream• Reduce the sticking tendencies of wet clays, thereby eliminating mud rings and wall packing• Reduce erosion of poorly consolidated formations• Lowers the compressor requirements for a given depth or water Influx• Increase borehole stability• Reduce air-volume requirement• Suppress dust during air drilling operation	
Advantages	<ul style="list-style-type: none">• Produces high quality foam at low concentrations• Highly stable foam with excellent retention time• Versatile and compatible with in fresh, hard and saline make-up water• Readily undergoes primary and ultimate (>99%) biodegradation• Proven product for multi-discipline application	
Typical Properties	Appearance	Pale red liquid
	Specific gravity	1.03
	Flash point, PMCC °F, °C	NA
	Solubility	Completely soluble in water

© Copyright 2001 Bardol, a Halliburton PSI.

ULTRA-FOAM, SZ-FLUID, QUIK-TRICE, and QUIK-GEL are registered trademarks of Halliburton Energy Services, Inc.

Rev. 6/2001 - IOP 010

Because the conditions of use of this product are beyond the seller's control, Bardol suggests that the purchaser make its own test to determine the suitability for the purchaser's application. Purchaser assumes all risks of use and handling of this product. This product will be replaced if defective in manufacture or packaging. Except for such replacement, seller is not liable for any damages caused by this product or its use. EXCEPT AS EXPRESSLY PROVIDED FOR ABOVE, THIS PRODUCT IS PROVIDED "AS-IS" AND BARDOL MAKES NO OTHER WARRANTIES WITH RESPECT TO THIS PRODUCT. BARDOL DISCLAIMS ALL OTHER EXPRESS OR IMPLIED WARRANTIES, INCLUDING ANY WARRANTIES OF MERCHANTABILITY, ACCURACY OF DATA, FITNESS FOR A PARTICULAR PURPOSE, OR NON-INFRINGEMENT.

Recommended Treatment

Approximate Amounts of ULTRA-FOAM® Added to Injection Water			
Application	/100 gal	/bbl	Liters/m ³
Dry-air drilling (as a dust suppressant)	0.5 - 1 pints	0.2 - 0.5 pints	0.5 - 1.5
Mud-mist drilling in sticky clays	1 - 2 quarts	1 - 2 pints	2.5 - 5
Stiff Foam and gel-foam drilling	0.5 - 2 gallons	1.5 - 7 pints	5 - 20
As a slug to clean the annulus	1 pint*	0.5 pints*	0.5**

* In drill pipe, followed by 3 to 5 gallons of water; ** followed by 20 liters of water

Note:

Product Make-up for Air Drilling Injection Slurries				
Main Ingredient of Injection Slurry	Water (Litres)	QUIK-GEL® viscosifier (kg)	QUIK-TROL® polymer (kg)	ULTRA-FOAM foaming agent (% by volume)
Foam Drilling	1000	---	---	0.02 - 3.0
Mixing/Injection Procedure Add ULTRA-FOAM to injection water. Inject into the air stream at a rate necessary to maintain hole stability and penetration rate. Increase amount of ULTRA-FOAM as required to compensate for downhole water dilution.				
Stiff-Foam Drilling	1000	---	0.25 - 0.5	0.1 - 2.0
Mixing/Injection Procedure Mix polymer with water before adding ULTRA-FOAM. 0.5-1.0 Litre of EZ MUD® may be used as a substitute for QUIK-TROL. Inject into the air stream at a rate necessary to maintain hole stability and penetration rate.				
Mud-Mist Drilling System	1000	30	---	0.3 - 1.0
Mixing/Injection Procedure Mix viscosifier with water before adding ULTRA-FOAM. Inject into the air stream at a rate necessary to maintain hole stability and penetration rate. Resulting viscosity is 32-40 sec/qt as measured by Marsh Funnel.				
Gel-Foam Drilling System	1000	15-18	0.5	0.3 - 1.0
Mixing/Injection Procedure Mix viscosifier and polymer with water before adding ULTRA-FOAM. Inject into the air stream at a rate necessary to maintain hole stability and penetration rate. Resulting viscosity is 32-40 sec/qt as measured by Marsh Funnel.				

Note:

In some states, it is illegal to discharge any foreign substance into the water shed due to potential contamination of ground water. After use, the foam mixture must be localized in an earthen pit or some type of containment and allowed to biodegrade naturally.

Packaging ULTRA-FOAM® is packaged in 25 Litre plastic containers or in 205 Litre drums.

Availability ULTRA-FOAM can be purchased through any Baroid Industrial Drilling Products Distributor. To locate the Baroid IDP distributor nearest you contact the Customer Service Department in Houston or your area IDP Sales Representative.

Baroid Industrial Drilling Products,
A Product and Service Line of Halliburton Energy Services, Inc.
3000 N. Sam Houston Pkwy E.
Houston, TX 77032

Customer Service (800) 735-6075 Toll Free (281) 871-4612

Technical Service (877) 379-7412 Toll Free (281) 871-4613

IDP Australasian +61 (0)417 099 354 +61 (0)414 557 917

Appendix C. Quick Gel

The appendix contains the specifications of quick gel used to prepare the foam for this research.



QUIK-GEL®

Viscosifier

Description QUIK-GEL is an easy-to-mix, finely ground (200-mesh), premium-grade, high-yielding Wyoming sodium bentonite. QUIK-GEL imparts viscosity, fluid loss control and gelling characteristics to freshwater-based drilling fluids.

Applications/Functions

- Mix with fresh water to form a low-solids drilling fluid for general drilling applications
- Viscosity water-based drilling fluids
- Reduce filtration by forming a thin filter cake with low permeability
- Improve hole-cleaning capability of drilling fluids
- Mix with foaming agents to make "gel/foam" drilling fluids for air/foam drilling applications

Advantages

- ANSI/NSF Standard 60 certified
- Single-sack product and cost effective
- Provides lubricity for drilling fluids
- Mixes easily and quickly reaches maximum viscosity
- Yields more than twice as much mud of the same viscosity as an equal weight of API oilfield grades of bentonite

Typical Properties

- Appearance Grey to tan powder
- Bulk density, lb/ft³ 68 to 72 (compacted)
- pH (3% solution) 8.9

Recommended Treatment Mix slowly through a jet mixer or sift slowly into the vortex of a high-speed stirrer.

Approximate Amounts of QUIK-GEL Added to Freshwater			
Application/Desired Result	lb/100 gal	lb/bbl	kg/m ³
Normal Drilling Conditions	15-25	6-10	18-30
Unconsolidated Formations	35-50	15-21	42-60
Make-Up For Gel/Foam Systems	12-15	5-7	14-18

• 1 bbl = 42 U.S. gallons

Additional Information *Note:*

- For optimum yield, pre-treat make-up water with 1-2 pounds of soda ash per 100 gallons of water (1.2-2.4 kg/m³).

© Copyright 2001 Baroid, a Halliburton PSL

QUIK-GEL is a registered trademark of Halliburton Energy Services, Inc.

Rev. 6/2001 - IDP 009

Because the conditions of use of this product are beyond the seller's control, Baroid suggests that the purchaser make its own tests to determine the suitability for the purchaser's application. Purchaser assumes all risk of use and handling of this product. This product will be replaced if defective in manufacture or packaging. Except for such replacement, seller is not liable for any damages caused by this product or its use. EXCEPT AS EXPRESSLY PROVIDED FOR ABOVE, THIS PRODUCT IS PROVIDED "AS-IS", AND BAROID MAKES NO OTHER WARRANTIES WITH RESPECT TO THE PRODUCT. BAROID DISCLAIMS ALL OTHER EXPRESS OR IMPLIED WARRANTIES, INCLUDING ANY WARRANTIES OF MERCHANTABILITY, ACCURACY OF DATA, FITNESS FOR A PARTICULAR PURPOSE, OR NON-INFRINGEMENT.

Packaging QUIK-GEL® is packaged in 50-lb (22.7-kg) multiwall paper bags.

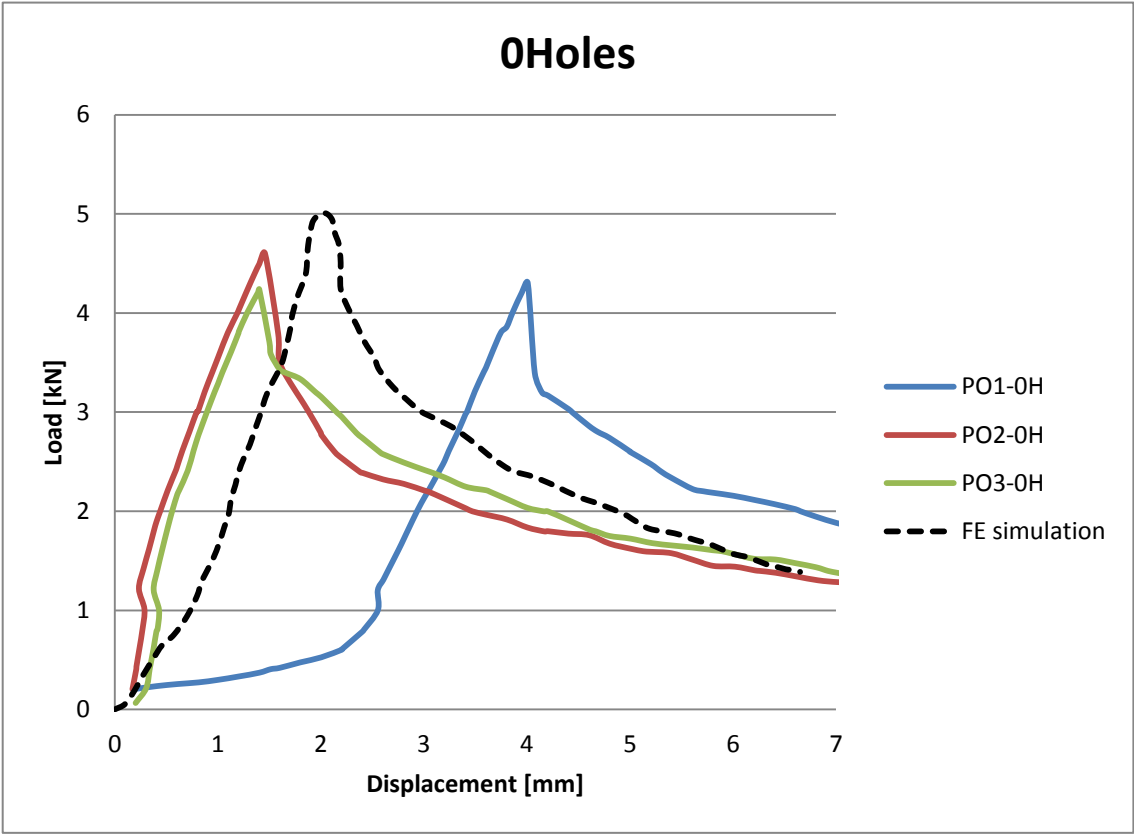
Availability QUIK-GEL can be purchased through any Baroid Industrial Drilling Products Distributor. To locate the Baroid IDP distributor nearest you contact the Customer Service Department in Houston or your area IDP Sales Representative.

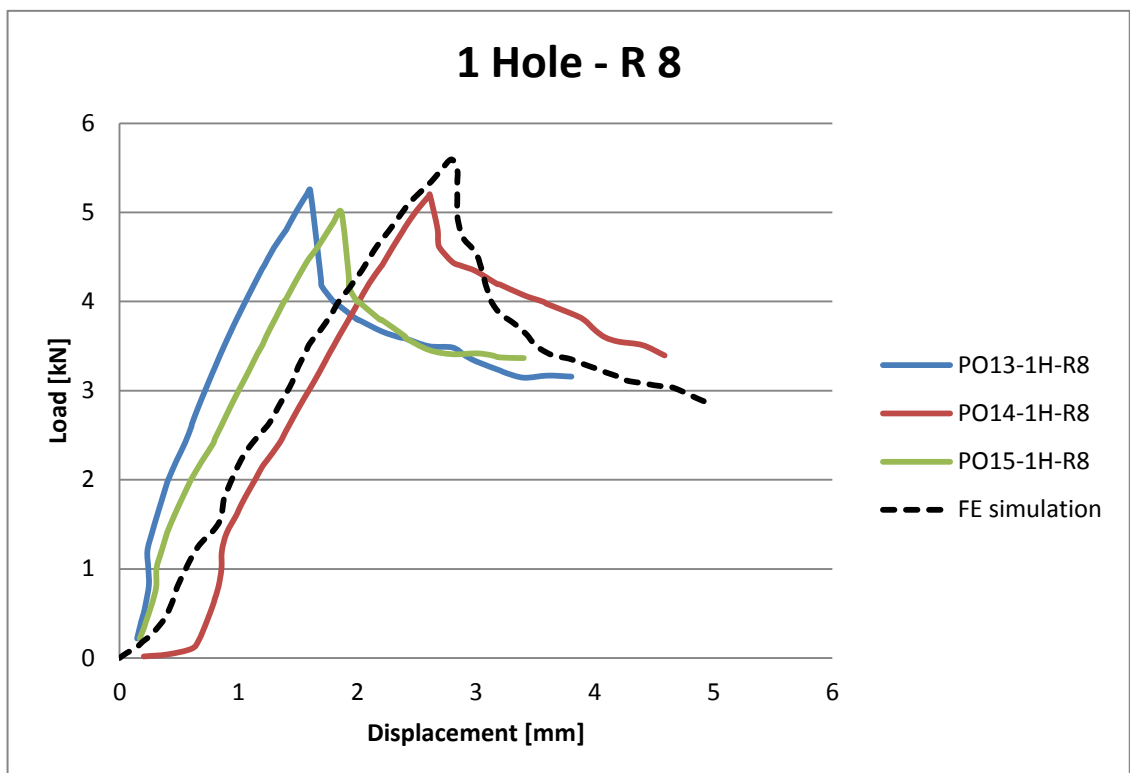
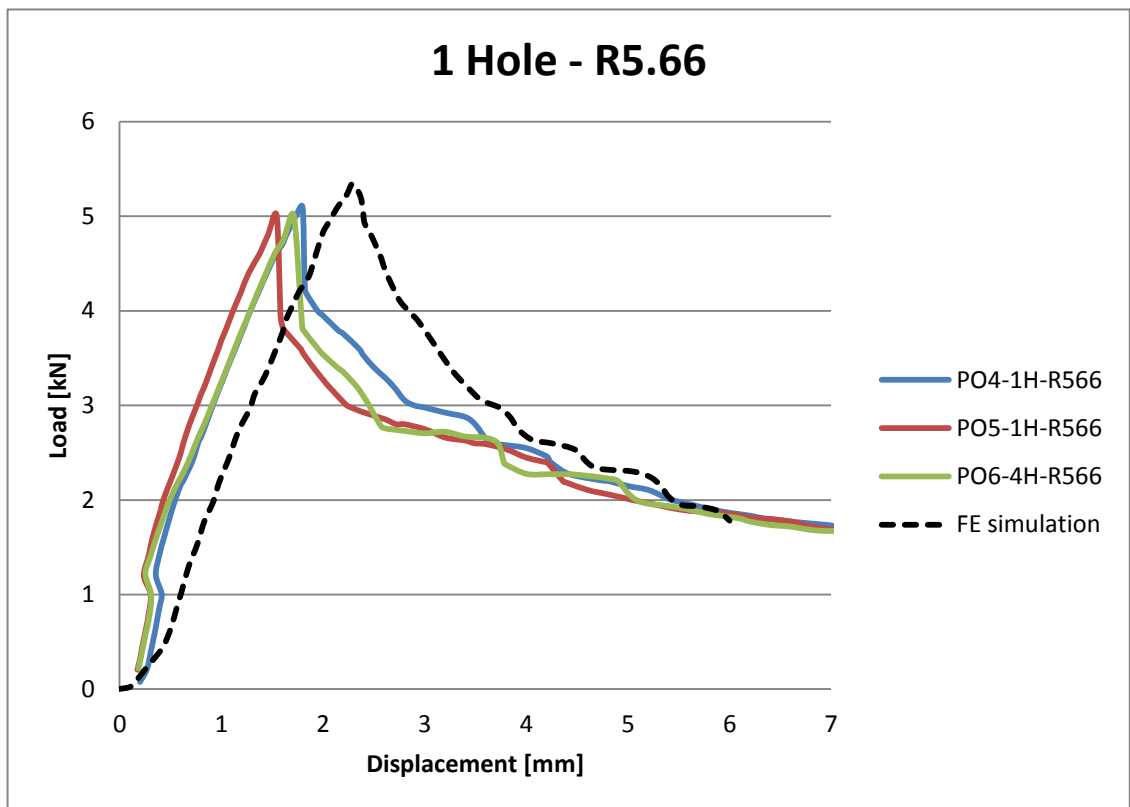
Baroid Industrial Drilling Products,
A Product and Service Line of Halliburton Energy Services, Inc.
3000 N. Sam Houston Pkwy. E.
Houston, TX 77032

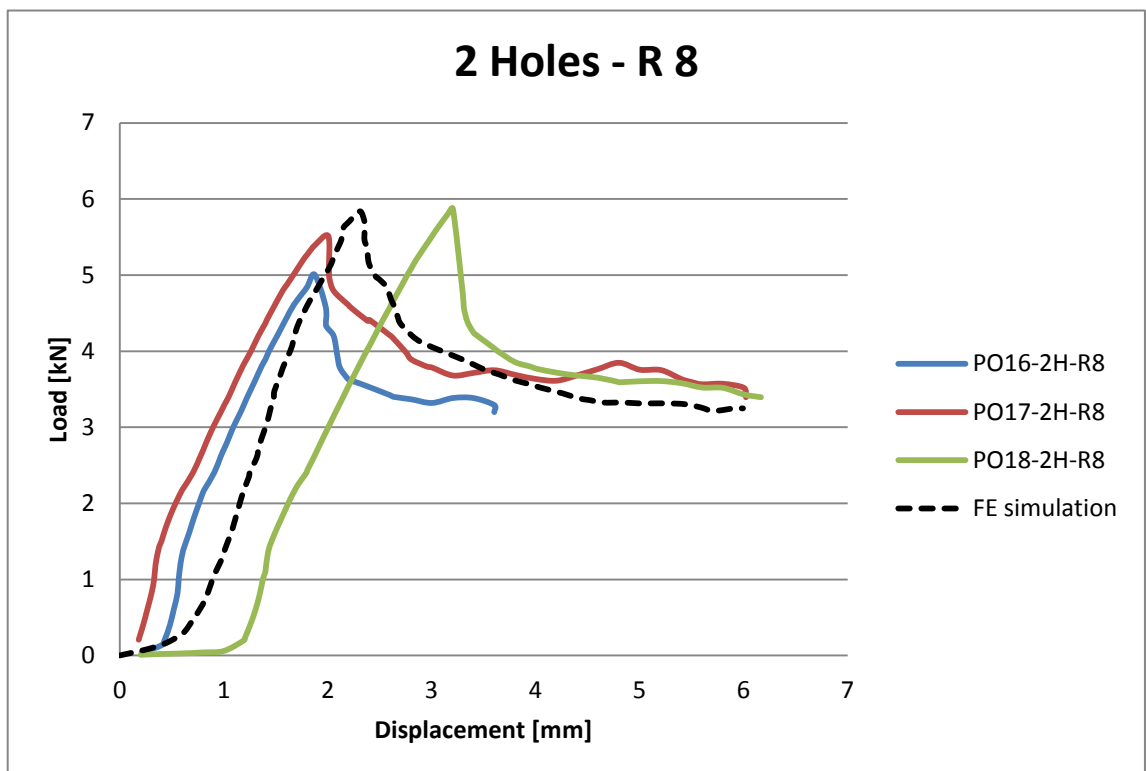
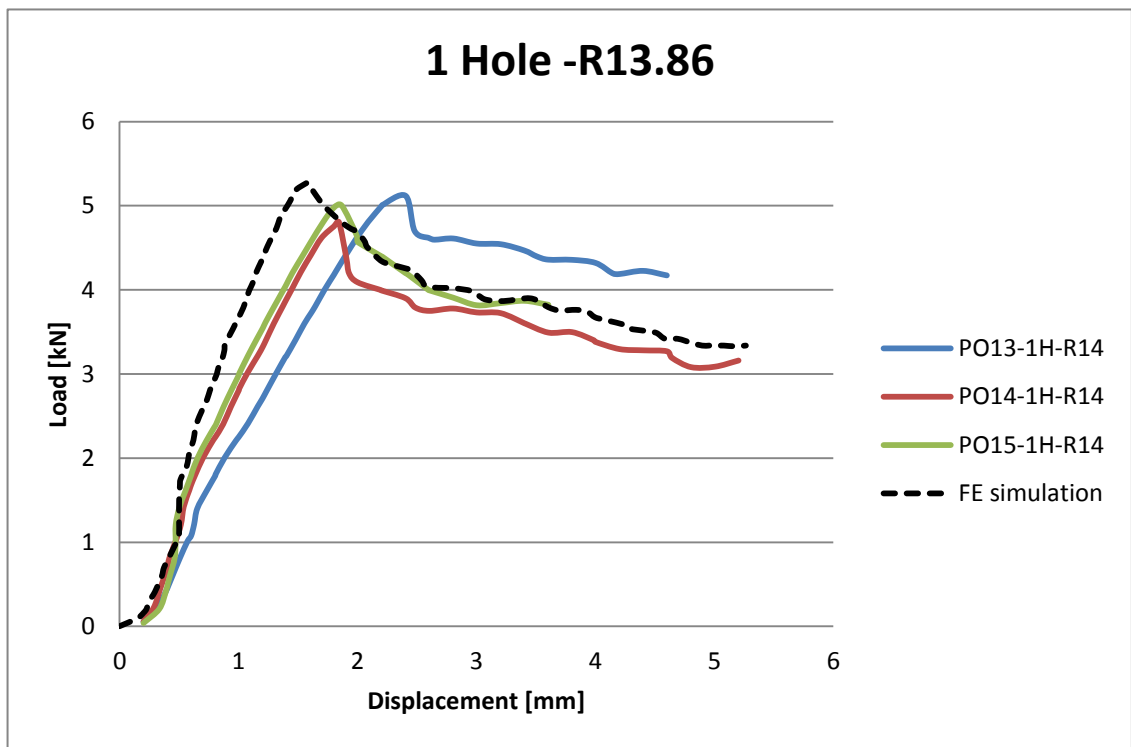
Customer Service (800) 735-6075 Toll Free (281) 871-4612
Technical Service (877) 379-7412 Toll Free (281) 871-4613

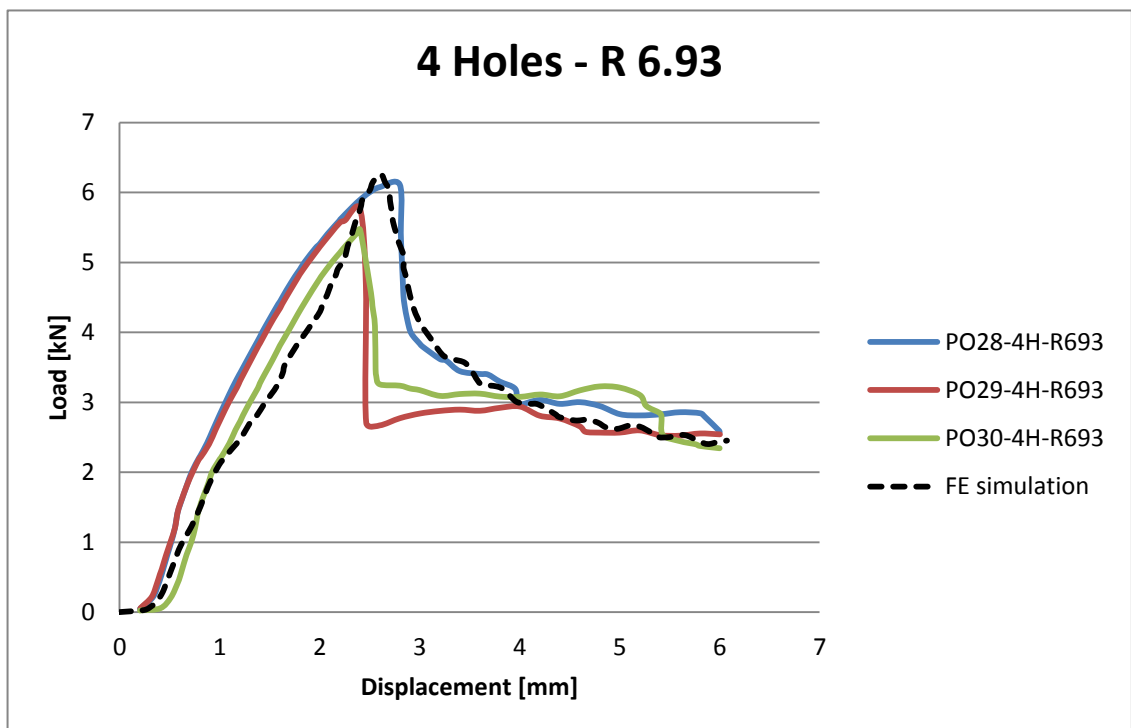
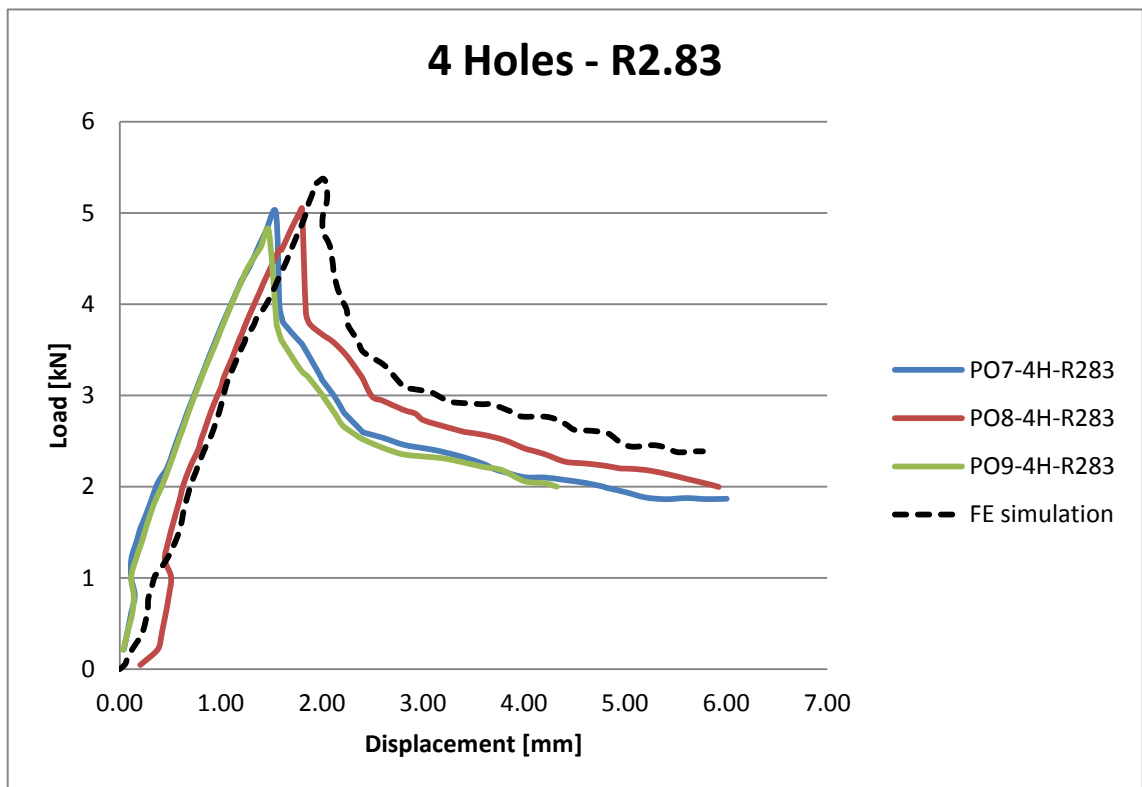
Appendix D. Load Displacement Curves

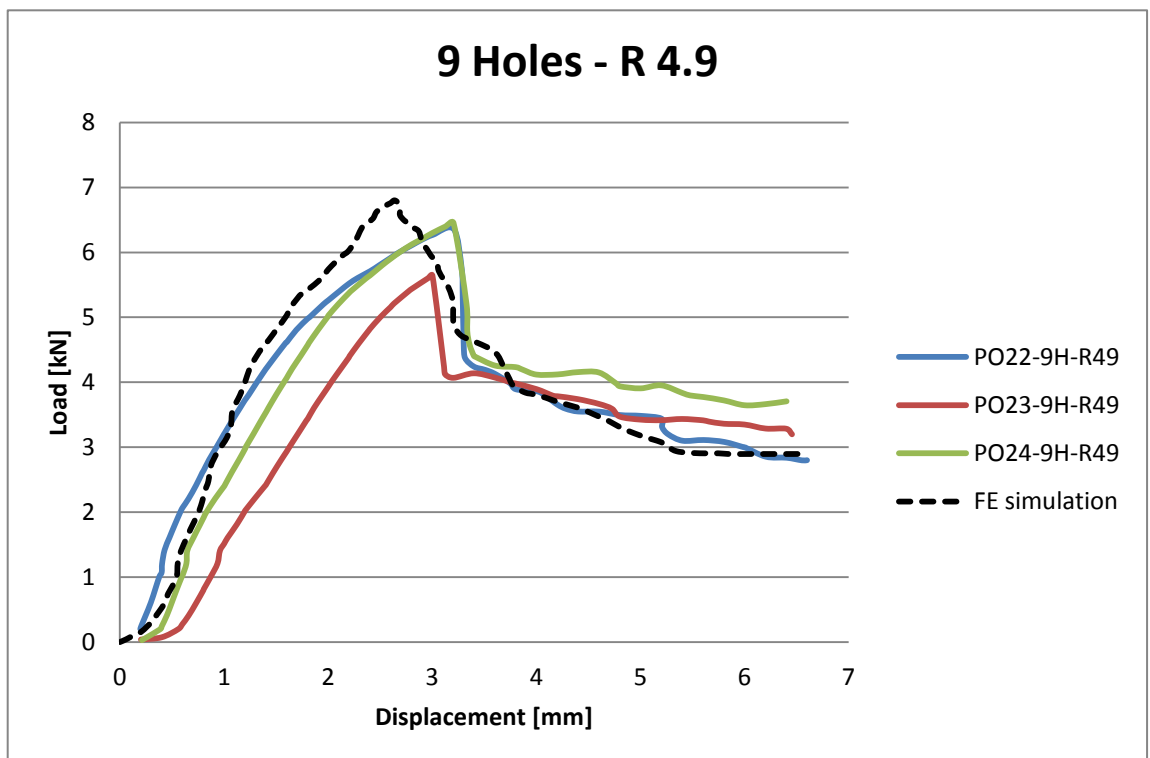
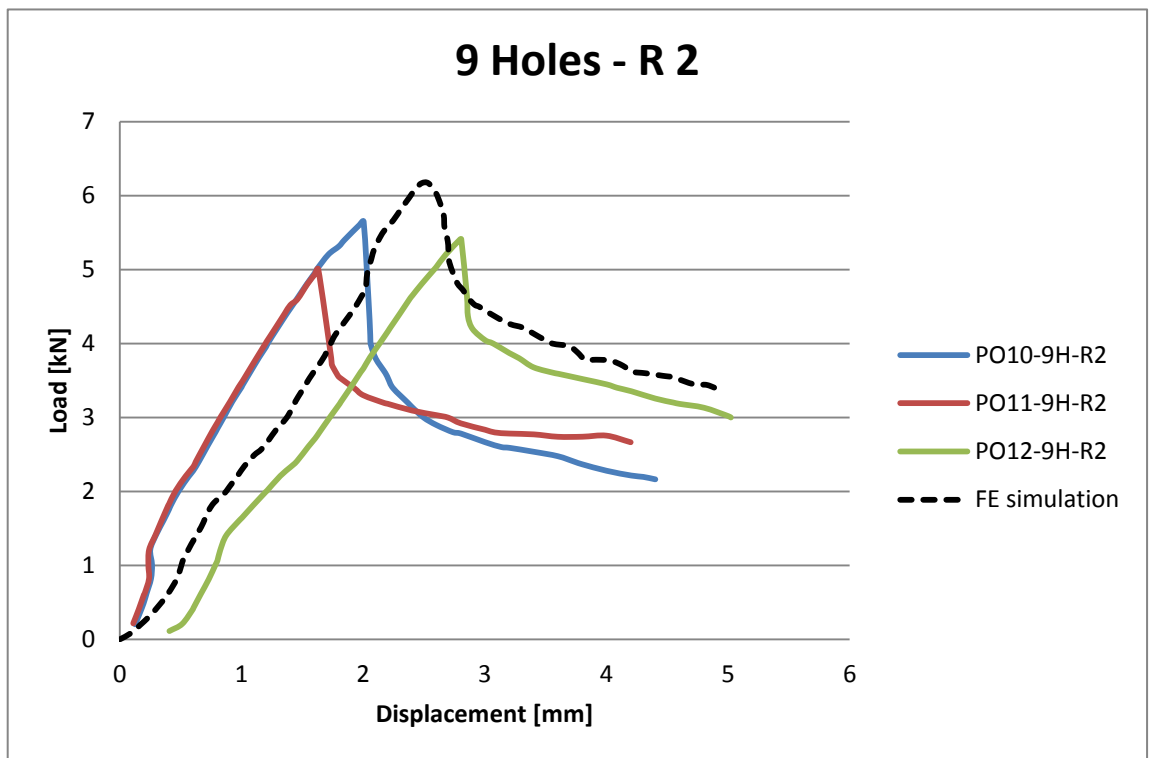
The appendix contains detailed load-displacement curves for the ten hole pattern for this research.

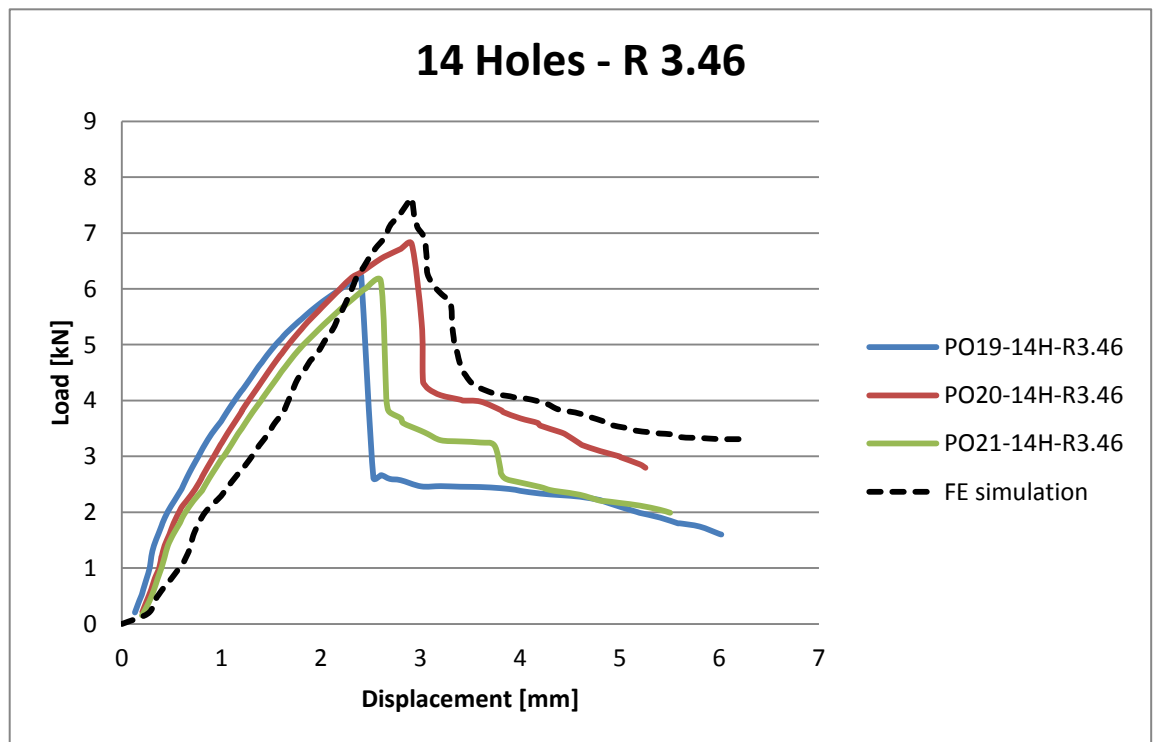












Appendix E. Publications resulting from the research.

The appendix contains the publications resulting from the research.

Alterman D., Vilches J., and Neitzert T., "An Analysis of the Bonding Energy through Pull-out Tests for Aerated Concrete with Various Steel Strip Geometries," *Advanced Material Research*, vol. 275, pp. 55-58, 2011.

Alterman D., Vilches J., and Neitzert T., "Effect of steel strip geometry on pull-out strength of aerated concret," Edited by A.M.Brandt, *Brittle Matrix Composites*, ZTUREK and Woodhead Publ. Ltd., pp. 439-448, 2009.

Ramezani M., Vilches J., and Neitzert T., "Evaluation of the pull-out strength of galvanised steel strips in a cement-based material," *Journal of Zhejiang University SCIENCE A*, vol. 14, pp. 843-855, 2013.

7. References

- [1] C. S. A. Project, "<http://www.uaceer.auckland.ac.nz/uoa/uaceer-csa-research>," 2010.
- [2] C. S. A. Project, "CSA GEMINI Marketing Brochure," *Heavy Engineering Research Association (HERA), Manukau, New Zealand*, 2010.
- [3] Akin O., Gül R., and Cüneyt A., "Effect of steel fibers on the mechanical properties of natural lightweight aggregate concrete," *Materials letters*, vol. 59, pp. 3357-3363, 2005.
- [4] Qian C.X. and S. P., "Development of hybrid polypropylene-steel fibre-reinforced concrete," *Cement and Concrete Research*, vol. 30, pp. 63-69, 2000.
- [5] Balendran R.V., Zhou F., Nadeem A., and Leung A., "Influence of steel fibres on strength and ductility of normal and lightweight high strength concrete," *Building and Environment*, vol. 37, pp. 1361-1367, 2002.
- [6] Song P., Hwang S., and Sheu B., "Strength properties of nylon- and polypropylene-fiber-reinforced concretes," *Cement and Concrete Research*, vol. 35, pp. 1546-1550, 2005.
- [7] Chen B. and Liub J., "Contribution of hybrid fibers on the properties of the high-strength lightweight concrete having good workability," *Cement and Concrete Research*, vol. 35, pp. 913-917, 2005.
- [8] Bekir I. and Canbaz M., "Effect of different fibers on the mechanical properties of concrete containing fly ash," *Construction and Building Materials*, vol. 21, pp. 1486–149, 2007.
- [9] Kunhanandan E.K. and Ramamurthy K., "Air void characterisation of foam concrete," *Cement and Concrete Research*, vol. 37, pp. 221-230, 2007.
- [10] Ramamurthy K., Kunhanandan E.K., and Indu Siva G., "A classification of studies on properties of foam concrete," *Cement & Concrete Composites*, vol. 31, pp. 388-396, 2009.
- [11] Davies J.M., "Lighthweight Sandwich Construction (Book)," *Blackwell Science Ltd*, p. 367, 2001.
- [12] Holm T. and Ries J., "Lightweight Concrete and Aggregates," *ASTM International*, pp. 548-560, 2006.
- [13] Newman J. and Owens P., "Advanced Concrete Technology. Part 2: Properties of Lightweight Concrete," *Elsevier Ltd.*, pp. Chapter 2, 1-27, 2003.
- [14] Neville A., "Properties of Concrete. The English Language Book Society and Pitman Publishing (3rd edition)." 1981.
- [15] Yasar E., Duran C., Kilic A., and Gulsen H., "Strength properties of lightweight concrete made with basaltic pumice and fly ash," *Materials Letters*, vol. 57, pp. 2267– 2270, 2003.
- [16] Gündüz L., "The effects of pumice aggregate/cement ratios on the low-strength concrete properties," *Construction and Building Materials*, vol. 22, pp. 721-728 2008.
- [17] Khandaker M. and Hossain A., "Blended cement and lightweight concrete using scoria: mix design, strength, durability and heat insulation characteristics," *International Journal of Physical Sciences*, vol. 1, pp. 5-16, 2006.

- [18] Kılıç A., Duran C., Yaşar E., and Özcan F., "High-strength lightweight concrete made with scoria aggregate containing mineral admixtures," *Cement and Concrete Research*, vol. 33, pp. 1595-1599, 2003.
- [19] Wang H. and Tsai K., "Engineering properties of lightweight aggregate concrete made from dredged silt," *Cement & Concrete Composites*, vol. 28, pp. 481-485, 2006.
- [20] Le R., Parant E., and Boulay C., "Taking into account the inclusions' size in lightweight concrete compressive strength prediction," *Cement and Concrete Research*, vol. 35, pp. 770– 775, 2005.
- [21] Chen B. and Liu J., "Experimental application of mineral admixtures in lightweight concrete with high strength and workability," *Construction and Building Materials*, vol. 22, pp. 655–659, 2008.
- [22] Jones M. and McCarthy A., "Utilising unprocessed low-lime coal fly ash in foamed concrete," *Fuel*, vol. 84, pp. 1398–1409, 2005.
- [23] Arisoy B. and Wu H., "Material characteristics of high performance lightweight concrete reinforced with PVA," *Construction and Building Materials*, vol. 22, pp. 635-645 2008.
- [24] Karakurt C., Kurama H., and Bekir I., "Utilization of natural zeolite in aerated concrete production," *Cement & Concrete Composites*, vol. 32, pp. 1-8, 2010.
- [25] Kearsley E. and Mostert H., "Designing Mix Composition of Foam Concrete with High Fly Ash Contents," *Use of Foamed Concrete in Construction, International Conference held at the University of Dundee, Scotland, UK*, pp. 29-36, 2005.
- [26] Narayanan N. and Ramamurthy K., "Structure and properties of aerated concrete: a review," *Cement & Concrete Composites*, vol. 22, pp. 321-329, 2000.
- [27] Kearsley E. and Wainwright P., "Porosity and Permeability of Foamed Concrete," *Cement and Concrete Research*, vol. 31, pp. 805-812, 2001.
- [28] "ASTM. Standard test method for foaming agents for use in producing cellular concrete using preformed foam, ASTM C 796-97," 1997.
- [29] Kearsley E. and Wainwright P., "Ash content for optimum strength of foamed concrete," *Cement and Concrete Research*, vol. 32, pp. 241-246, 2002.
- [30] Kunhanandan E. and Ramamurthy K., "Models for strength prediction of foam concrete," *Materials and Structures*, vol. 41, pp. 247-254, 2008.
- [31] Kearsley E. and Wainwright P., "The Effect of Porosity on the Strength of Foamed Concrete," *Cement and Concrete Research*, vol. 32, pp. 233-239, 2002.
- [32] Kunhanandan E.K. and Ramamurthy k., "Influence of filler type on the properties of foam concrete," *Cement & Concrete Composites*, vol. 28, pp. 475-480, 2006.
- [33] Fouad H., "Cellular Concrete," *Significance of Tests and Properties of Concrete and Concrete -Making Materials, Lamond J. and Pielert J., ASTM International, Standard Worldwide STP169D*, pp. 561-569, 2006.
- [34] Wu Z., Zhang Y., Zheng J., and Ding Y., "An experimental study on the workability of self-compacting lightweight concrete," *Construction and Building Materials*, vol. 23, pp. 2087-2092, 2009.

- [35] Kayali O., Haque M., and Zhu B., "Some characteristics of high strength fiber reinforced lightweight aggregate concrete," *Cement & Concrete Composites*, vol. 25, pp. 207-213, 2003.
- [36] Kan A. and Demirboga R., "A novel material for lightweight concrete production," *Cement & Concrete Composites*, vol. 31, pp. 489-495, 2009.
- [37] Othuman A., "Lightweight Foamed Concrete (LFC) Thermal and Mechanical Properties at Elevated Temperatures and its Application to Composite Walling System (PhD Thesis)," 2010.
- [38] Laukaitis A., Zurauskas R., and Keriene J., "The effect of foam polystyrene granules on cement composite properties," *Cement & Concrete Composites*, vol. 27, pp. 41-47, 2005.
- [39] Chow W., "Fire hazard assessment on polyurethane sandwich panels for temporary accommodation units," *Polymer Testing*, vol. 23, pp. 973–977, 2004.
- [40] Pokharel N. and Mahendran M., "Finite element analysis and design of sandwich panels subject to local buckling effects," *Thin-walled structures*, vol. 42, pp. 589–611, 2004.
- [41] Ahmed N., Radin S., and Ramli M., "Ferrocement encased lightweight aerated concrete: A novel approach to produce sandwich composite," *Materials Letters*, vol. 61, pp. 4035-4038, 2007.
- [42] Mouritz A. and Gardiner C., "Compression properties of fire damaged polymer sandwich composites," *Composites Part A: Applied Science and Manufacturing*, vol. 33, pp. 609-620, 2002.
- [43] Gu P., Dao M., and Asaro R., "Structural stability of polymer matrix composite panels in fire," *Marine Structures*, vol. 22, pp. 354-372, 2009.
- [44] Dodds N., Gibson A.G., Dewhurst D., and Davies J.M., "Fire behaviour of composite laminates," *Composites Part A: Applied Science and Manufacturing*, vol. 31, pp. 689-702, 2000.
- [45] Kayali O., "Bond of Steel in Concrete and the Effect of Galvanizing," *Galvanized Steel Reinforcement in Concrete* vol. 8, pp. 229-270 2004.
- [46] Alterman D., Vilches J., and Neitzert T., "An Analysis of the Bonding Energy through Pull-out Tests for Aerated Concrete with Various Steel Strip Geometries," *Advanced Material Research*, vol. 275, pp. 55-58, 2011.
- [47] Bouazaoui L. and Li A., "Analysis of steel/concrete interfacial shear stress by means of pull out test," *International Journal of Adhesion & Adhesives*, vol. 28, pp. 101-108, 2007.
- [48] Tang W., Lo T., and Balendran R., "Bond performance of polystyrene aggregate concrete (PAC) reinforced with glass-fibre-reinforced polymer (GFRP) bars," *Building and Environment*, vol. 43, pp. 98-107, 2008.
- [49] Chu X. and Neitzert T., "Experimental and numerical modelling of interfacial behaviour between galvanised steel and aerated concrete," *International Journal of Modelling, Identification and Control (IJMIC)*, vol. 2, pp. 208-218, 2007.
- [50] Schilde K. and Seim W., "Experimental and numerical investigations of bond between CFRP and concrete," *Construction and Building Materials*, vol. 21, pp. 709–726, 2007.
- [51] Teo D., Mannan M., Kurian J., and Ganapathy C., "Lightweight concrete made from oil palm shell (OPS): Structural bond and durability properties," *Building and Environment*, vol. 42, pp. 2614-2621, 2007.

- [52] Banholzer B., Brameshuber W., and Jung W., "Analytical evaluation of pull-out tests—The inverse problem," *Cement & Concrete Composites*, vol. 28, pp. 564–571, 2006.
- [53] Cao J. and Chung D., "Degradation of the bond between concrete and steel under cyclic shear loading, monitored by contact electrical resistance measurement," *Cement and Concrete Research*, vol. 31, pp. 669-671, 2001.
- [54] AL-mahmoud F., Castel A., François R., and Tourneur C., "Effect of surface pre-conditioning on bond of carbon fibre reinforced polymer rods to concrete," *Cement & Concrete Composites*, vol. 29, pp. 677–689, 2007.
- [55] De Lorenzis L., Rizzo A., and La Tegola A., "A modified pull-out test for bond of near-surface mounted FRP rods in concrete," *Composites: Part B*, vol. 33, pp. 589–603, 2002.
- [56] Fang C., Lundgren K., Plos M., and Gylltoft K., "Bond behaviour of corroded reinforcing steel bars in concrete," *Cement and Concrete Research*, vol. 36, pp. 1931-1938, 2006.
- [57] Khandaker M. and Hossain A., "Bond characteristics of plain and deformed bars in lightweight pumice concrete," *Construction and Building Materials*, vol. 22, pp. 1491-1499, 2008.
- [58] Chang J., "Bond degradation due to the desalination process," *Construction and Building Materials*, vol. 17, pp. 281-287, 2003.
- [59] Won J., Park Ch., Kim H., Lee S., and Jang Ch., "Effect of fibers on the bonds between FRP reinforcing bars and high-strength concrete," *Composites: Part B*, vol. 39, pp. 747–755, 2008.
- [60] Khalfallah S. and Ouchenane M., "A numerical simulation of bond for pull-out tests: The direct problem," vol. 8, pp. 491-505.
- [61] Ferrer M., Marimom F., and Crisinel M., "Designing cold-formed steel sheets for composite slabs: An experimentally validated FEM approach to slip failure mechanics," *Thin-walled structures*, vol. 44, pp. 1261-1271, 2006.
- [62] Golden Bay Cement., "www.goldenbay.co.nz," 2011.
- [63] "ASTM C39 Standard Test Method for Compressive Strength of Cylindrical Concrete Specimens."
- [64] Fouad H., "Cellular concrete," *Significance of Tests and Properties of Concrete and Concrete-making Materials*, pp. 561-569, 2006.
- [65] Proshin A., Beregovoi V., and Eremkin I., "Unautoclaved foam concrete and its constructions, adapted to the regional conditions. ," *Use of Foamed Concrete in Construction, International Conference held at the University of Dundee, Scotland, UK*, pp. 113-20, 2005.
- [66] Alterman D., Vilches J., and Neitzert T., "Effect of steel strip geometry on pull-out strength of aerated concret," *Edited by A.M.Brandt, Brittle Matrix Composites, ZTUREK and Woodhead Publ. Ltd.*, pp. 439-448, 2009.
- [67] Affindy M., Rahman A., and Ahmad A., "Study on Behavior of Foamed Concrete under Quasi Static Indentation Test," *European Journal of Scientific Research*, vol. 51, pp. 424-432, 2011.
- [68] Jones M. and McCarthy A., "Preliminary views on the potential of foamed concrete as a structural material," *Magazine of Concrete Research*, vol. 57, 2005.

- [69] Suryani S. and Mohamad N., "Structural Behaviour of Precast Lightweight Foamed Concrete Sandwich Panel under Axial Load: An Overview," *International Journal of Integrated Engineering - Special Issue on ICONCEES*, vol. 4, pp. 47-52, 2012.
- [70] Abaqus, "Abaqus/CAE User's Manual " http://www.tu-chemnitz.de/projekt/abq_hilfe/docs/v6.9/books/usi/default.htm, 2012.
- [71] Behfarnia K. and Sayah A., "FRP strengthening of shear walls with opening," *Asian journal of civil engineering (Building and housing)*, vol. 13, pp. 691-704, 2012.
- [72] Ramezani M., Vilches J., and Neitzert T., "Evaluation of the pull-out strength of galvanised steel strips in a cement-based material," *Journal of Zhejiang University SCIENCE A*, vol. 14, pp. 843-855, 2013.